STUDIES ON HEAVY METALS

IN THE

SEDIMENTS OF A STORM WATER DRAIN

AND THE

AVON-HEATHCOTE ESTUARY

A Thesis Submitted in

Partial Fulfilment

of the

Requirements

for the

Degree of

Master of Science

in

Chemistry

in the University of Canterbury

R. L. HAY

1988

CONTENTS

CHAPTER **PAGE**

LIST OF TABLES

LIST OF FIGURES

FIGURE PAGE

LIST OF PLATES

ABSTRACT

The concentrations of chromium, copper, iron, manganese, nickel, lead, and zinc have been estimated,primarily by flame AAS, in the sediments of the City Outfall Drain and Avon-Heathcote Estuary, Christchurch, New Zealand. These, and other metals have also been determined by XRF, and the two sets of results are compared. Sediment samples were obtained by the use of a simple coring device where possible, or by sampling the top two centimetres of sediment where this was not possible.

The variation in metal concentration with location, depth, and rainfall are discussed, with reference to metal-metal correlations, organic matter content, particle size distribution, and a theory on the formation of the sediment units in the Avon-Heathcote Estuary. These results are then evaluated with regard to enrichment factors calculated from a set of local background levels defined in this study. The strongest metal-metal correlation is lead with zinc, although lead, zinc, copper, and to a lesser extent chromium, are commonly found in association with one another. Metal concentration generally decreases with depth , except in the case of the estuary core RH2, which exhibits a profile of concentration vs. depth consistent with MacPherson's proposals for the formation of the Estuaries sediment units. Lead and zinc are found to be the metals most highly enriched above background levels in the clay, then sand, then silt fractions. No obvious reason for this was found as for all other metals, including those that correlated well with lead and zinc, the order was clay > silt > sand.

The distribution of metal concentrations in the silt-clay size fraction wre investigated using a novel technique not requiring the separation of individual size fractions. The percentage of quartz present in each fraction was found to be the primary factor causing variation in metal concentration down to approximately 4 μm. Below this size metal speciation becomes dominant. The role of organic matter was not determined but is felt to be of possible significance.

The thesis concludes with reccomendations for areas of further research, including sediment dating, application of sequential extraction techniques, and a poosible method of treatment for waste waters.

CHAPTER I

GENERAL INTRODUCTION

1.1 THE ESTUARINE ENVIRONMENT

The word estuary is derived from the Latin aestuarium, meaning a tidal channel, and is commonly used to describe the tidal mouth of a large river (The Concise Oxford Dictionary 7th ed.). The Avon-Heathcote Estuary is a shallow, intertidal estuary, situated southeast of the city of Christchurch, New Zealand, and is roughly triangular in shape. The eastern edge of the estuary is bounded by a sandy spit, and the western edge by flat swampy land overlying alluvial shingle. To the south the volcanic mass of Banks Peninsula prevents further souhward migration of the estuary and the Heathcote River channel.

The Avon and Heathcote Rivers originally entered a bay with open access to the sea. The Avon probably entered the sea between New Brighton and Waimairi Beaches. Sediment from the Waimakariri River, transported by longshore drift, built up a spit, pushing the outlet of the Avon southward until the bay was cut off, except for a narrow channel, thus forming the present estuary 1000-2000 years ago (Knox and Kilner, 1973; Deely pers. comm., 1987; MacPherson, 1978). The River Avon has lower flood flows, though a higher dry weather level than the Heathcote. This is because the Heathcote catchment is largely on the hills above southern Christchurch, whereas, the Avon drains the Christchurch basin itself. The dissimilar catchments result in a difference in the type of sediment entering the estuary from the two rivers. Sediment from the Heathcote contains more loess (a quartz and feldspar rich, wind deposited soil), and volcanic particles, in addition to the greywacke derived sediments that the Avon carries.

The catchment flats are now extensively covered by impervious paved or roofed surfaces, in addition to being extensively drained. This is a marked change from the early 1850's, when Christchurch was first settled by europeans. The changes to the catchment have increased the peak water flow in the rivers and the Outfall Drain during rainfall, thus increasing both the amount and speed at which sedimet particles and any associated metal species reach the estuary. The low lying catchment was then covered in raupo and flax, with some tussock, fern, tutu, and small areas of swamp forest such as Kahikatea. The affect of this dramatic change in catchment use on the sediments of the estuary of is discussed in some detail by MacPherson (1978). A summary of his findings, together

with a brief review of the processes and theory of sedimentation and metal-sediment interactions is given in Section 1.2.3.

The Avon-Heathcote Estuary is a complex and transitional environment. Not only in physical terms such as the merging of different ecosystems and change in ambient chemical conditions, but also in terms of mans use of the estuary. The Christchurch Drainage Board (CDB) uses the estuary as a discharge point for processed sewage effluent from the Bexely sewage farm, and also storm water, via the Avon and Heathcote Rivers andthe City Outfall Drain. However, the estuary is also a natural focus for recreational and sporting activities such as yachting, windsurfing, swimming, and fishing. This conflict of interest, together with the richness, diversity, and delicate nature of the estuarine environment makes it an area of special interest. As an indication of the importance of the estuary as a wildlife habitat, the population survey conducted by Knox and Kilner has been summarised below.

The estuary supports 20 species of polycheate worms (at densities of 40 - 8000 m^{-2} dependant on species and location). Polycheate worms work through large quantities of sediment, sometimes as much as 6 g day^{-1} $individual^{-1}$. Five species of mollusc (the cockle, or chione stuchburyi at 2500 m^{-2}), six gastropods (amphibola crenata at up to 425 m^{-2}), seven crustaceans, and two species of anenomes complete the mudflat community. Of these 40 species, 30 are common or relatively common. In addition, a little further up the food chain, 28 species of fish (some of which are transitional only), and 29 species of birds live or feed in, and on, the estuary. The fish and birds feed upon either members of the mudflat community or other fish, which have themselves fed from that source, and therfore act as potential accumulators of heavy metal taken up by the sediment dwelling and/or feeding species. As examples an average Pied Oyster Catcher, of 425 g dry weight, consumes 109,710 cockles per year, or 52.12 kg dry weight; the Sand Flounder (a not atypical example) was found to contain 32.4% mud in its gut contents, with the remainder being detritus and sediment/detritus feeding organisms.

As heavy metals are known to have deleterious effects on most animal and plant species (see Section 1.3), and fish, such as flounder, are caught from the estuary for human consumption, it is advisable that metal inputs to the estuary are limited and estimated. This study is, however, more concerned with the levels of metal enrichment and physical mechanisms of metal-sediment interaction (past and present), and the interpretation of these, than in the affects of any metal pollution. It is hoped that the information obtained from this study will be of use at a later date, for both physical and environmental studies.

1.2 ESTUARY SEDIMENTS, SEDIMENTATION, AND METAL-SEDIMENT BINDING

1.2.1 Introduction

When there was no heaven,/ no earth, no height, no depth, no name,/ when Apsu was alone,/ the sweet water, the first begetter; and Tiamat/ the bitter water, and that,/ return to the womb, her Mummu,/ when there were no gods- When sweet and bitter/ mingled together, no reed was plaited, no rushes/ muddied the water,/ the gods were nameless, natureless, futreless, then/ from Apsu and Tiamat/ in the waters gods were created, in the waters/ silt precipitated,...

The Babylonian Creation, Sanders (1971)

The above quotation aptly demostrates an early knowledge of an important sediment forming process in any place where fresh (sweet) and salt (bitter) waters meet. This is the flocculation and settling out of clay particles, and will be discussed more fully below.

Sediments are a complex and variable mixture of quartz, feldspar, carbonates, clays, amorphous hydroxides (of Fe, Mn, Si, Al), and organic material. Other minerals and substances may be present, depending upon the source of the sediment and its history of transport. Quartz, feldspar, and carbonate are all relatively low in heavy metals, and do not absorb metals from other sources to any significant degree. Clay minerals, hydrous oxides (especially those of Fe and Mn), and organic matter all interact extensively with metal ions by a variety of mechanisms.

Before describing these it is necessary to define the terms used. The nomenclature used is that of Folk, Andrews, and Lewis (**Fig. 7**) who used the Wentworth size classification system as a basis for classifying particles. The Wentworth scale takes the $-\log_2$ of the particle diameter (in mm), producing a whole number (phi) which is negative for particles >1 mm, 0 = 1 mm, and positive for particles <1 mm (see **Table 1.0**).

Table 1.0 The Wentworth Size Classification

size class	particle diameter in mm	phi
very coarse sand	2 - 1	-1 - 0
coarse sand	1 - 0.5	0 - 1
medium sand	0.5 - 0.25	1 - 2
fine sand	0.25 - 0.125	2 - 3
very fine sand	0.125 - 0.063	3 - 4
coarse silt	0.063 - 0.032	4 - 5
medium silt	0.032 - 0.016	5 - 6
fine silt	0.016 - 0.008	6 - 7
very fine silt	0.008 - 0.004	7 - 8
clay	< 0.004	> 8

Division of size classes in this study were: sand, 563 μm to 63 μm; silt, 63 μm to 4 μm; and clay, < 4 μm. Sand and coarse silt are predominantly carried in rivers and streams as bed load, by a series of small hops called saltation, heavy metal rich particles may also be transported in this manner. Finer particles, clays, colloids, and organic matter are predominantly transported as suspended sediment. Thus deposition of heavy metal contaminants is dependant upon the particle size fraction with which it associates, the processes these particles are subject to, and reflects pollution in a given area (Salomons and Förstner, 1984; deGroot et al., 1976).

Figure 1 depicts the chemical properties of a typical sediment. The quantities of the species shown, and the pH and E_h levels of any given sediment, will vary from location to location, depending upon local conditions. Layer (1) represents yellow-brown oxidised sediment, layer (2) represents the redox potential discontinuity (RPD), which is typically grey in colour, and layer (3) represents reduced sediment, and is typically black in colour due to the presence of FeS.

Figure 1 Chemical Properties of a typical sediment

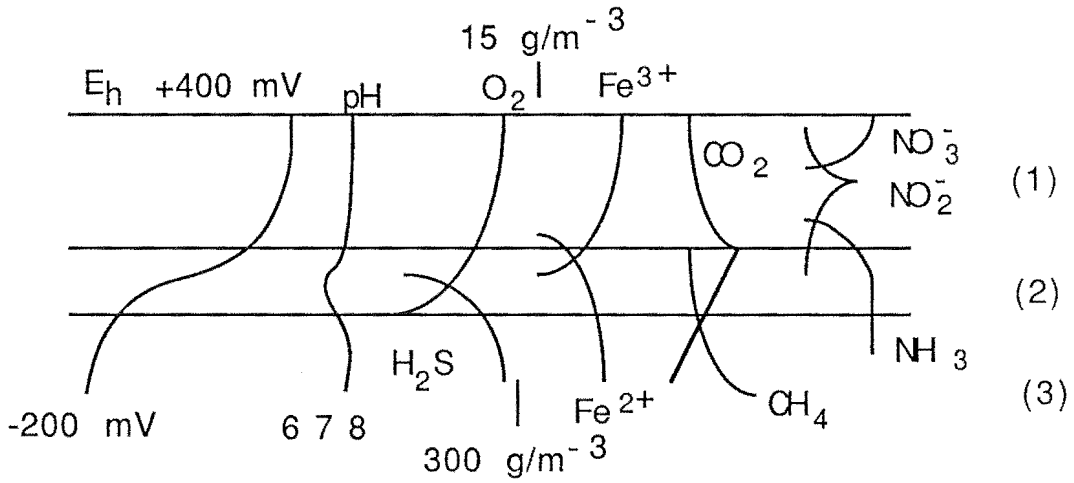

After Fenchel (1970), from Knox and Kilner (1973).

At the outfall to the City Drain (the location of core RH2, this study) the sediment E_h at a depth of 30 mm was determined as approximately -200 mV (Knox and Kilner). At this location then, layers (1) and (2) are absent, and only a small oxidised microzone exists above layer (3). Manganese and iron oxyhydrates are therefore chemically unstable, and may dissolve, releasing bound metals into the surrounding pore water. Knox and Kilner note that the oxidised microzone is known to inhibit release of nutrients to the surface waters, and it seems possible that this may also apply to heavy metals.

1.2.2 Sedimentary Processes and Metal Binding

1) Clay Flocculation: The most common clay minerals in the Avon-Heatcote Estuary are illite and chlorite (MacPherson, 1978; Deely, 1987). Illite is a nonexpandable clay formed by either the weathering of feldspars (low MgO) or diagenisis of montmorillinite (high MgO), whereas chlorite, although often formed insitu, is mostly derived from macroscopic chlorite in catchment soils (Weaver and Pollard, 1973). Clay particles have a negative charge on their surface due to substitution of principal structural cations (Si, Al) by cations of lower valance (primarily Al substituting Si lattice positions, and Fe substituting Al lattice positions). The charge is counteracted by an electrical double layer of counter ions which can undergo ion exchange. In fresh water the negatively charged particles tend to be kept apart by repulsion. In more saline water the repulsive forces are reduced, leading to destabilisation of the colloid or suspension, and an increased tendency to flocculate (clump together) on collision. Four flocculating mechanisms have been recognised, these are: (1) neutralisation of -ve charge by specific adsorption of +ve ions; (2) compression of the double layer by increased counter ion charge and/or concentration; (3) interparticle bridging by adsorbed material; and (4) enmeshment of clay and hydroxide particles (Burton, 1976). Heavy metal binding to clays is primarily by sorption in the double layer, with isomorphous replacement in lattice sites a secondary factor. Deposition of the floccules formed is dependant on water velocity and flow patterns, and the estuary floor type. A hard rocky bottom may lead to disaggregation and resuspension of floccules (Postma, 1980).

2) Hydrated Oxides: A number of workers have reported the influence of Fe and Mn hydroxides on trace metal transport and speciation. Due to the difficulty in obtaining undisturbed, isolated, and identifiable natural samples, much work in this field has been done on simplified model systems. This has led to variation in the relative significace of the oxyhydrates as metal scavengers when compared with organic matter, the mechanism of metal binding, and the speciation and surface areas of compounds reported in the literature. It is generally agreed that hydrated oxides may occur as discrete particles, clusters, or as coatings on minerals (Jenne, 1968; Förstner and Wittmann, 1981; and Dawson, 1982). Förstner and Wittmann considered the primary mode of transport of the oxyhydrates is as coatings on particles <16 μm diameter (clay to fine silt).

Iron and manganese hydrated oxides are formed when groundwater containing Mn^{2+} and Fe^{2+} enter oxidising surface water for the first time (Förstner and Wittmann; Chao and Theobald, 1976). The mechanism of formation is dependant on the ambient conditions and ligands, with the dominant forms produced being "FeOOH" and "MnO_2". The primary means of metal-hydrated oxide binding is by surface sorption, probably by exchange with protons, although other mechanisms are discussed (Dawson; Chao and

Theobald). Manganese oxyhydrates are considered better scavangers than iron, largely because of their greater surface area. Iron oxyhydrates typically have surface areas of 6.4-164 $m^2\ g^{-1}$ (Crosby et al., 1983), which compares poorly with manganese species such as Birnessite with a surface area of 350 $m^2\ g^{-1}$ (Dawson). The equilibrium between the Fe and Mn oxyhydrates is, however, dependant on a large number of factors which will not be discussed here. Dawson found that Ni, Cu, and Zn correlated largely with Mn, and to a lesser extent with Fe in soil concretions. This is in contrast with Snodgrass (1980), who states that Fe oxyhydrates dominate both organic matter and Mn oxyhydrates when competing for Ni. Swallow et al. (1980) found that lead was sorbed by $Fe_2O_3.xH_2O$ with no influence from the ageing (increasing crystalinity) of the oxide.

3) Organic Matter: Organic surfaces for trace metal adsorption can arise in three ways: (1) organisms; (2) decomposition of plant and animal matter; and (3) low molecular weight material being sorbed onto clay or metal oxide surfaces (Salomons and Förstner, 1984). Interactions between organic matter and metals will be dependant upon the type and quantity of organic matter present, the degree of competition with other chelating or binding phases and ligands, and the type of donor atoms available to bond to metal ions. Dawson (1982) found that in soils the order of correlation of trace metals with organic content was $Fe^{3+} > Al^{3+} > Cu^{2+} >> Zn^{2+} > Ni^{1+} > Mn^{2+}$, whereas Timperly and Allen (1974), studying lake sediments, found the order to be $Cu^{2+} > Ni^{2+} > Pb^{2+} > Co^{2+} > Fe^{2+} > Zn^{2+} > Mn^{2+}$. The differences between the two studies are attributed to the different conditions applying.

1.2.3 Geological Description of the Sediments of the Avon-Heathcote Estuary (AHE)

MacPherson (1978) concluded from his study of the AHE that during the period 1850-1920 the tidal compartment of the estuary decreased by 30%, and then returned to its origional volume, and is now 30% larger than its pre-european volume. He links this with the process of urbanisation in the catchment area, noting that overseas studies had shown an initial silting of waterways with drainage and denudation of the land, followed by erosion as greater areas of impervious surface, and improved drainage, increase the volume and speed of runoff water. The sediment supplied is also of a coarser nature.

In the AHE an abiologic pre-estuarine / estuarine pre-european / estuarine post-european sequence is recognised. The four units of this sequence are described in **Table 1.1**. MacPherson concluded "The AHE is experiencing ongoing nett erosion, and the sediment-water interface is continually deepening. As a result the inhabitants of the bioturbate zone are efficiently 'eating' their way downwards into progressively older sediment, which is mixed into the bioturbate zone (and the fine suspendible fraction is added to the water column)..."

Table 1.1 Geological Description of the Sediments of the AHE

unit	description	date
I	An upper zone of dark grey and black mottled, bioturbate sediment, inhabited by a number of burrowing animals, seperated from the underlying sediment by a bioturbation interface.	present - 1850
C	Thin, massive, muddy unit, olive grey plastic mud or very fine sandy mud - may show laminations. (b) - (c) contact often abrupt. Deposited throughout the estuary, often rich in organic matter. Cohesive. Depostied relatively rapidly and at uniform rates.	1900 - 1850
B	Intermediate layered muddy unit - stratified sediment - laminated muddy very fine sand, often with centimetre to decimetre interbeds of massive muddy fine sand and muddy very fine sand. Interpreted as estuarine, and deposited under essentially the same conditions as those applying today.	1850 - ?
A	Basal massive sand unit. Pre-estuarine, open ocean sediment (uppermost Christchurch Formation).	

1.3 TOXICITY OF HEAVY METALS TO AQUATIC PLANTS, FISH, INVERTEBRATES, AND HUMANS

1.3.1 Use and Occurence of Heavy Metals

Before outlining the toxicity of the elements studied it is perhaps best to briefly list man's use of these metals and significant natural sources.

1) Chromium: The earliest recorded use of chromium was as a paint pigment in France (c.1800). Chromium is now widely used in the fields of metallurgy, refractory compounds, and the chemical industry (58, 21, and 21% of world production respectively). The metal or its compounds have found uses as diverse as pigments, tanning of leather, and the plating of metals, through to saccharin manufacture and the purification of fats and oils. Primary discharges into soil and water are by electroplating, laundary chemicals, animal glue manufacture (Cr^{6+}), and tanning and dyeing (Cr^{3+}). Some fertilisers contain up to 10,000 ppm chromium. Studies from the USA and Britain show that sewage teatment works are a major source of chromium (and also Cu, Ni, and Zn) (Moore and Ramamoorthy, 1984; Purves, 1985). In Christchurch the primary sources of Cr are leather tanning (especially in the late 1800's, now less important), road markings, and sewage effluent.

2) Copper: Copper is widely used in industry and also as a timber preservative. Major anthropogenic sources are fertilisers and the combustion of coal, oil, wood, and petrol. Natural sources include volcanic particles, sea salt spray, and especially dust (type not specified) (Moore and Ramamoorthy, 1985). These are also likely to constitute the major natural and anthropogenic sources for Christchurch.

3) Nickel: Commonly used for coinage, and like chromium in the electroplating and metallurgical fields. Enrichment in sediments is commonly due to the activities of electroplating, and battery manufacturing industries, with photoengraving and urban run off contributing. Common contributers to the nickel and chromium load carried by urban runoff are corroding roofs, tins, and plated objects. Less common are fires and flaking paint (Purves, 1985). Combustion of diesel fuel has also been implicated as a source of nickel (Nriagu, 1979), though at 0.07 ppm in New Zealand diesel (Wilson, pers. comm.) this is unlikely to be an important factor. No single significant source of nickel in the Christchurch environment has been identified, and all of the above are likely to contribute to anthropogenic nickel in the environment to some degree.

4) Iron and Manganese: Both of these metals are derived largely from the surronding soil. However, both elements are also commonly used as structural materials and in alloys in a number of diverse applications. This, as will be seen later, leads to enrichment above background levels which is not normally expected, especially in the case of manganese. The most significant source of these metals in the City Outfall Drain sediments is likely to be roofing iron, and particulate from engine wear (especially for manganese).

5) Lead: Lead has probably the longest history of use by man of any of the metals studied here. Although known by other civilisations the Romans were the first great users of the metal. Interested readers are referred to Nriagu (1983). The extraction and industrial application of lead accounts for approximately 20% of anthropogenic lead, with the automotive combustion of leaded petrols accounting for a further 60% (Nriagu, 1979). Two major sources of lead in Christchurch have been identified - house paint and leaded petrol (Day, 1977). Day concluded that as the concentration of lead in soil fell off rapidly with distance and depth from houses, petrol was the major source of the metal in the Christchurch environment. A battery factory in Heathcote is a significant source of lead pollution for the local area, and in the past has discharged into the Heathcote River (Purchase and Fergusson, 1986). The amount of this discharge has since been reduced (Robb, pers. comm. 1987).

6) Zinc: Coal and especially wood combustion are important anthropogenic sources of zinc. Galvinizing, printing, dyeing, and paints also contribute, although the affect of these is probably more localised. Nriagu (1979) estimated that for Cu, Pb, and Zn eroded soils accounted for 60-80% of the natural abundance, with volcanoes accounting for a further 15-20% and natural fires <10%. Interestingly he estimated that plant exudates accounted for 20% of atmospheric zinc. The most significant sources of anthropogenic zinc in the Christchurch environment are the combustion of solid fuels, and runoff from galvanised roofs.

1.3.2 Metal Toxicity Towards Aquatic Plants, Invertebrates, and Fish

Unless otherwise stated the following summary is based on information in Moore and Ramamoorthy (1985).

1) Chromium: Chromium is less toxic to aquatic plants than Cu, Pb, Zn, and Ni. In salt water this is due to competitive inhibition with cations. Sublethal and chronic exposure effects include decreased growth and a reduction in the reproduction and survival abilities of progeny. The order of toxicity and effects of exposure for invertebrates and fish are the same as those described above.

2) Copper and Nickel: The effects of exposure to copper include growth inhibition, loss of potassium due to increased cell permiability, decreased photsynthesis, and decreased levels of particulate carbon and nitrogen fixation. Some algaes may become tolerant to prolonged high exposure and have been found to contain up to 600 ppm dry weight (Stokes, 1975). Copper is also highly toxic to aquatic invertebrates and fish, with a higher level of toxicity in fresh than in marine, and hard than in soft water (see also Brković-Popović and Popović, 1977). The affects of exposure to nickel are similar, although nickel is somewhat less toxic.

3) Lead: The most toxic form of lead is Pb^{2+}. Increaing pH, or increasing the concentration of chelating agents in the water, decreases the toxicity. Lead is less toxic towards plants and invertebrates than copper, and under some conditions zinc, but more so than nickel, chromium and manganese.

4) Zinc: The toxic effects of zinc are highly variable due to the ability of species to adapt. The presence of PO_4^{3-} significantly reduces toxic effects. For fish exposure to zinc ions gives four marked effects: increased concentration of lactic and pyruvic acid, therefore a decrease in tissue pH; kidney tissue and enzyme dysfunction (due to the former); decrease in growth, maximum size, and reproductive potential; and, altered reproductive and schooling behaviour.

In summary, there is a decreased diversity and density of population in areas highly contaminated by heavy metals, but not necessarily so for moderate to lightly contaminated areas. Many variables affect the outcome of contamination in a given area, such as adaption, light, temperature, and cation concentration.

1.3.3 Metal Toxicity Towards Humans

Förstner (1980) considers Fe as being "non-critical" in its toxic action towards humans. Nickel, copper (in contrast to Moore and Ramamoorthy), lead, and zinc he rates as "very toxic and easily accessible".

1) Chromium: Mammalian organisms can tolerate up to 100-200 times their total body Cr content as stomach acidity converts the more toxic Cr^{6+} to Cr^{3+}, which is also less easily absorbed through the gastro-intestinal tract (<1% abs.). Chromium is therefoe not considered acutely toxic to humans although it is a suspected mutagen for workers of ferrechrome and chrome pigments (Moore and Ramamoorthy).

2) Copper: Copper is not very toxic to humans, largely because it does not inhibit the operation of S containing proteins and enzymes (toxicity to aquatic animals is due to precipitation of essential carboxylic acids). There is no evidence of carcinogenic or mutagenic properties.

3) Lead: Lead mimics Ca in deposition and mobilisation in human skeletal components. A major pathway of lead into the body is by inhalation, as 35% of inhaled lead is absorbed compared with 10% of ingested lead (WHO, 1977). At low levels lead inhibits the enzymes which convert protoporphyrin into heam molecules. As the concentration of lead in the blood increases aenemia develops. Above 50-60 µg/1000 ml blood the nervous system is affected, and as the concentration reaches 80-100 µg/1000 ml nerve loss and muscle weakness develops. Eventually convulsions, coma, and death follow prolonged exposure at high concentrations. A summary of the effects and mechanisms of lead poisoning may be found in Simmonds, (1982).

4) Nickel: Nickel is essential for health at 200-300 µg day^{-1}, however, in excess of this amount is acutely toxic by competitive interaction with Ca, Co, Cu, Fe, and Zn. The major effect is interference with the synthesis and degradation of cellular heme due to strong binding of of sulpher and the rigid geometry of complexes formed. Nickel inhalation has also been shown to cause cancers (Pederson et al., 1978).

5) Zinc: Toxic effects of zinc appear to be related to interactions with Cd. Zinc is essential for formation and functioning of a variety of enzymes and hormones, and also immune system response.

1.4 AIMS OF THIS STUDY

The location of this study was the main City Outfall Drain, located on the western edge of the Avon-Heathcote Estuary. This drain carries storm water away from the central city area and discharges it into the estuary. The Outfall Drain was constructed in 1871 as an open timbered drain, and was intended to be used as a canal to bring barges into Christchurch as an alternative to Port Lyttelton.

Two major renovations of the drain have been carried out, one in the 1930's when a section of concrete channel was laid, and another in the mid 1970's when the

existing precast concrete sections were laid between Olliviers Rd. and St. John St. The catchment area and drain location may be seen in **Figure 2.**

The aims of this study are to establish the current concentrations of the metals chromium, copper, iron, manganese, nickel, lead, and zinc at a number of sites along the length of the City Outfall Drain, and to examine any variation of metal concentration with time, rainfall, location, or particle size. Due to the construction of the drain the time dependancy study has been divided into two parts. The first is an examination of historical metal concentrations using sediment cores. The second uses surface samples collected over a comparativly short period of time. Particular attention has been paid to concentration variation with particle size, in the silt and clay size fraction, and also enrichment factors.

CHAPTER II

GEOLOGY AND HEAVY METAL CONCENTRATIONS OF CORE SAMPLES

2.1 INTRODUCTION

Sediment core samples have a major advantage over surface samples in that they are capable of yielding both chemical and geological data relating to the past history of a site. Provided care is taken in the interpretation of these results much useful information can be obtained. Factors that will affect the reliability of data from a core include bioturbation (the reworking of the top centimetres of sediment by burrowing and feeding organisms) and diagenesis. Bioturbation may lead to the mixing of polluted and unpolluted sediments and so change concentration gradients and grain size disribution. Diagenisis refers to the changes that take place in the sediment column during its formation. Changes such as: consolidation, expulsion of water, change in the type and quantity of organic matter, and change in the E_h and pH properties. The important aspects of diagenesis in the present study are; changes to organic matter, E_h, and pH. Organic matter is probably a controlling factor or, at least, a major influence on E_h/pH, as it will determine the amount of free oxygen present. An example of the importance of both E_h and pH may be seen from the various species of manganese that can exist under differing conditions. Under oxidising conditions manganese forms trivalent and tetravalent oxyhydrates, which are insoluble and good scavengers by sorption of trace metals. The manganese (and iron) oxyhydrates are deposited with the sediment. Upon burial, and the exclusion of oxygen, reducing conditions will produce divalent manganese oxyhydrates. The manganese (II), iron (II), and any trace metals bound to the oxyhydrates are released into the sediment pore water, where they may be complexed by organic material and migrate up or down the sediment column, perhaps being released into the surface waters (Duchart and others, 1973; Robbins and Callender, 1975; Presby and Trefry, 1980; Aston and Chester, 1976; deGroot and others, 1976). If this has occurred to any considerable degree caution must be exercised, as high localised metal concentrations may be due, at least in part, to diagenetic effects rather than anthropogenic influences.

In this work sediment cores were collected along the drain, to approximately 30 m into the estuary. Sample treatment and analytical procedures are described in Chapter VI. In addition, a core collected but not analysed by Burgess (1985) was studied. In

addition to determining the concentration of heavy metals some additional information has been obtained on the sediments. This information largely comprises textural description and total organic matter content. Particle size is also an important factor in the interpretation of metal concentration results. Higher results are expected in mud (a mixture of silt and clay as defined in **Fig.7**), silt, and clay than in sand (Ramamoorthy and Rust, 1978; Jaffé and Walters,1977; see also Chapter IV). Obviously therefore the grain size composition of a sediment must be taken into consideration in the interpretation of trace metal concentrations. A method has been devised for correcting metal concentrations for grain size effects by Ackermann (1980), using ^{137}Cs. This was not done in this study. Methods used for grain size analysis in this study are based on those of Lewis (1981). For textural description of sediments the Folk,Andrews,Lewis (1970) terminology is used [as reported in Lewis (1981)].

2.2 SAMPLING PLAN AND SITE DESCRIPTION

Three cores were collected at irregular intervals along the length of the drain from St. John St. to the mouth of the drain on Humphries Drive. An additional core had also been collected by another worker (Burgess, 1985) at a location approximately 115 m due east of the drain mouth, in the estuary. The locations of these cores are shown in **Figure 2**. Factors influencing the location chosen for coring included: the distance from other cores, the position along the drain, and access. Cores were numbered by order of collection, however, as great difficulty was experienced in collecting one core, numbering is not sequential. The core collected by Burgess was labelled 13.2 as it was collected from the Christchurch Drainage Board (CDB) transept 13, site 2.

The study area can be seen from plates 1,2,3. Plate 1 gives a view of the estuary end of the drain. Core 13.2 was collected slightly above and to the right of the centre of the photograph. Core RH2 was collected 30 m on the estuary side of the drain mouth (centre-left), the drain itself runs along Linwood Ave. (centre-left to left). Plates 2 and 3 are photographs taken at the site of core RH3. Plate 2 looks south east towards the estuary, plate 3 looks west towards Christchurch city. Downstream of the St. John St. bridge the drain has a sediment bottom and is 6-20 m wide, and has a typical water depth of 0.1- 0.8 m. Above the bridge the drain has a concrete bottom, and only surface samples could be collected - see Chapter III.

2.3 RESULTS

2.3.1 Geological

After collection the cores containers were opened and the cores logged. The results may be seen in **Figures 3, 4, 5, and 6**. Little information was available on core 13.2, although four subsamples have been described texturally in this study.

Out of the twenty eight samples analysed during the study period, twenty subsamples were chosen from the four cores for more detailed analysis. These samples were separated into their component sand, silt, and clay fractions for later analysis. A by product of the particle size separation, is that useful textural information can be obtained and that sand and silt fractions could be examined under a microscope. The Folk, Andrews, Lewis classification of these samples is presented in **Figure 7**, and the percentage sand, silt, and clay in **Table 2.0**.

Ten of the samples are classified as silty-sand, eight as sandy-silt, and two as sand. As can be seen from the data in **Figure 7** the samples do not cluster, but rather represent a gradational change from silt through to sand. The samples range in clay content from 0.5 % (RH2/21) to 18.1 % (RH3/11), with only five samples below 4 % and one sample above 11 %. The mean clay content is 6.4 %, with a standard deviation (s) of 4.1 %. However, if samples below 4 % and above 11 % are excluded the mean becomes 7.2 % and s = 2.2 %. Illite and chlorite were identified as the primary clay species from the XRD traces of the clay fractions.

All of the cores have stratification typical of estuarine deposits,with the bulk of the sediment being silty-sand or sandy-silt laminated by irregular 5-15 mm thick silt or sand bands, with occasional beds of either medium to coarse clean sand or fine clayey silt. MacPherson (1978) identified a number of stratigraphic units typical of the estuary which are described in Chapter 1.2. The most positive identification of these units has been made in core RH2 (**Fig. 5**) (the core taken near the edge of the estuary) with unit c beginning at a depth of 310 mm, and ending with a sharp mud-sand interface at a depth of 965 mm. The section 965-1170 mm was unit b. No unit a was present. The core from 0-310 mm appears to represent "modern" sediments, and certainly the heavy metal concentration data to be discussed supports this. The other estuarine core, 13.2 contains modern (0-160 mm) and unit c (160-300 mm) sediments only. The length of core 13.2 was insufficient to reach the bottom of unit c. The horizion at 160 mm is believed to be equivalent to that at 310 mm in core RH2.

Cores RH3 and RH1 are rather more difficult to interpret. Sediments below 180 mm in RH3, and 240 mm in RH1 most probably represent estuarine deposits. However, how these sediments relate to MacPherson's units is not clear. Between 170-180 mm in

RH3 and 205-240 mm in RH1 is a layer of distinctly brown clayey silt with a major very fine sand component. Above this layer the sediments are distinctly higher in organic matter, darker in colour, and sandier in composition. In addition in RH3 the top 100 mm or so of sediment has an oily odour, and an oily sheen appears on the water surface when the sediment is disturbed.

Interpretation of the sedimentation pattern in RH3 and RH1 is limited by the lack of a dating of the sediment column, and any history of dredging. The most likely location for the 1871 drain bottom in RH3 is at a depth of 290 mm. Above this depth the uniform grey silt is laminated by thin bands of sand which may represent episodes of high water flow. The brown coloured sediment layer resembles the surronding soil. This may have arisen from either a major flood event, or a renovation of the drain, or a considerable change in the activities carried out in the drainage basin. Identification of the likely 1871 drain bottom in RH1 was not possible.

2.3.2 Heavy Metal Concentrations and Correlations

The concentrations of the metals were obtained by digesting samples in conc. HNO_3/HF, by the method given in Section 6.3, followed by flame AAS analysis (see Chap. 6.4). The results of these analyses are listed in **Table 2.1**. Samples are listed according to location, upstream to downstream, and surface to bottom of cores. Figures in brackets are the depths to the centre of each sample, and are the values used for plotting depth versus metal concentration , for total, sand, silt, and clay fractions, and percent organic content. These graphs may be seen in **Figures 8-11**. Dashed lines connect samples which are too far apart for reliable interpolation to be made and are not to be considered as a continuum. No plots for core RH1 silt and clay were drawn, as two of the four samples (RH1/9 and RH1/14) had negligible silt, and the clay fraction became contaminated when the centrifuge tubes broke during the separation procedure. Depths are plotted as "below surface" as a common datum point for all of the samples is not known. From map 1 (see MacPherson, 1978), it would appear that the top of core 13.2 lies 100 mm below the top of core RH2. Lowering the curve for 13.2 by the appropriate amount would place the two plotted curves in the correct position relative to one another but would not necessarily correctly align corresponding stratigraphic units. Trends and features of interest in the depth versus concentration graphs will be discussed in Section 2.4.

Metal-metal and metal organic correlations were calculated using the program STATCALC (© 1984 Alan Lee, Peter McInerney, Peter Mullins). The resulting correlation coefficients are presented in **Tables 2.3 - 2.20**. Significant correlations and any implications these may have will be discussed in Section 2.4.

2.3.3 Experimental Factors Influencing Results

During the course of this study a variety of factors were noticed which had an influence on the results obtained. These are discussed below.

1) Fe and Mn by Standard Additions: In the course of the analyses samples to be analysed for iron were diluted 1000 times and those to be analysed for manganese 40 times. Normally the diluted samples were analysed immediately. However, on two occasions a delay of 2-3 days was unavoidable. On both occasions erratic results were obtained for iron, while high results were obtained for manganese. The following experiment was performed. Four separate samples, each in duplicate, were prepared for manganese analysis in the usual manner. One set of duplicates was used for analysis by AAS, and the other for E_h and pH measurements. Analysis was carried out immediatly after preparation, and repeated after three days, and again after four days. The results are presented below.

Table 2.2 Change in Concentration of Mn, E_h, and pH, in Four Samples with Time.

	DATE								
	16/9/87			19/9/87			23/9/87		
sample	ppm	E_h	pH	ppm	E_h	pH	ppm	E_h	pH
1	265	0.427	2.21	227	0.415	2.29	192	0.431	2.21
2	118	0.425	2.34	157	0.424	2.37	194	0.430	2.28
3	286	0.430	2.30	276	0.426	2.37	296	0.434	2.24
4	139	0.426	2.32	101	0.428	2.46	93	0.428	2.31

All of the samples showed a small increase in pH after the three day period, followed by a decrease back to, or even below, the initial pH at the end of the four day period. Samples one to three experienced a small decrease in E_h over the three day period followed by an increase in E_h to greater than the origional E_h by the end of the four day period. Sample four did not undergo any significant shift in E_h over the duration of the experiment.

It is clear from the E_h and pH diagram for the manganese/water system (Campbell and Whitekar, 1969; see **Fig. 12**) that the $Mn^{2+}_{(aq)}$ ion is the most stable state.

Figure 12 E_h, pH Diagram for the Manganese/Water System

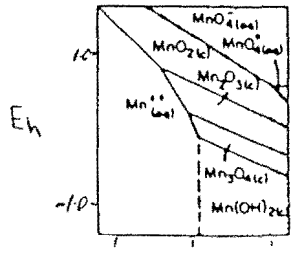

In fact, the stable state is the $M^{2+}_{(aq)}$ for all of the metals studied, except for Na^{1+} and Cr^{3+}. However, aluminium will exist as the $Al(OH)_2{}^{1+}_{(aq)}$ complex, and silicon as colloidal silica, $SiO_{2\,(c)}$ for the above E_h and pH conditions. It seems therefore, though it has not been proven, that the possibility of some colloidal silica that is slowley formed may cause the reduction in the manganese levels. To circumvent this problem iron samples for standard additions were made up in 0.5 M HNO_3, the same acid concentration as in the initial sample, and both iron and manganese solutions were analysed immediatly after preparation.

2) Formation of a Precipitate in the Digested Solution: The formation of insoluble compounds in the digested solutions is of concern as they may absorb analyte elements on to their surfaces, or trap them in their crystal lattices, thereby lowering the metal concentration in solution.The initial digestion technique used was that of Burgess (1985), based on Hulse (1983). A precipitate was often found to form in the digested solution, although neither Burgess nor Anderson (1985) (who used the same technique) have stated whether or not an insoluble residue formed. Both Hulse and also Dawson (1982) found that a residue formed and examined the precipitate by XRD. They concluded that the precipitate was most likely insoluble aluminofluorides ($NaAlF_4.xH_2O$, $MgAlF_5.xH_2O$). Increasing the amount of HF used in the digestion method was found to avoid the formation of precipitates. Only one out of one hundred or so samples produced a precipitate after this modification.

2.4 DISCUSSION

2.4.1 Introduction

In interpreting the heavy metal levels in sediments three approaches were used during this study. Firstly, the concentrations of the metals were studied for trends and anomolies.Secondly, relationships between particle size, organic matter, and metal concentration were examined, and lastly, the reltionships between the different metal concentrations were examined. This last point was also examined by testing the statistical significance of metal-metal and metal-organic correlations. The manner in which the degree of significance changed with depth, location, and different grain size fractions was noted.

2.4.2 Metal Concentration versus Particle Size and Organic Matter

As a general rule it was noted, in this study, that the organic content of sediments in relation to particle size follows the order silt < sand < clay. This unexpected order arises from the presence of fewer, but larger, pieces of organic debris in the sand fraction (563-63 μm), boosting the % organic matter above that of the silt fraction (63-4 μm).

The normal ranges of % organic matter found are 1.5-3.5%, 1,75-2.5%, and 4.3-10%, for the sand, silt, and clay fractions respectively . The sample with the highest organic content for all fractions was RH3/3, with 7.67, 8.74, and 16.22%, in the sand, silt, and clay fractions respectively.

An examination of the data in **Figures 8-11** indicates that Pb, Zn, and Cu, have a consistent and similar change in concentration to that of organic matter with depth, regardless of size fraction. Exceptions to this occurred for the clay fractions of RH3, and the total samples for 13.2, in which there was no relationship between metal concentrations and organic matter content. Chromium also exhibited some similarity with organic content with depth for the sand fractions of RH2, RH3, and 13.2; the silt fractions of RH2; the clay fractions of RH2 and 13.2; and the total sample for RH1. Iron and nickel demonstrated rather less similarity, with reasonable matches in the sand fraction of RH3 (Fe,Ni). the silt fraction of RH2 (Fe), the clay fraction of RH3 (Ni), and the total samples for RH1 and RH3 (Ni). As previously mentioned no data was available for RH1 silt and clay.

Examination of the correlation coefficients between the metal and organic content given in **Tables 2.3-2.20** yield a number of significant features which are summarised in **Table 2.21**. Lead and zinc most frequently correlate with organic matter at a significant level, whereas chromium, copper, and nickel correlate significantly, but less frequently. Manganese and iron correlate at a significant level in RH3 clay only, although when all core samples are taken into consideration the only significant Mn and Fe correlations with organic matter are in the sand and silt, and sand size fractions respectively.

For all metals, except lead, the concentrations decreased in the order clay > silt > sand. For both lead and organic matter (as mentioned above) the order is clay > sand > silt. This could be due to lead being enriched in hydroxide/organic coatings on the sand grains. However, as similar behaviour was not observed for Cu, Zn, or Cr, and these metals also correlated well with organic matter, it seems that for some reason particulate matter > 63 μm, is high in Pb in the drain sediments. This is somewhat surprising, as the levels of lead in urban street dust are generally greater in the smaller sized particles (Harrison and Wilson, 1985b).

When the concentrations of the metals in the total sample are compared with the concentrations in the various grain size fractions, the following patterns occur: clay > total > silt > sand, for Cu, Zn, Org.; clay > total > sand > silt for Pb; clay > total = silt > sand for Cr, Mn, and Ni; and clay > silt > total > sand for Fe.

2.4.3 Variation of Metal Concentration with Depth

1) Core RH3: Plots of concentration vs. depth for all the elements in core RH3 (total sample) show a maxima in concentration at a depth of 145 mm (RH3/3). This pattern is not observed (surprisingly) for the separate sand, silt, and clay fractions, with the exception of iron in the sand and silt fractions. In both of the latter cases the maximum concentration is at a depth of 490 mm (RH3/11). Most elements in all fractions reach a minimum concentration between approximately 210-330 mm, or level out to a "background" concentration. Exceptions are Zn (in all fractions), and Pb, Fe, and Cr in the clay fraction which all continue to decrease.

2) Core RH1: With the exception of Mn (total and sand) and Ni (sand), which show an overall increase in concentration with depth; and Fe (total and sand) and Pb (sand), which show no overall change in concentration, the concentrations of all elements decreased with depth. For the total sample all elements display a slight minima at a depth of 305 mm. There is no geological evidence in the sediment column to suggest why this should be so.

3) Core RH2: In all cases, other than for iron, the elements studied all decreased in concentration between samples 8a and 8b, and then remained relatively constant in concentration before increasing in concentration at a depth of around 790 mm (the exact depth varied slightly from element to element). Iron often showed a marked increase in concentration across the modern-unit c sediment interface for all size fractions. A number of elements demonstrated a marked pattern of minima and maxima between 790-1060 mm, that does not match up with either organic content or changes in sediment type in a way that can be predicted. It is therefore assumed that the variation is due to anthropogenic activities.

4) Core 13.2: With the exception of lead and zinc, all elements were lowest in concentration at the top of the core, and highest at 100-180 mm depth. The concentration of lead changed little with depth in the total sample, while the concentration of zinc declined at a steady rate with depth. The clay size fraction departs from this pattern, notably for lead and zinc for which concentrations increased greatly at the top of the core. Only the concentrations of nickel and manganese do not increase at the top of the core.

2.4.4 Relationships Between Metal Concentrations

The significant metal to metal and metal to organic correlations are summarised in **Table 2.21**, in which correlations are ranked according to element, level of significance, core, and location. The correlations are, on the whole, well supported by the graphical comparison of change in concentration with depth for all elements and size

fractions. The following metal associations have been consistently found. Lead, zinc, and copper, by far the strongest grouping, being found in all cores and size fractions with the exception of 13.2 total. Rather less common associations are lead and chromium, copper and chromium, and iron and manganese. Minor associations occur between iron and chromium, manganese with both zinc and chromium, and zinc and copper with chromium. A selection of typical dendograms which portray these relationships pictorially were obtained by cluster analysis of the correlation coefficients and are presented in **Figures 13-17.**

As a general rule the correlation coefficients are of a higher significance, and of a greater frequency, in the clay and silt size fractions, and at the upstream (RH3) rather than downstream (RH2) end of the drain. Relatively few significant correlations are found at 13.2, and none at the 0.001 level.

2.4.5 Comparison of AAS and XRF Analytical Data

The concentrations of the elements Ba, Ce, Cr, La, Nb, Nd, Ni, Sr, V, Zn, and Zr were determined by XRF using the method described in Chapter VI. The results are presented in **Table 2.22.** Comparison of the XRF and AAS results are possible for Cr, Ni, and Zn.

Chromium values obtained by XRF are approximately 46% higher than those obtained by AAS. A number of the standards used to calibrate the XRF spectrometer also gave rather higher values than were recommended. It is thought that this may be partially due to the background correction used for this element. The value of σ/x (the coefficient of variation, cv) for the two sets of data also indicated that the AAS results were more consistent, with a cv = 27% c.f. 59.5% for XRF, despite the AAS values having a greater overall range. XRF results for nickel have a rather limited range (10-19 ppm c.f. 9-31 ppm for AAS), although in this case the concentrations obtained by AAS are considerably higher, averaging 17.3 ppm, compared with 12.6 ppm by XRF. In the case of zinc the average concentration obtained by AAS is some 23% lower than that obtained by XRF (172 compared with 211 ppm). The coefficient of variation though, is only 6% lower, despite having a smaller range (29-1388 c.f. 31-1833 ppm).

As nickel is present in low concentrations it seems likely that a combination of detection problems and matrix effects are responsible for the lack of variation in XRF results, the XRF method is more susceptible to matrix effects and has a higher detection limit than for AAS. In the case of zinc the metal concentrations are well above the detection limit, and therefore will not play a significant role in influencing the result obtained. The difference in the results may be due in part to experimental procedure, and partly the two different sets of matrix effects in operation.

Appendix A contains XRF results for major elements (with the exception of Na, which could not be reliably determined) from a selection of core samples, and two surface samples. No detailed analyses of these results has been made, their main purpose being as a comparison with AAS. Both iron and manganese by XRF gave a lower mean, cv, and more restricted range than results for the same samples by AAS. Manganese was particularily affected. A summary of the results gives: (x, cv, range) Fe by XRF (2.30, 23.3%, 1.70-3.24), by AAS (2.95, 28.0%, 1.95-4.40); Mn by XRF (400, 21.6%, 232-542), by AAS (533, 59%, 121-997). As standards run concurrently with these samples gave excellent results for both iron and manganese, bead preperation may have played a significant role in the reduction in sensitivity for the XRF Fe and Mn results.

Table 2.0 % sand, silt, and clay for core samples

sample	No.	% sand	% silt	% clay	type
RH3/3	1	55.1	38.3	2.9	silty sand
RH3/5	2	65.8	27.5	6.0	silty sand
RH3/8	3	52.6	36.7	9.1	silty sand
RH3/11	4	12.0	69.0	18.1	sandysilt
RH1/1	5	57.5	26.3	8.5	silty sand
RH1/3	6	57.3	28.0	8.9	silty sand
RH1/9	7	98	neg.	*	sand
RH1/14	8	98	neg.	*	sand
RH2/2	9	42.5	48.1	9.4	sandy silt
RH2/8a	10	42.6	49.2	8.2	sandy silt
RH2/8b	11	57.6	38.2	4.2	silty sand
RH2/16	12	39.7	52.9	6.2	sandy silt
RH2/19	13	15.5	72.3	10.6	sandy silt
RH2/21	14	83.3	16.2	0.5	silty sand
RH2/22	15	43.2	50.8	5.1	sandy silt
RH2/23	16	29.6	59.0	9.8	sandy silt
13.2/1	17	76	20	2	silty sand
13.2/3	18	56	38.6	4.4	sandy silt
13.2/5	19	51	42.6	5	silty sand
13.2/7	20	52.5	41.5	6	silty sand

neg. : negligible * : lost during separation

Table 2.1 Metal Concentration and % Organic Content for Core Samples (ppm)

sample	depth (mm)	Cu	Cr	Fe%	Mn	Ni	Pb	Zn	Org.
RH3/1	30-70 (50)	26.7	31.7	1.95	659	11.9	170	665	2.22
RH3/3	120-170 (145)	19.0	61.8	4.09	909	23.8	760	1388	9.74
RH3/3s		97.6	45.9	3.37	1079	13.0	518	1436	7.67
RH3/3z		177	63.6	4.43	1154	26.9	2933	1760	8.74
RH3/3c		162	165	11.20	2684	135	3296	6215	16.22
RH3/4	170-180 (175)	49.5	41.5	4.09	701	18.4	309	634	6.13
RH3/5	180-230 (210)	10.9	32.2	2.94	597	14.5	46.4	129	2.43
RH3/5s		11.7	23.3	2.63	833	6.8	38.8	109	1.67
RH3/5z		17.1	34.2	3.52	844	9.8	74.5	110	2.42
RH3/5c		120	75.7	6.54	1684	47.3	212	527	4.65
RH3/8	310-350 (330)	14.4	32.0	3.54	620	14.8	46.8	98.5	2.46
RH3/8s		6.2	26.5	2.72	862	7.0	19.3	96.5	1.84
RH3/8z		12.4	38.2	4.05	898	25.9	36.0	64.8	2.15
RH3/8c		51.7	75.2	6.29	1399	40.7	160	251	4.43
RH3/9	350-400 (375)	7.9	33.5	3.65	953	13.0	14.9	62.5	2.12
RH3/10	400-440 (420)	11.9	34.9	4.07	1154	16.5	22.2	88.9	3.02
RH3/11	460-520 (490)	9.6	32.5	3.60	997	19.3	16.2	84.4	3.39
RH3/11s		12.9	37.9	4.97	702	9.0	29.9	79.8	3.63
RH3/11z		13.0	41.6	5.30	635	25.0	31.2	45.7	2.23
RH3/11c		58.7	71.1	5.52	1651	40.9	42.7	171	4.43
RH1/1	0-180 (90)	25.0	34.0	2.47	269	31.0	138	217	4.44
RH1/1s		6.8	25.0	1.77	165	8.8	36.0	99.9	1.76
RH1/1z		19.9	47.1	3.13	854	10.5	112	285	3.30
RH1/1c		53.6	83.0	6.90	1245	31.1	297	747	9.48
RH1/3	205-240 (223)	21.0	28.0	2.40	339	30.0	108	173	3.67
RH1/3s		5.1	27.7	1.72	191	9.2	25.3	77.2	1.73
RH1/3z		12.0	39.6	3.82	692	9.9	73.5	222	2.79
RH1/3c		50.0	79.1	7.59	1242	24.8	29	644	11.37
RH1/6	290-320 (305)	9.0	23.0	2.30	439	27.0	51.0	64.0	1.92
RH1/9	395-430 (413)	6.0	24.0	1.51	256	22.0	58.0	35.0	1.44
RH1/9s		5.1	25.7	1.68	286	9.7	10.5	21.6	1.37
RH1/9z		-	-	-	-	-	-	-	-
RH1/9c		-	-	-	-	-	-	-	-
RH1/12	490-530 (510)	7.0	27.0	2.04	170	24.0	49.0	29.0	1.72

Table 2.1 Continued

sample	depth (mm)	Cu	Cr	Fe%	Mn	Ni	Pb	Zn	Org.
RH1/14	570-590 (580)	7.0	19.0	2.11	319	21.0	37.0	32.0	1.45
RH1/14s		4.7	21.2	1.74	139	10.0	10.7	19.0	1.27
RH1/14z		-	-	-	-	-	-	-	-
RH1/14c		-	-	-	-	-	-	-	-
RH2/2	45-85 (65)	15.2	48.6	3.52	875	7.3	151	146	3.84
RH2/2s		13.0	37.2	1.97	221	10.3	89.1	74.4	3.58
RH2/2z		11.1	39.4	3.47	954	7.3	22.7	82.2	1.95
RH2/2c		62.7	202	7.57	1120	42.9	244	528	8.93
RH2/8a	245-285 (265)	15.1	64.1	3.32	782	9.3	67.6	112	-
RH2/8as		19.9	41.6	2.13	265	11.2	17.4	39.9	2.63
RH2/8az		11.0	56.9	4.12	890	11.6	15.5	76.6	2.47
RH2/8ac		96.3	268	7.69	1585	63.3	151	413	8.35
RH2/8b	250-290 (270)	7.8	36.6	3.78	556	12.5	26.1	42.0	2.52
RH2/8bs		6.2	29.6	2.11	153	11.3	14.2	28.4	2.09
RH2/8bz		7.3	34.2	4.34	868	14.7	9.8	48.9	2.28
RH2/8bc		43.8	96.5	10.94	1329	39.3	55.1	276	6.42
RH2/16	560-600 (580)	8.4	33.4	3.28	600	14.3	28.6	38.0	2.55
RH2/16s		6.0	31.9	1.87	136	10.9	13.8	29.0	2.06
RH2/16z		7.0	33.7	3.72	767	11.2	12.1	42.3	1.91
RH2/16c		39.0	80.9	8.71	1521	58.2	85.1	170	5.88
RH2/19	680-740 (710)	10.4	36.6	2.84	1073	14.6	48.8	65.9	-
RH2/19s		6.9	36.0	1.89	145	11.3	14.1	29.8	2.51
RH2/19z		6.6	31.8	3.56	696	11.5	11.5	39.7	2.00
RH2/19c		31.9	77.9	7.19	1240	53.1	79.3	170	5.58
RH2/20	740-775 (758)	9.3	37.3	5.57	1090	9.3	42.3	57.2	2.69
RH2/21	775-810 (793)	7.0	37.4	3.70	835	11.7	32.8	50.6	-
RH2/21s		6.5	27.8	2.07	118	12.0	13.5	26.6	1.90
RH2/21z		9.3	35.4	4.16	994	15.1	9.3	49.6	2.15
RH2/21c		88.1	96.4	9.30	3071	102	152	282	7.51
RH2/22	810-850 (830)	12.2	47.2	4.40	795	17.4	43.0	59.5	2.18
RH2/22s		9.3	38.8	2.49	147	16.3	14.8	29.6	3.02
RH2/22z		9.0	37.8	4.26	745	15.7	12.6	50.4	2.45
RH2/22c		55.0	88.1	9.02	1097	65.7	122	216	6.95
RH2/23	850-890 (870)	17.7	52.5	5.61	694	19.2	49.4	75.7	3.00
RH2/23s		10.4	39.7	3.02	202	16.1	17.3	34.7	3.19
RH2/23z		10.6	36.7	3.86	1124	14.1	12.2	54.5	2.57
RH2/23c		41.5	86.6	8.08	1218	61.7	89.4	190	5.93

Table 2.1 Concluded

sample	depth (mm)	Cu	Cr	Fe%	Mn	Ni	Pb	Zn	Org.
RH2/27	1010-1050 (1030)	5.5	36.0	2.80	237	12.0	32.0	38.4	3.27
13.2/1	0-40 (20)	8.7	44.2	1.99	121	9.7	16.9	84.6	2.74
13.2/1s		6.2	29.5	1.09	76.7	7.6	28.3	47.2	2.34
13.2/1z		8.3	40.0	1.30	119	10.5	18.8	52.5	1.74
13.2/1c		71.8	205	4.31	789	35.9	187	664	9.77
13.2/3	80-120 (100)	17.1	50.7	2.67	119	16.1	16.7	74.2	3.23
13.2/3s		8.8	36.4	1.51	90.3	14.4	32.6	50.2	2.72
13.2/3z		7.4	38.7	1.52	83.0	12.1	5.7	30.2	1.94
13.2/3c		70.1	151	4.08	839	51.7	68.5	280	7.45
13.2/5	160-200 (180)	7.7	44.4	2.89	171	17.1	17.1	51.2	3.15
13.2/5s		7.8	29.8	1.52	109	13.7	23.6	34.1	2.51
13.2/5z		6.6	39.2	1.76	156	24.0	3.6	31.3	1.91
13.2/5c		48.2	116	4.19	861	48.2	38.6	200	7.05
13.2/7	240-280 (260)	8.6	47.5	2.85	167	14.0	11.1	43	3.14
13.2/7s		6.9	31.5	1.56	95.9	12.6	28.5	31.5	2.57
13.2/7z		7.6	36.9	1.71	168	16.6	5.4	31.8	1.93
13.2/7c		40.7	114	4.35	849	44.8	40.7	129	5.34

Significant values of r for the tables below are as follows:

n	n-2	p =	0.1	0.05	0.01	0.001
4	2	r =	0.988	0.997	1.000	1.000
6	4		0.729	0.811	0.917	0.974
8	6		0.622	0.707	0.834	0.925
7	5		0.669	0.755	0.875	0.951
10	8		0.549	0.632	0.765	0.872
18	16		0.400	0.468	0.590	0.708
20	18		0.378	0.444	0.561	0.679
25	23		0.338	0.398	0.507	0.619
28	25		0.318	0.375	0.479	0.589

Table 2.3 Correlation Coefficients for Core RH3 Totals n = 8

	Cu	Cr	Fe	Mn	Ni	Pb	Zn	Org.
Cu	1.000							
Cr	0.256	1.000						
Fe	0.053	0.487	1.000					
Mn	-0.383	0.175	0.544	1.000				
Ni	0.158	0.827	0.672	0.354	1.000			
Pb	0.401	0.964	0.280	-0.024	0.734	1.000		
Zn	0.472	0.882	0.078	-0.097	0.606	0.971	1.000	
Org.	0.403	0.971	0.531	0.134	0.891	0.948	0.867	1.000

Table 2.4 Correlation Coefficients for Core RH3 Sand n = 4

	Cu	Cr	Fe	Mn	Ni	Pb	Zn	Org.
Cu	1.000							
Cr	0.861	1.000						
Fe	8.5×10^{-3}	0.566	1.000					
Mn	0.871	-0.465	-0.465	1.000				
Ni	0.950	0.956	0.314	0.692	1.000			
Pb	0.999	0.796	-0.032	0.892	0.938	1.000		
Zn	0.997	0.789	-0.049	0.902	0.933	1.000	1.000	
Org.	0.958	0.947	0.287	0.712	1.000	0.947	0.943	1.000

Table 2.5 Correlation Coefficients for Core RH3 Silt n = 4

	Cu	Cr	Fe	Mn	Ni	Pb	Zn	Org.
Cu	1.000							
Cr	0.968	1.000						
Fe	0.077	0.311	1.000					
Mn	0.850	0.736	-0.388	1.000				
Ni	0.388	0.582	0.669	0.216	1.000			
Pb	1.000	0.970	0.083	0.850	0.399	1.000		
Zn	1.000	0.965	0.065	0.857	0.384	1.000	1.000	
Org.	1.000	0.967	0.076	0.847	0.380	1.000	1.000	1.000

Table 2.6 Correlation Coefficients for Core RH3 Clay n = 4

	Cu	Cr	Fe	Mn	Ni	Pb	Zn	Org.
Cu	1.000							
Cr	0.824	1.000						
Fe	0.861	0.992	1.000					
Mn	0.878	0.970	0.954	1.000				
Ni	0.848	0.999	0.991	0.982	1.000			
Pb	0.828	1.000	0.992	0.972	0.999	1.000		
Zn	0.839	0.999	0.992	0.978	1.000	1.000	1.000	
Org.	0.823	0.999	0.998	0.977	0.999	0.999	0.999	1.000

Table 2.7 Correlation Coefficients for Core RH1 Totals n = 6

	Cu	Cr	Fe	Mn	Ni	Pb	Zn	Org.
Cu	1.000							
Cr	0.818	1.000						
Fe	0.731	0.453	1.000					
Mn	0.094	-0.330	0.394	1.000				
Ni	0.912	0.805	0.786	0.254	1.000			
Pb	0.972	0.892	0.571	-0.034	0.876	1.000		
Zn	0.997	0.816	0.709	0.133	0.919	0.978	1.000	
Org.	0.997	0.878	0.725	0.056	0.924	0.979	0.994	1.000

Table 2.8 Correlation Coefficients for Core RH1 Sand n = 4

	Cu	Cr	Fe	Mn	Ni	Pb	Zn	Org.
Cu	1.000							
Cr	0.253	1.000						
Fe	0.635	-0.336	1.000					
Mn	-0.539	-0.171	-0.810	1.000				
Ni	-0.857	-0.568	-0.569	0.783	1.000			
Pb	0.867	0.432	0.696	-0.852	-0.986	1.000		
Zn	0.805	0.521	0.628	-0.862	-0.990	0.991	1.000	
Org.	0.703	0.691	0.448	-0.797	-0.968	0.938	0.974	1.000

Table 2.9 Correlation Coefficients for Core RH2 Totals n = 10

	Cu	Cr	Fe	Mn	Ni	Pb	Zn	Org.
Cu	1.000							
Cr	0.834	1.000						
Fe	0.399	0.187	1.000					
Mn	0.334	0.127	0.327	1.000				
Ni	0.160	-0.051	0.290	-0.167	1.000			
Pb	0.597	0.470	-0.074	0.304	-0.502	1.000		
Zn	0.757	0.722	-0.013	0.368	-0.455	0.937	1.000	
Org.	0.287	0.289	-0.267	-0.078	-0.550	0.766	0.718	1.000

n = 7 for organic

Table 2.10 Correlation Coefficients for Core RH2 Sand n = 8

	Cu	Cr	Fe	Mn	Ni	Pb	Zn	Org.
Cu	1.000							
Cr	0.757	1.000						
Fe	0.140	0.454	1.000					
Mn	0.941	0.756	0.210	1.000				
Ni	-0.162	0.307	0.866	-0.183	1.000			
Pb	0.319	0.199	-0.197	0.430	-0.324	1.000		
Zn	0.505	0.364	-0.137	0.611	-0.333	0.976	1.000	
Org.	0.500	0.761	0.444	0.598	0.328	0.674	0.733	1.000

Table 2.11 Correlation Coefficients for Core RH2 Silt n = 8

	Cu	Cr	Fe	Mn	Ni	Pb	Zn	Org.
Cu	1.000							
Cr	0.665	1.000						
Fe	-2.9×10^{-4}	0.218	1.000					
Mn	-0.699	0.174	0.066	1.000				
Ni	-0.221	-0.199	0.824	0.063	1.000			
Pb	0.615	0.408	-0.558	0.140	-0.828	1.000		
Zn	0.851	0.737	-0.149	0.413	-0.565	0.847	1.000	
Org.	0.458	0.455	0.642	0.402	0.605	-0.220	0.146	1.000

Table 2.12 Correlation Coefficients for Core RH2 Clay n = 8

	Cu	Cr	Fe	Mn	Ni	Pb	Zn	Org.
Cu	1.000							
Cr	0.670	1.000						
Fe	-0.050	-0.384	1.000					
Mn	0.591	-0.062	0.248	1.000				
Ni	0.543	-0.205	0.301	0.911	1.000			
Pb	0.586	0.634	-0.472	0.130	2.4×10^{-3}	1.000		
Zn	0.612	0.849	-0.203	3.0×10^{-4}	-0.209	0.817	1.000	
Org.	0.789	0.828	-0.175	0.172	0.045	0.878	0.943	1.000

Table 2.13 Correlation Coefficients for Core 13.2 Totals n = 4

	Cu	Cr	Fe	Mn	Ni	Pb	Zn	Org.
Cu	1.000							
Cr	0.884	1.000						
Fe	0.049	0.348	1.000					
Mn	-0.648	-0.331	0.728	1.000				
Ni	0.297	0.398	0.892	0.465	1.000			
Pb	0.242	-0.221	-0.386	-0.486	0.053	1.000		
Zn	0.413	0.010	-0.855	-0.942	-0.555	0.669	1.000	
Org.	0.444	0.917	0.917	0.393	0.925	-0.235	-0.598	1.000

Table 2.14 Correlation Coefficients for Core 13.2 Sand n = 4

	Cu	Cr	Fe	Mn	Ni	Pb	Zn	Org.
Cu	1.000							
Cr	0.793	1.000						
Fe	0.659	0.440	1.000					
Mn	0.457	-0.064	0.802	1.000				
Ni	0.868	0.598	0.943	0.761	1.000			
Pb	0.325	0.827	-0.023	-0.587	0.073	1.000		
Zn	0.237	0.501	-0.524	-0.704	-0.262	0.681	1.000	
Org.	0.876	0.890	0.800	0.374	0.884	0.530	0.076	1.000

Table 2.15 Correlation Coefficients for Core 13.2 Silt n = 4

	Cu	Cr	Fe	Mn	Ni	Pb	Zn	Org.
Cu	1.000							
Cr	0.149	1.000						
Fe	-0.839	-0.617	1.000					
Mn	-0.292	-0.460	0.645	1.000				
Ni	-0.881	-0.178	0.867	0.682	1.000			
Pb	0.857	0.598	-0.911	-0.279	-0.683	1.000		
Zn	0.784	0.631	-0.840	-0.156	-0.555	0.987	1.000	
Org.	-0.709	-0.692	0.804	0.129	0.472	-0.965	-0.994	1.000

Table 2.16 Correlation Coefficients for Core 13.2 Clay n = 4

	Cu	Cr	Fe	Mn	Ni	Pb	Zn	Org.
Cu	1.000							
Cr	0.864	1.000						
Fe	-0.417	0.085	1.000					
Mn	-0.731	-0.971	-0.313	1.000				
Ni	-0.227	-0.686	-0.758	0.818	1.000			
Pb	0.738	0.976	0.279	-0.989	-0.825	1.000		
Zn	0.782	0.979	0.176	-0.962	-0.771	0.990	1.000	
Org.	0.847	0.930	-0.076	-0.847	-0.591	0.907	0.956	1.000

Table 2.17 Correlation Coefficients for All Cores: Totals n = 28

	Cu	Cr	Fe	Mn	Ni	Pb	Zn	Org.
Cu	1.000							
Cr	0.218	1.000						
Fe	0.150	0.461	1.000					
Mn	0.100	0.181	0.668	1.000				
Ni	0.214	-0.350	-0.279	-0.313	1.000			
Pb	0.499	0.391	0.151	0.208	0.265	1.000		
Zn	0.571	0.360	0.109	0.215	0.193	0.960	1.000	
Org.	0.535	0.630	0.297	0.236	0.205	0.896	0.841	1.000

n = 25 for organic

Table 2.18 Correlation Coefficients for All Cores: Sand n = 20

	Cu	Cr	Fe	Mn	Ni	Pb	Zn	Org.
Cu	1.000							
Cr	0.580	1.000						
Fe	0.389	0.430	1.000					
Mn	0.631	0.221	0.698	1.000				
Ni	0.177	0.559	-0.003	-0.287	1.000			
Pb	0.981	0.498	0.320	0.600	0.139	1.000		
Zn	0.983	0.464	0.351	0.635	0.116	0.991	1.000	
Org.	0.910	0.796	0.494	0.530	0.365	0.895	0.868	1.000

Table 2.19 Correlation Coefficients for All Cores: Silt n = 18

	Cu	Cr	Fe	Mn	Ni	Pb	Zn	Org.
Cu	1.000							
Cr	0.738	1.000						
Fe	0.242	0.182	1.000					
Mn	0.365	0.259	0.819	1.000				
Ni	0.465	0.319	0.247	0.027	1.000			
Pb	0.998	0.724	0.222	0.340	0.467	1.000		
Zn	0.993	0.749	0.230	0.369	0.416	0.991	1.000	
Org.	0.983	0.764	0.304	0.436	0.423	0.977	0.991	1.000

Table 2.20 Correlation Coefficients for All Cores: Clay n = 18

	Cu	Cr	Fe	Mn	Ni	Pb	Zn	Org.
Cu	1.000							
Cr	0.402	1.000						
Fe	0.298	-0.079	1.000					
Mn	0.635	-0.058	0.623	1.000				
Ni	0.665	0.171	0.625	0.780	1.000			
Pb	0.754	0.219	0.466	0.534	0.735	1.000		
Zn	0.762	0.244	0.448	0.512	0.712	0.998	1.000	
Org.	0.575	0.449	0.359	0.306	0.463	0.783	0.804	1.000

Table 2.21 Significant Correlations Ranked by Location, Element, and Degree of Significance

total samples																									
surface*					RH3					RH1					RH2					13.2					
0.001	0.01	0.02	0.05	0.1	0.001	0.01	0.02	0.05	0.1	0.001	0.01	0.02	0.05	0.1	0.001	0.01	0.2	0.05	0.1	0.001	0.01	0.02	0.05	0.1	
Pb-Cu Pb-Cr Pb-Ni	Pb-Zn Pb-Fe			Pb-Mn	Pb-Zn Pb-Org Pb-Cr			Pb-Ni		Pb-Zn Pb-Org	Pb-Cu	Pb-Cr	Pb-Ni		Pb-Zn			Pb-Org	Pb-Cu						Pb
Mn Zn Zn-Cu	Pb-Zn Zn-Cr Zn-Cr Zn-Ni	Zn-Fe			Pb-Zn Zn-Cu	Zn-Org				Pb-Zn Zn-Org	Zn-Ni	Zn-Cr	Zn-Cr		Pb-Cr		Zn-Cu		Zn-Org						Zn-
Pb-Cu Cu-Ni	Zn-Cu Cu-Cr			Cu-Fe						Zn-Cu Cu-Org	Pb-Cu	Cu-Ni	Cu-Cr	Cu-Fe		Cu-Cr	Zn-Cu		Pb-Cu						Cu
Org					Pb-Org Org-Cr	Zn-Org Org-Ni				Pb-Org Zn-Org	Org-Ni	Cu-Org	Org-Cr					Pb-Org	Zn-Org					Org-Fe Org-Ni	
Pb-Cr Cr-Fe Cr-Ni	Zn-Cr Cu-Cr				Org-Cr Pb-Cr	Zn-Cr	Cr-Ni					Pb-Cr	Zn-Cr Cu-Cr Org-Cr			Cu-Cr	Zn-Cr								Cr
Pb-Ni Cu-Ni Cr-Ni	Zn-Ni Ni-Fe					Org-Ni	Cr-Ni	Pb-Ni	Ni-Fe		Zn-Ni Org-Ni	Cu-Ni	Pb-Ni	Ni-Fe										Org-Ni	Ni
Cr-Fe	Pb-Fe Ni-Fe	Zn-Fe		Cu-Fe Mn-Fe					Ni-Fe					Cu-Fe Ni-Fe										Org-Fe	Fe
				Fe-Mn Pb-Mn																				-Zn-Mn	Mn

*Included here for ease of comparison with other samples, refer to Chapter 3.

Table 2.21 continued

sand samples																					
RH3					RH1					RH2					13.2						
0.001	0.01	0.02	0.05	0.1	0.001	0.01	0.02	0.05	0.1	0.001	0.01	0.02	0.05	0.1	0.001	0.01	0.02	0.05	0.1	
Pb-Zn Pb-Cu				Pb-Org Pb-Ni		Pb-Zn	-Pb-Ni		Pb-Org	Pb-Zn				Pb-Org	Pb-Zn				Pb-Org	Pb
Pb-Zn	Zn-Cu			Zn-Ni Zn-Mn Zn-Org		Pb-Zn	-Zn-Ni	Zn-Org		Pb-Zn			Zn-Org							Zn
Pb-Cu	Zn-Cu		Cu-Org	Cu-Ni						Cu-Mn			Cu-Cr							Cu
Org-Ni			Cu-Org	Pb-Org Org-Cr Zn-Org				Zn-Org -Org-Ni	Pb-Org				Zn-org Org-Cr	Pb-Org						Org
			Cr-Ni	Org-Cr									Cu-Cr Org-Cr							Cr
Org-Ni			Cr-Ni	Pb-Ni Zn-Ni Cu-Ni			-Pb-Ni -Zn-Ni	-Org-Ni			Ni-Fe									Ni-Fe	Ni
											Ni-Fe									Ni-Fe	Fe
				Zn-Mn						Cu-Mn											Mn

Table 2.21 continued

silt samples																				
RH3					RH1					RH2					13.2					
0.001	0.01	0.02	0.05	0.1	0.001	0.01	0.02	0.05	0.1	0.001	0.01	0.02	0.05	0.1	0.001	0.01	0.02	0.05	0.1	
Pb-Zn Pb-Cu Pb-Org			Pb-Cr								Pb-Zn	-Pb-Ni					Pb-Zn	Pb-Org	Pb-Fe	Pb
Pb-Zn Zn-Cu Zn-Org			Zn-Cr								Pb-Zn Zn-Cu		Zn-Cr			-Zn-Org	Pb-Zn			Zn
Pb-Cu Zn-Cu Cu-Org			Cu-Cr								Zn-Cu			Cu-Cr -Cu-Mn Cu-Org						Cu
Pb-Org Zn-Org Cu-Org			Org-Cr											Cu-Org		-Org-Zn		Org-Pb		Org
			Pb-Cr Zn-Cr Cu-Cr Org-Cr										Zn-Cr	Cu-Cr						Cr
												-Pb-Ni Ni-Fe								Ni
												Ni-Fe							-Pb-Fe	Fe
														-Cu-Mn						Mn

Table 2.21 continued

clay samples																				
RH3					RH1					RH2					13.2					
0.001	0.01	0.02	0.05	0.1	0.001	0.01	0.02	0.05	0.1	0.001	0.01	0.02	0.05	0.1	0.001	0.01	0.02	0.05	0.1	
Pb-Zn Pb-Org Pb-Cr Pb-Ni	Pb-Fe		Pb-Mn								Pb-Org	Pb-Zn		Pb-Cr		Pb-Zn	-Pb-Mn	Pb-Cr	Pb-Org	Pb
Pb-Zn Zn-Ni Zn-Cr Zn-Org	Zn-Fe		Zn-Fe							Zn-Org	Zn-Cr	Pb-Zn				Pb-Zn		Zn-Cr -Zn-Mn Zn-Org		Zn
													Cu-Org							Cu
Pb-Org Zn-Org Org-Cr Org-Ni		Org-Fe	Org-Mn							Zn-Org	Pb-Org	Org-Cr	Cu-Org					Zn-Org	Pb-Org Org-Cr	Org
Pb-Cr Zn-Cr Org-Cr Cr-Ni	Cr-Fe		Cr-Mn								Zn-Cr	Org-Cr		Pb-Cr				Pb-Cr -Cr-Mn Zn-Cr	Org-Cr	Cr
Pb-Ni Zn-Ni Org-Ni Cr-Ni	Ni-Fe	Ni-Mn									Ni-Mn									Ni
	Pb-Fe Zn-Fe Cr-Fe Ni-Fe	Org-Fe	Fe-Mn																	Fe
		Ni-Mn	Pb-Mn Zn-Mn Org-Mn Cr-Mn Fe-Mn								Ni-Mn						-Pb-Mn	-Zn-Mn -Cr-Mn		Mn

Table 2.21 concluded

all samples																				
all totals					all sand					all silt					13.2					
0.001	0.01	0.02	0.05	0.1	0.001	0.01	0.02	0.05	0.1	0.001	0.01	0.02	0.05	0.1	0.001	0.01	0.02	0.05	0.1	
Pb-Zn Pb-Org	Pb-Cu		Pb-Cr		Pb-Zn Pb-Cu Pb-Org	Pb-Mn		Pb-Cr		Pb-Cu Pb-Zn Pb-Org Pb-Cr				Pb-Ni	Pb-Zn Pb-Org Pb-Cu Pb-Ni			Pb-Mn	Pb-Fe	Pb
Pb-Zn Zn-Org	Zn-Cu			Zn-Cr	Pb-Zn Zn-Cu Zn-Org	Zn-Mn		Zn-Cr		Pb-Zn Zn-Cu Zn-Org Zn-Cr				Zn-Ni	Pb-Zn Zn-Org Zn-Cu Zn-Ni			Zn-Mn	Zn-Fe	Zn
	Pb-Cu Zn-Cu Cu-Org				Pb-Cu Zn-Cu	Cu-Cr Cu-Mn			Cu-Fe	Pb-Cu Zn-Cu Cu-Org Cu-Cr				Cu-Ni	Pb-Cu Zn-Cu	Cu-Ni Cu-Mn	Cu-Org		Cu-Cr	Cu
Pb- Org Zn-Org Org-Cr	Cu-Org				Pb-Org Zn-Org Cu-Org Org-Cr		Org-Mn	Org-Fe		Pb-Org Zn-Org Cu-Org Org-Cr				Org-Ni Org-Mn	Pb-Org Zn-Org		Org-Cu		Org-Cr Org-Ni	Org
Org-Cr		Cr-Fe	Pb-Cr	Zn-Cr -Cr-Ni	Org-Cr	Cu-Cr	Cr-Ni	Zn-Cr Pb-Cr		Pb-Cr Zn-Cr Org-Cr Cu-Cr									Cu-Cr Org-Cr	Cr
				-Cr-Ni			Cr-Ni							Pb-Ni Zn-Ni Cu-Ni Org-Ni	Pb-Ni Zn-Ni Ni-Mn	Cu-Ni Ni-Fe			Org-Ni	Ni
Fe-Mn		Cr-Fe			Fe-Mn			Org-Fe	Cu-Fe	Fe-Mn						Ni-Fe Fe-Mn			Pb-Fe Zn-Fe	Fe
Fe-Mn					Fe-Mn	Pb-Mn Zn-Mn Cu-Mn	Org-Mn			Fe-Mn				Org-Mn	Ni-Mn	Cu-Mn Fe-Mn		Pb-Mn Zn-Mn		Mn

Table 2.22 Metal Concentration by XRF for Core Samples

sample	element concentration (ppm)										
	Ba	Ce	Cr	La	Nb	Nd	Ni	V	Zn	Zr	Sr
RH3/1	563	52	38	23	9	32	11	55	37	175	283
RH3/3	665	84	128	35	10	37	19	70	1833	172	233
RH3/4	580	69	71	34	13	44	15	64	832	187	263
RH3/5	596	61	46	32	12	42	10	55	155	269	275
RH3/8	598	75	41	32	12	34	11	68	87	210	265
RH3/9	591	55	36	30	11	39	11	64	66	181	274
RH3/10	586	72	54	34	13	38	12	75	106	199	250
RH3/11	568	73	47	33	13	32	14	82	67	210	247
RH1/1	565	56	49	27	10	33	12	67	301	187	260
RH1/3	580	63	47	33	13	37	12	63	250	204	269
RH1/6	607	53	35	28	10	31	13	52	57	191	285
RH1/9	596	48	29	19	9	30	11	50	38	126	291
RH1/12	618	69	32	27	10	33	11	62	43	184	287
RH1/14	575	50	35	26	10	32	11	55	37	175	283
RH2/2	512	72	63	33	13	35	12	60	175	276	280
RH2/8b	581	63	40	33	11	33	11	60	54	230	267
RH2/16	563	81	44	34	14	39	13	71	50	237	263
RH2/19	542	69	44	35	13	38	15	71	57	220	258
RH2/20	596	69	39	29	11	35	11	63	46	227	266
RH2/22	593	77	43	39	14	44	17	77	59	260	240
RH2/23	560	82	53	43	16	49	14	83	68	254	232
RH2/27	610	62	37	32	11	45	11	56	31	337	281
13.2/1	553	54	42	24	10	36	10	41	90	425	340
13.2/3	532	67	59	29	11	36	13	64	117	292	278
13.2/5	527	64	49	35	12	37	15	64	66	271	268
13.2/7	587	73	43	28	12	40	13	63	47	262	267

Figure 2 Catchment Area of the City Outfall Drain, and Location of Sampling Sites

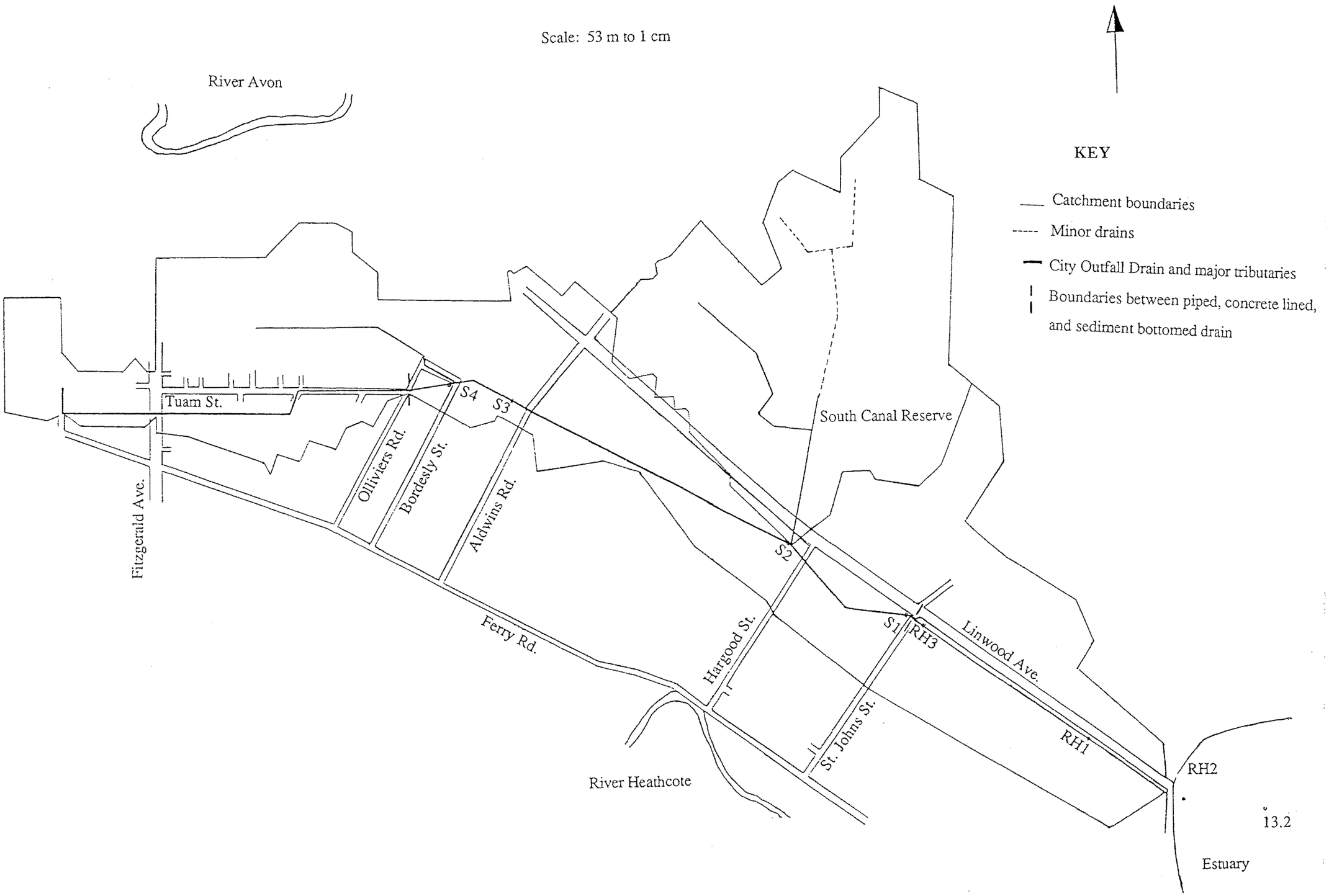

Figure 3 CORE RH3

The cross hatched area represents material lost during removal of water from the core or discarded due to contamination.

Verticle scale 1:3

Very organic rich dark grey/green silty med. to coarse sand. Percentage sand increases upwards. Solitary small rounded pebble at base of layer. Strong odour of oil, three small (3-5 mm) bivavle halves.

Brown silt, soft and plastic. One small pebble

Med. grey silt with irregular med. to fine sand inclusions (3-6 mm diameter), grading upwards into fine grey silty sand with med. sand inclusions.

Fine-medium grey sand with irregular silt bands. Has burrowed contact with underlying layer

Very uniform grey silt, One med. to fine sand inclusion.

Estimated compression 20-35 % largely in top 20 cm.

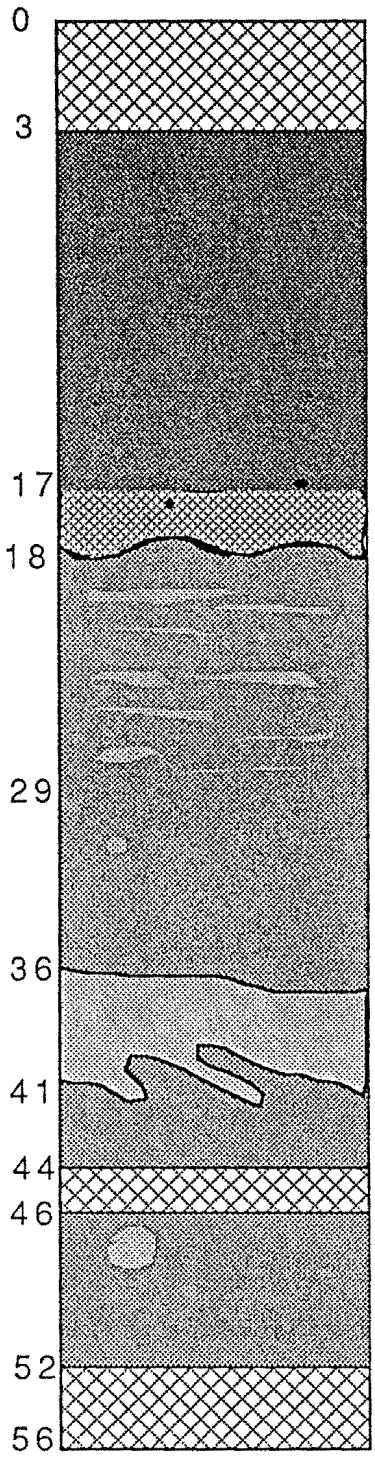

Figure 4 CORE RH1

Verticle scale 1:3

Black fine sand. Fines upwards to silty sand with common organic debris - plant, algae, snails, e.t.c. Very high water content, on opening of core loss of verticle definition made it necessary to treat the top 18 cm as one subsample (RH1/1).

Black-grey medium to fine silty sand.

Brown-green silty fine-v. fine sand.

Dark grey sand with light brown-grey silty sand bands 0.5-1 cm thick

Grey sand - has a creamy grey appearence when wet. Traces of decomposed organic material.

Silty lenses approx. 0.5 cm thick in grey med. sand matrix. Laminations of decoposed organic material.

Very clean med.-fine dark grey sand.

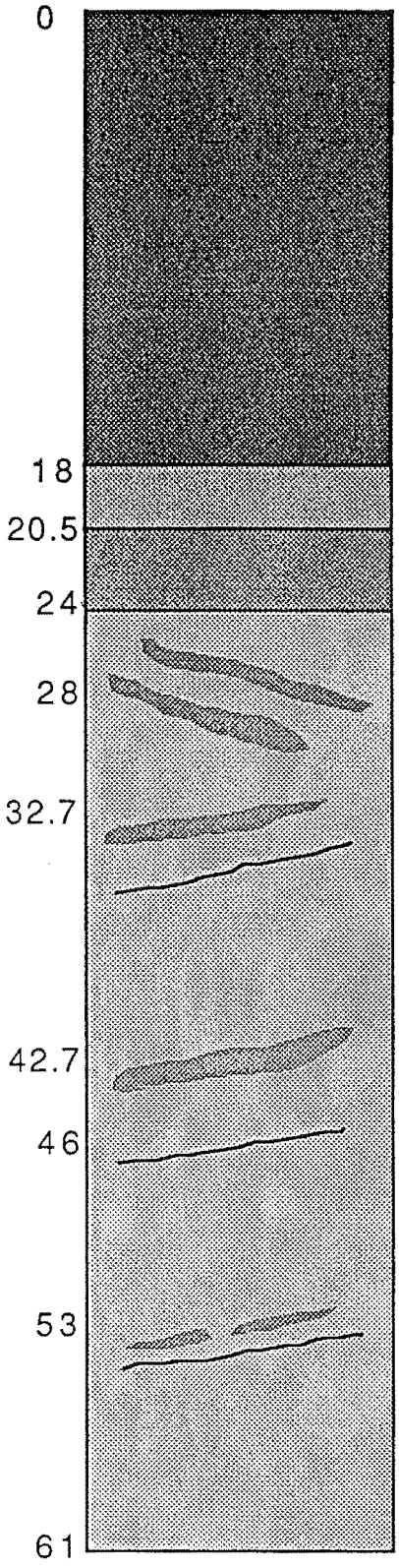

Figure 5 CORE RH2

Verticle scale 1:3

"Modern Sediments"

Very dark grey muddy fine to medium sand becoming black at the surface. Small number of 'cockle' shells, often brittle and badly corroded. Three live specimans were recovered from the pit dug to retrieve the core.

Fragments of sticks, cockle shells, and snail (amphibola crenata) were found at lower levels

Unit c

No evidence of bioturbation on the moder-unit c boundary.

uniform light grey silty sand passing into sandy silt and back without any obvious layering

Traces of plant matter. Fragment of thick, white opaque glass found at a depth of 42 cm indicating that this sediment is post european in origion.

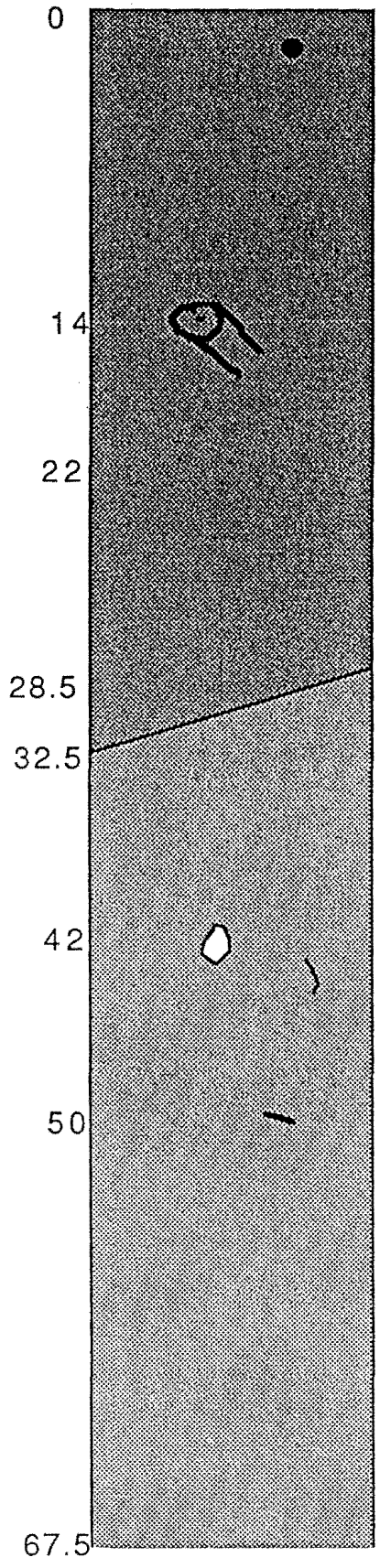

Light grey mud. Very clayey and cohesive.

muddy sand- faint organic bands. becomes sandier at the bottom of the bed.

green-grey fine sandy, fine to very fine silt.

Unit b

Dark grey sand fining slightly towards a shrp unit c-unit b interface.

upper few centimetres banded by 0.5-1 cm silty layers, with red-brown traces of organic material. Bottom few centimetres has very fine silt banding 0.5-1.5 cm in thickness.

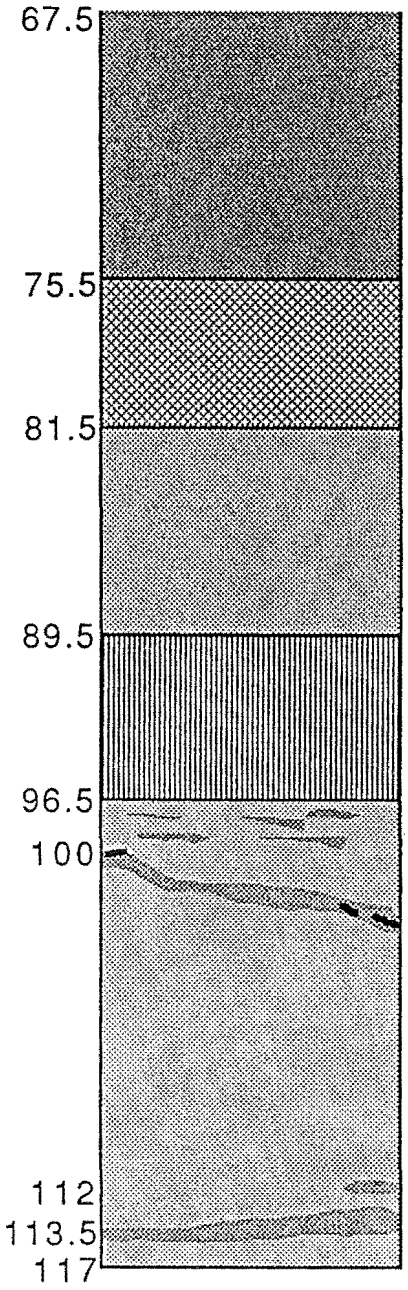

Figure 6 CORE 13.2

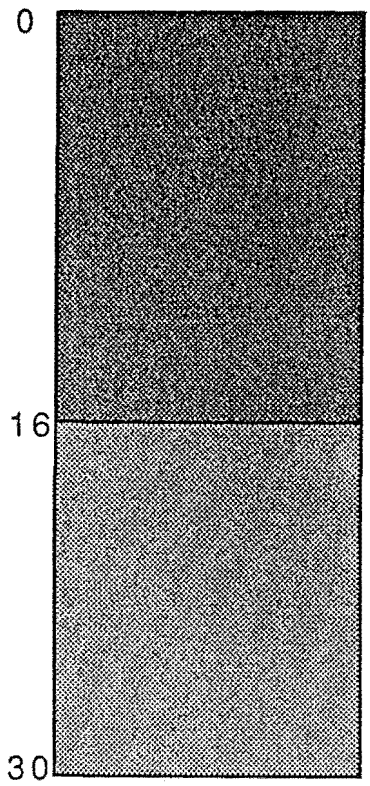

Vertical scale 1:3

Little information was available about this core. The top 16 cm is recorded as being moderately dark in colour and of medium "grainsize".

The bottom 14 cm were described as light in colour and slightly finer than above.

The upper layer most probably represents modern sediments, and the lower layer the top of unit c.

Figure 7 The Folk, Andrews, Lewis Classification of Non-Gravel Bearing Sediments

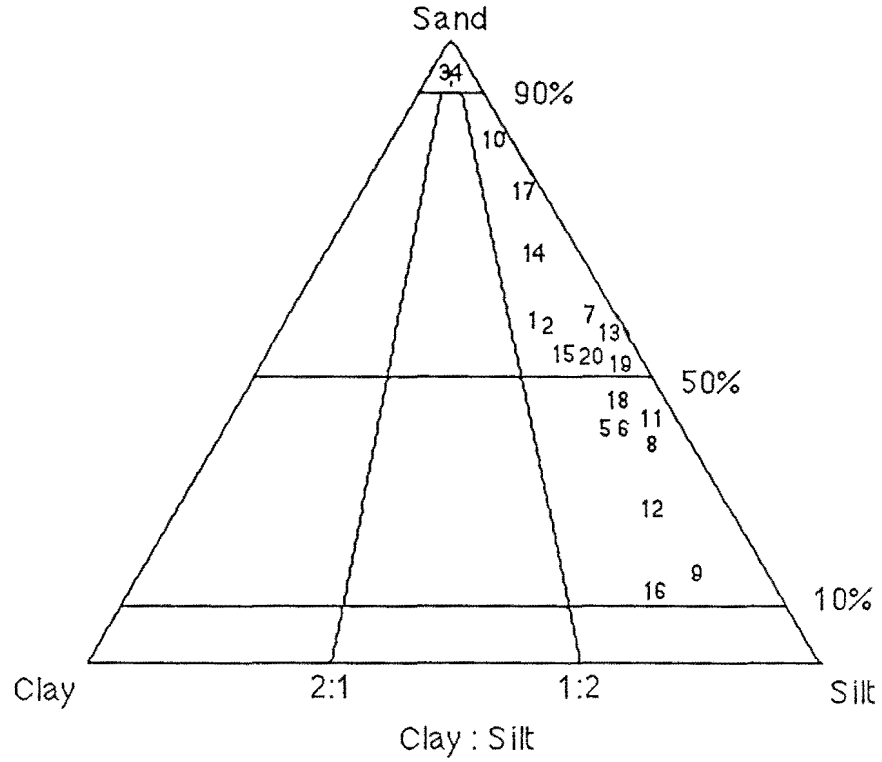

S = sand
cS = clayey sand
mS = muddy sand
zS = silty sand
sC = sandy clay
sM = sandy mud
sZ = sandy silt
C = clay
M = mud
Z = silt

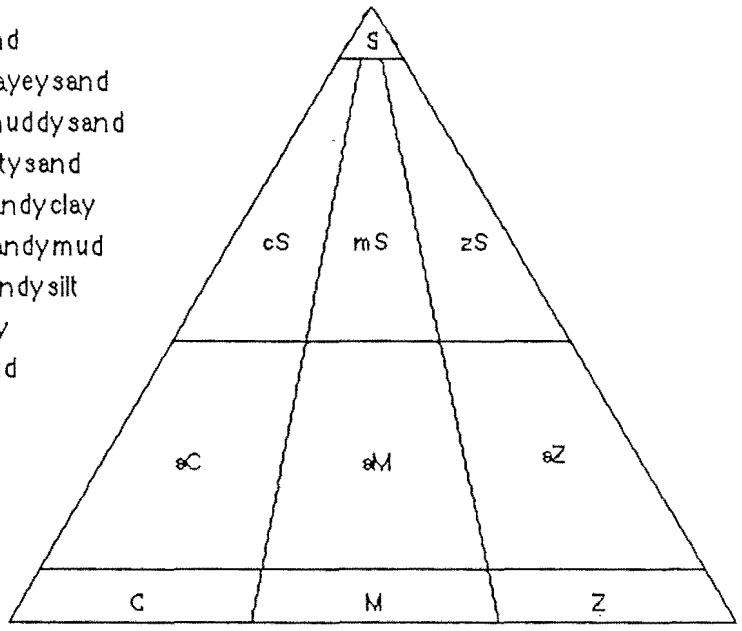

Figure 8 Depth versus Concentration in Total Samples

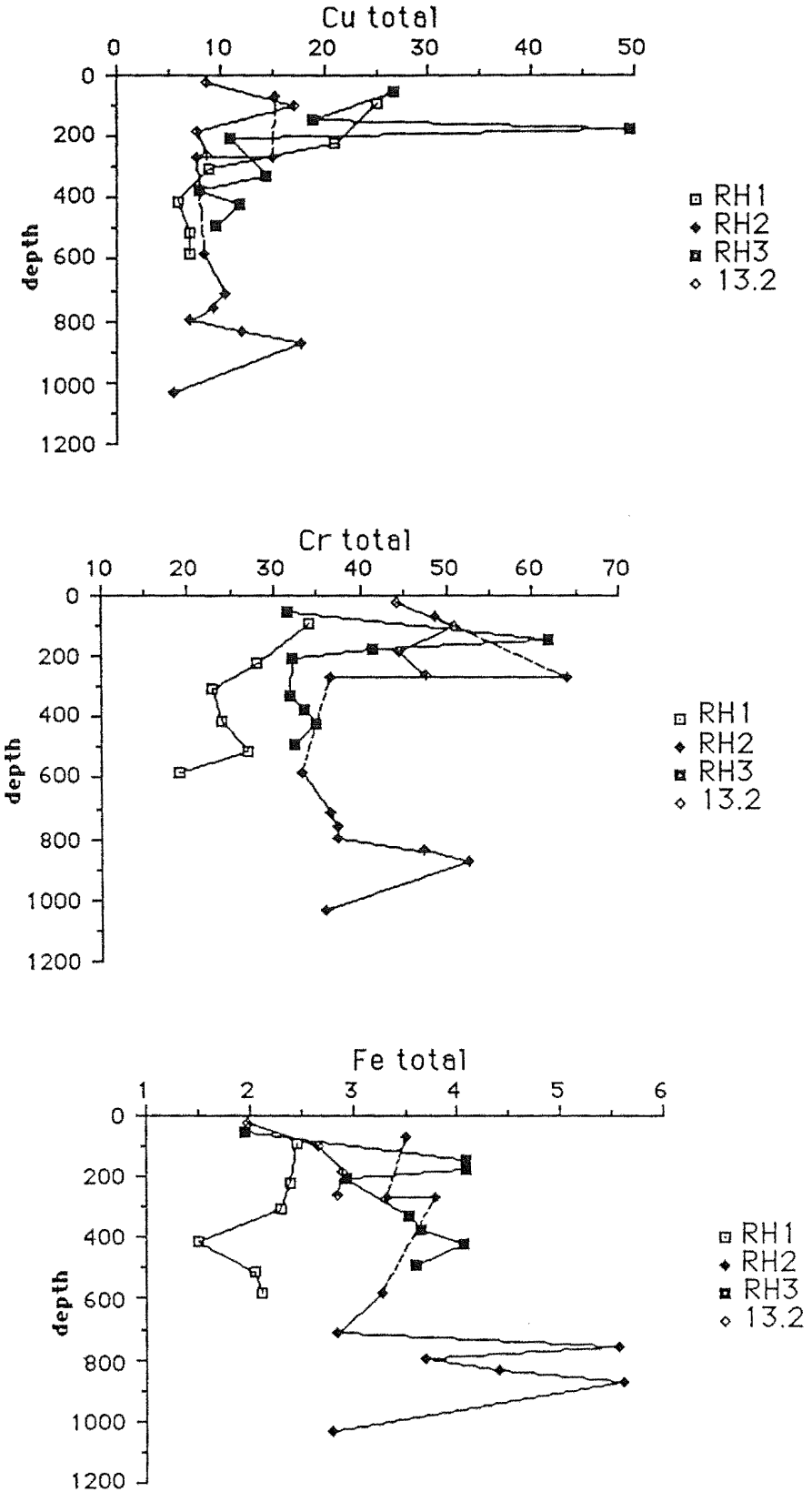

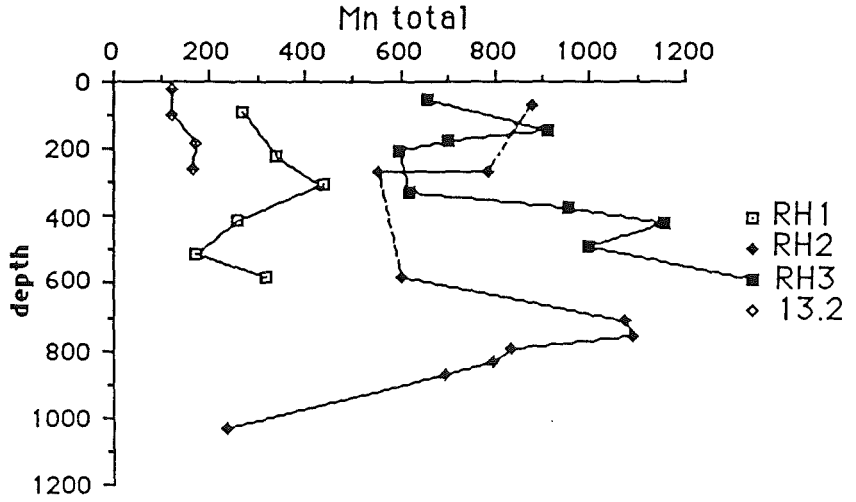
Mn total
0
200
400
600
800
1000
1200
depth
RH1
RH2
RH3
13.2

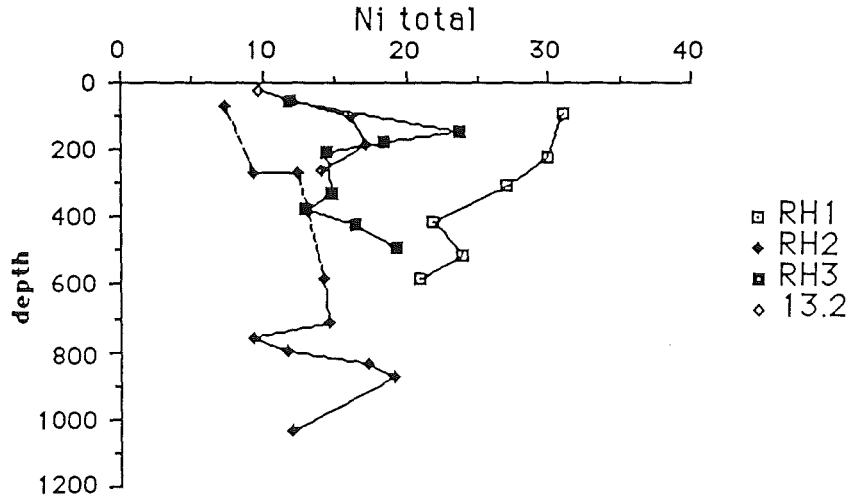
Ni total
0
10
20
30
40
depth
RH1
RH2
RH3
13.2

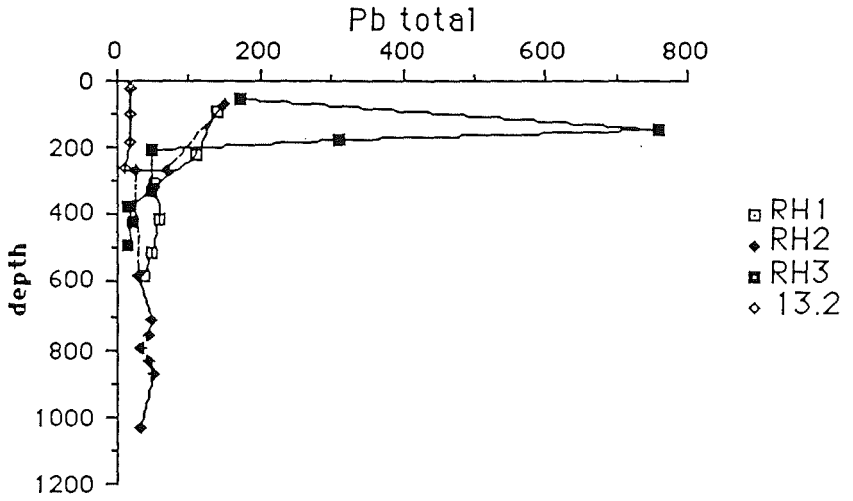
Pb total
0
200
400
600
800
depth
RH1
RH2
RH3
13.2

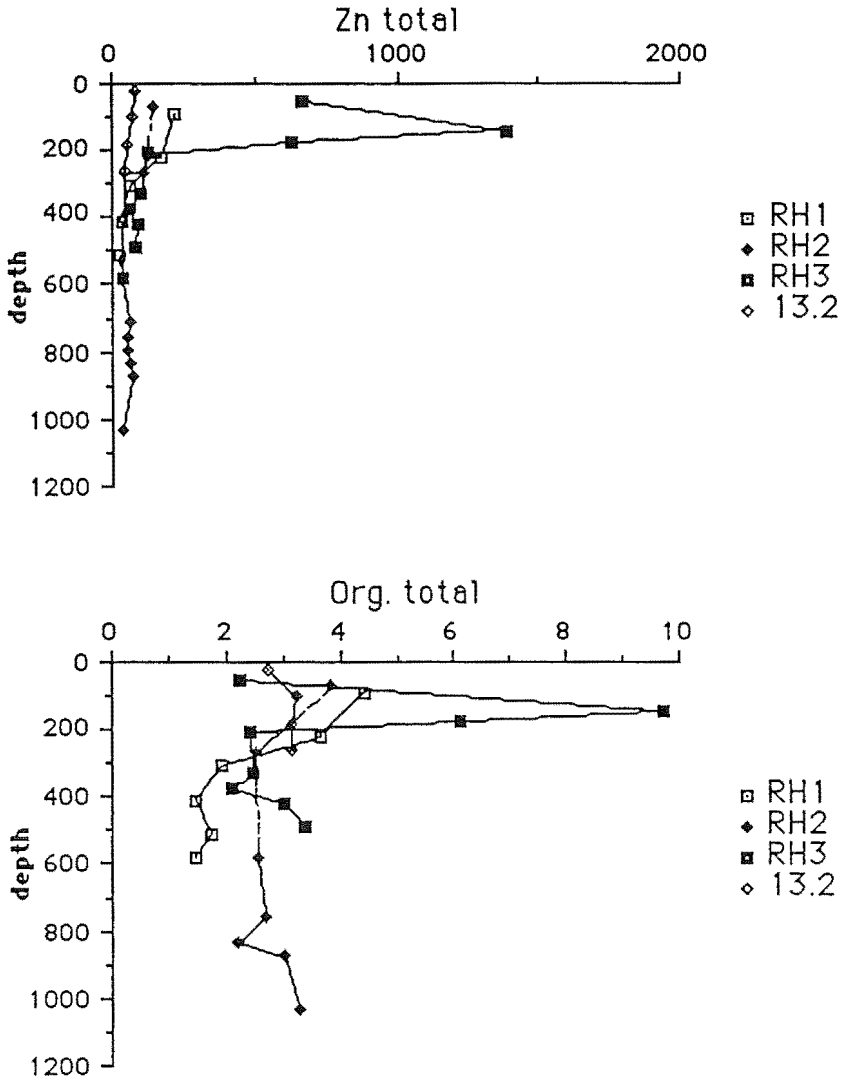

Figure 9 Depth versus Concentration in Sand Samples

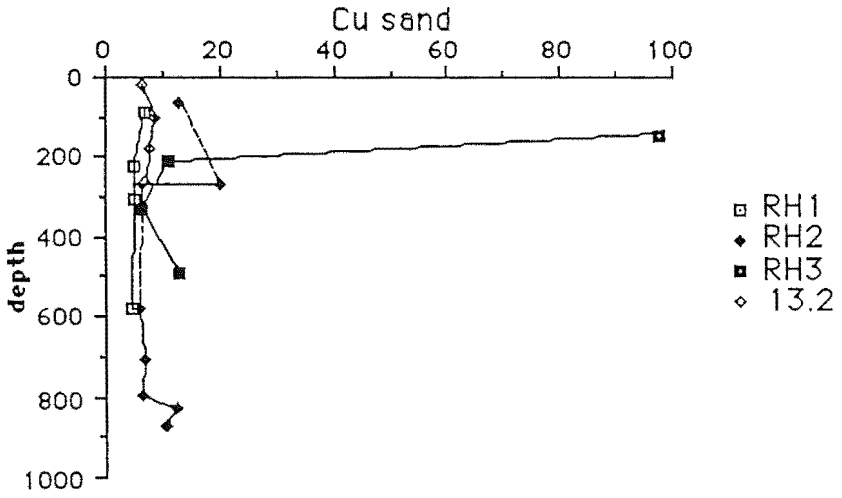

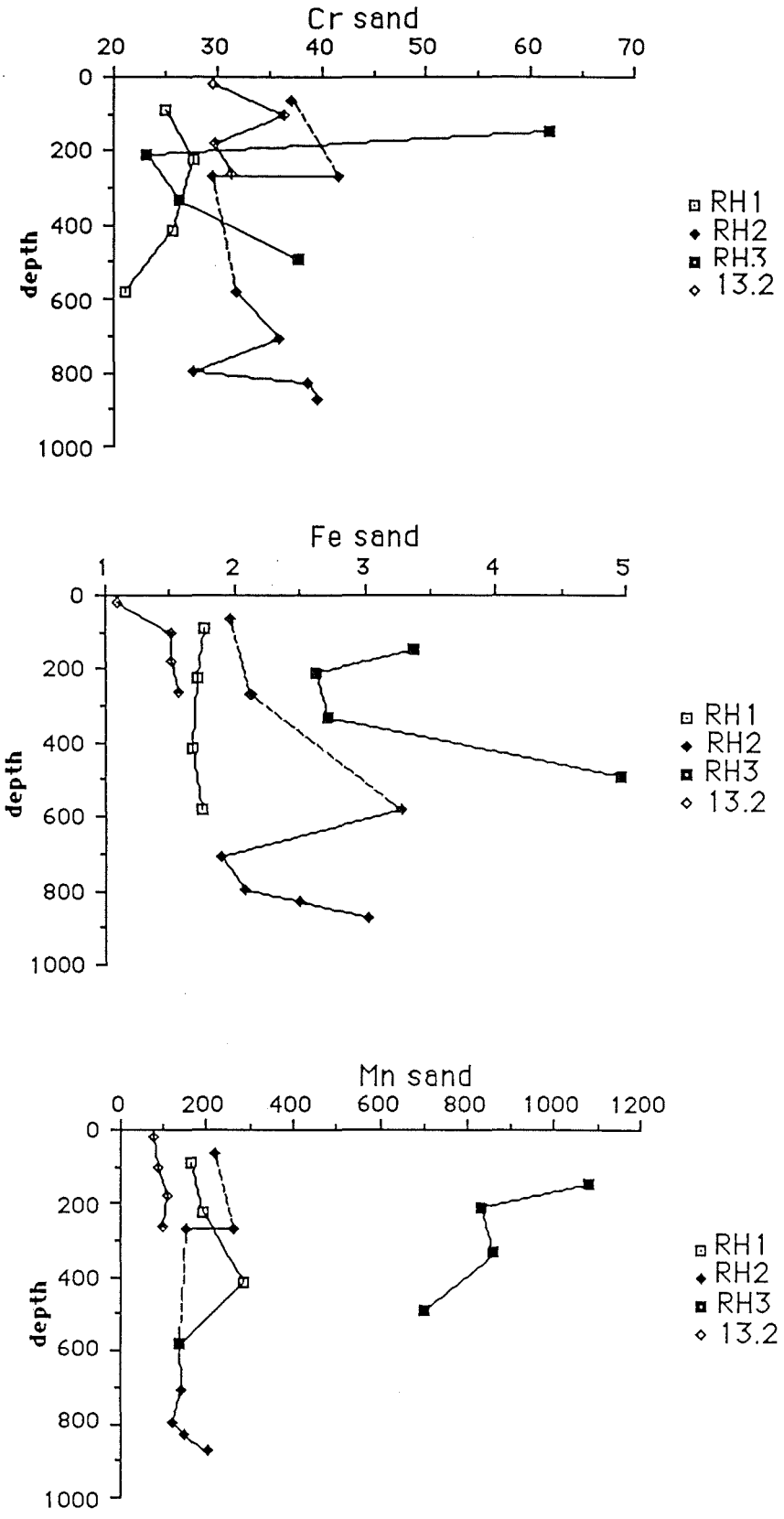
Cr sand
20
30
40
50
60
70
0
200
400
600
800
1000
depth
RH1
RH2
RH3
13.2
Fe sand
1
2
3
4
5
0
200
400
600
800
1000
depth
RH1
RH2
RH3
13.2
Mn sand
0
200
400
600
800
1000
1200
0
200
400
600
800
1000
depth
RH1
RH2
RH3
13.2

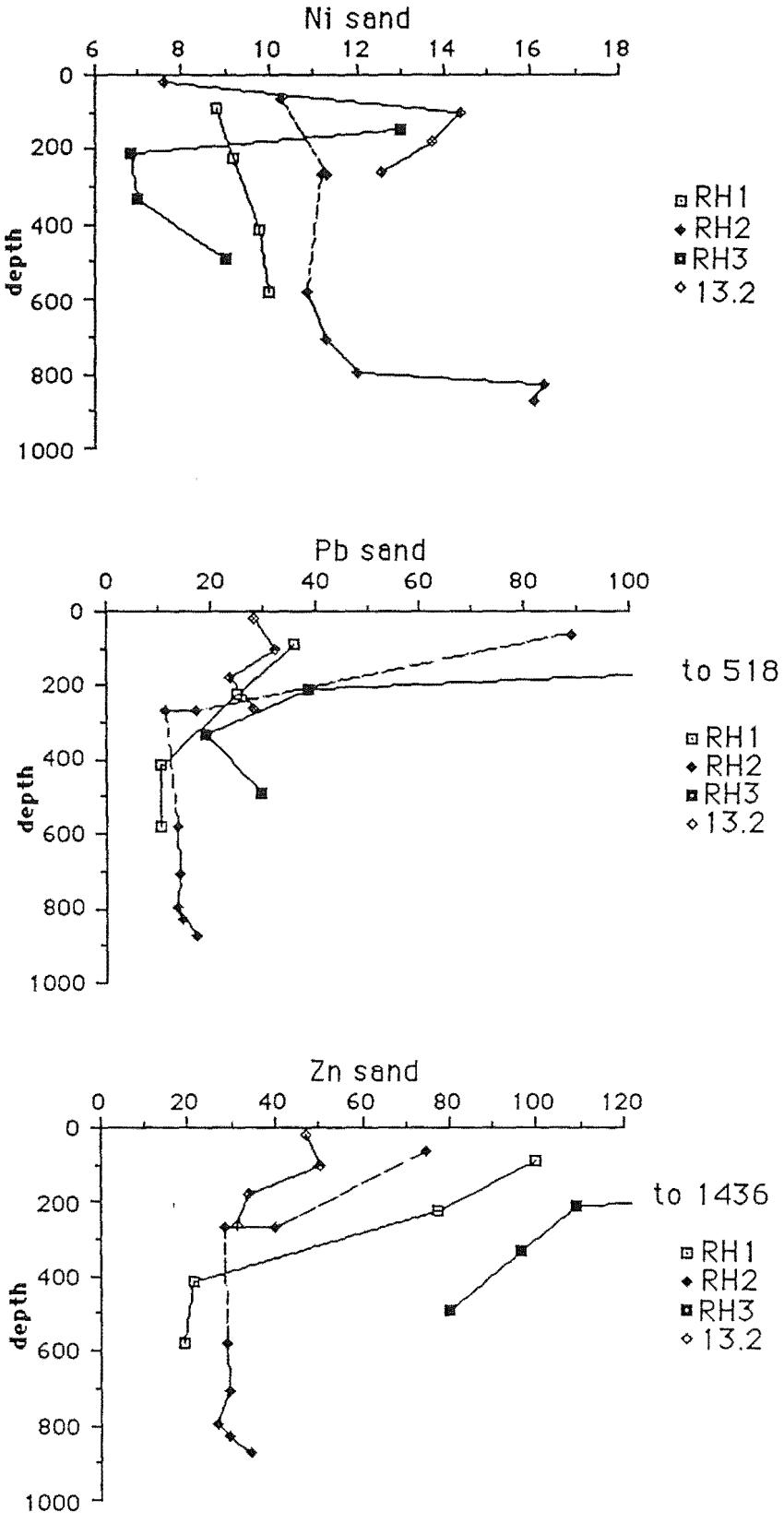
Ni sand
6
8
10
12
14
16
18
0
200
400
600
800
1000
depth
RH1
RH2
RH3
13.2
Pb sand
0
20
40
60
80
100
0
200
400
600
800
1000
depth
to 518
RH1
RH2
RH3
13.2
Zn sand
0
20
40
60
80
100
120
0
200
400
600
800
1000
depth
to 1436
RH1
RH2
RH3
13.2

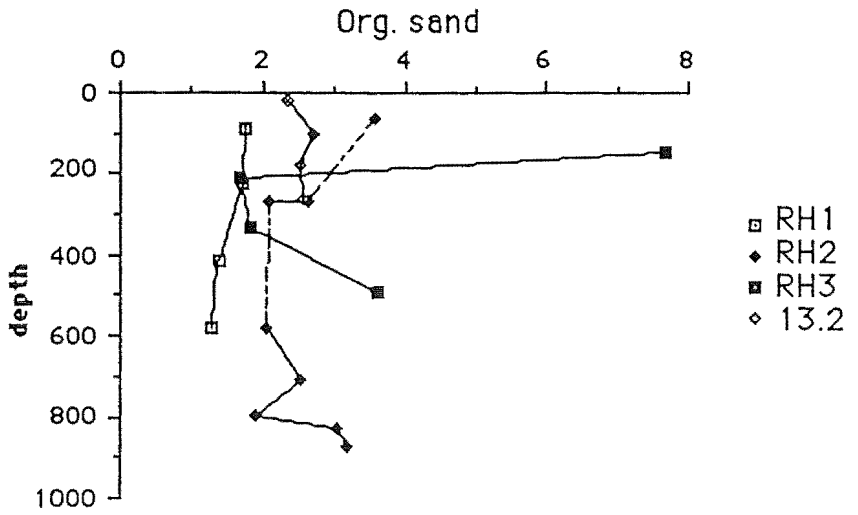

Figure 10 Depth versus Concentration in Silt Samples

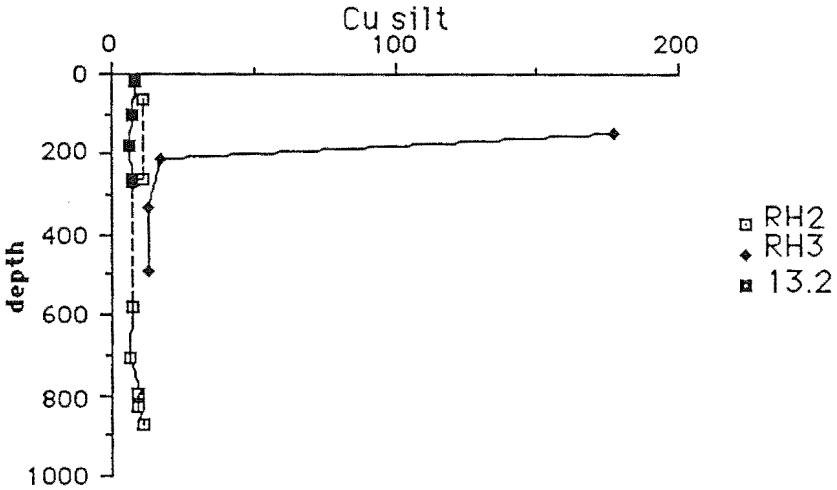

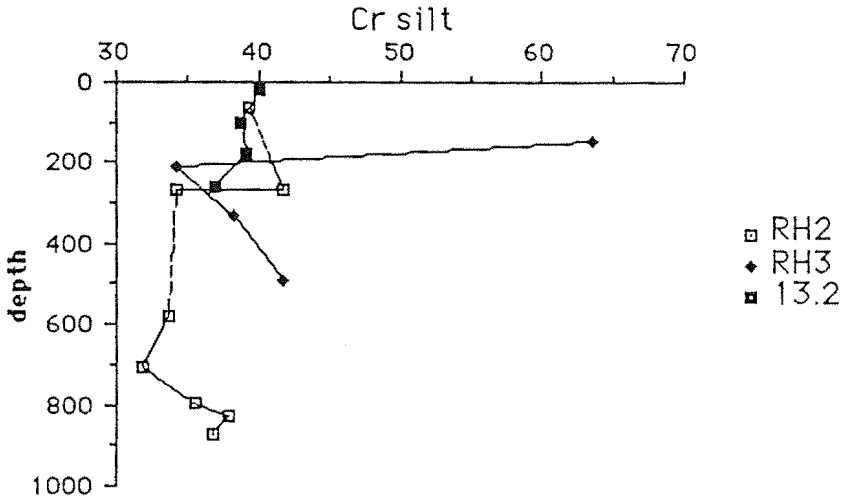

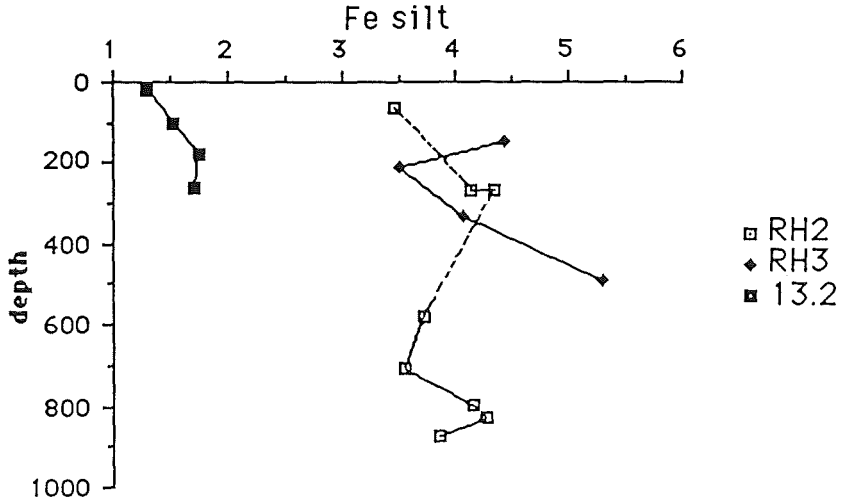
Fe silt
1
2
3
4
5
6
0
200
400
600
800
1000
depth
RH2
RH3
13.2

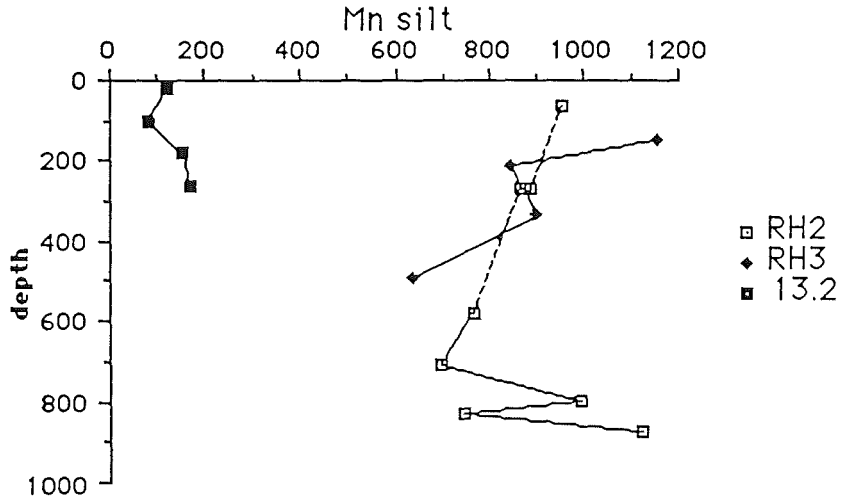
Mn silt
0
200
400
600
800
1000
1200
0
200
400
600
800
1000
depth
RH2
RH3
13.2

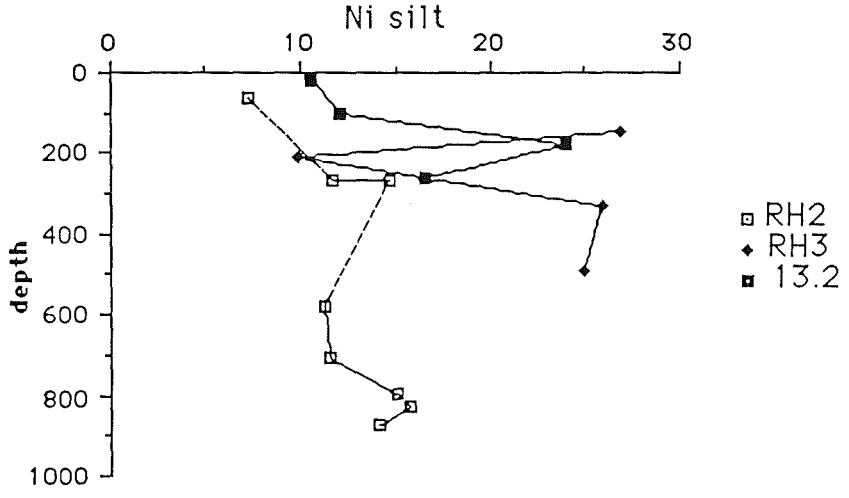
Ni silt
0
10
20
30
0
200
400
600
800
1000
depth
RH2
RH3
13.2

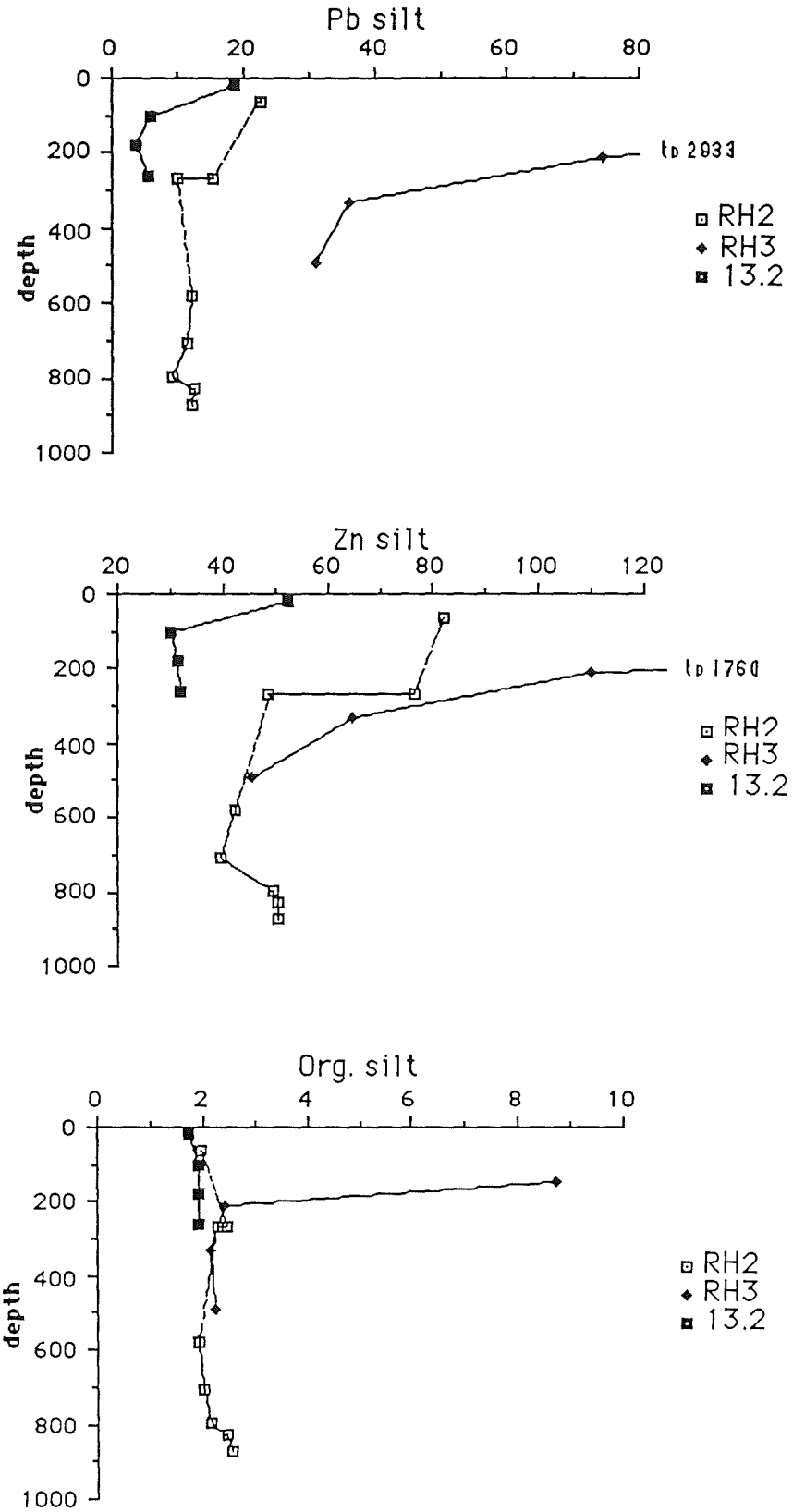
Pb silt
0
20
40
60
80
0
200
400
600
800
1000
depth
RH2
RH3
13.2
Zn silt
20
40
60
80
100
120
0
200
400
600
800
1000
depth
RH2
RH3
13.2
Org. silt
0
2
4
6
8
10
0
200
400
600
800
1000
depth
RH2
RH3
13.2

Figure 11 Depth versus Concentration in Clay Samples

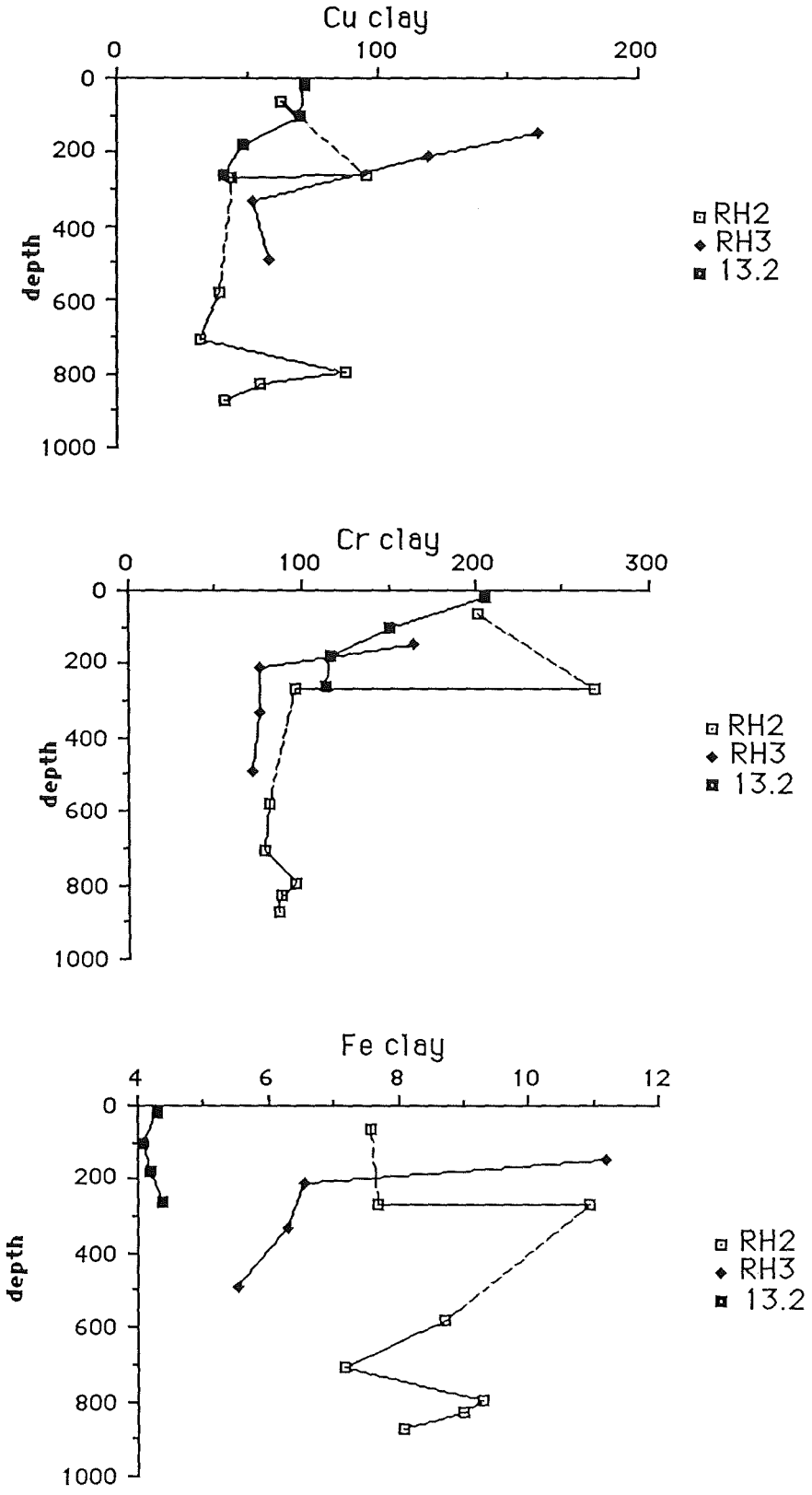

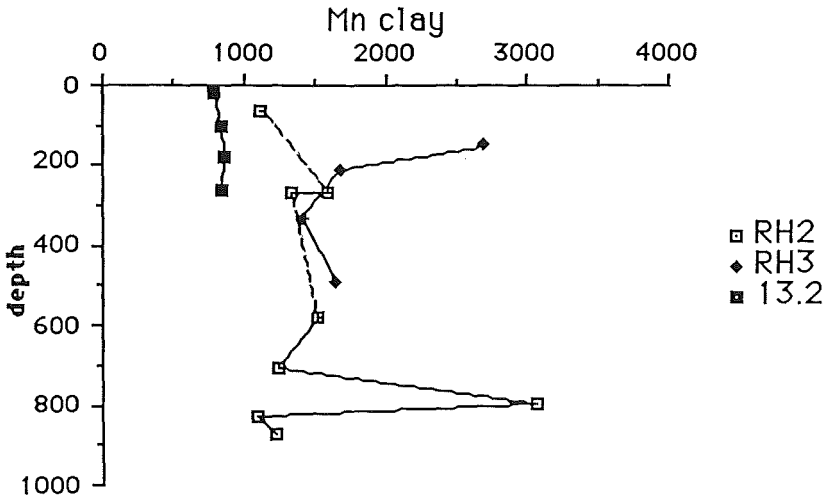
Mn clay
0
1000
2000
3000
4000
depth
0
200
400
600
800
1000
RH2
RH3
13.2

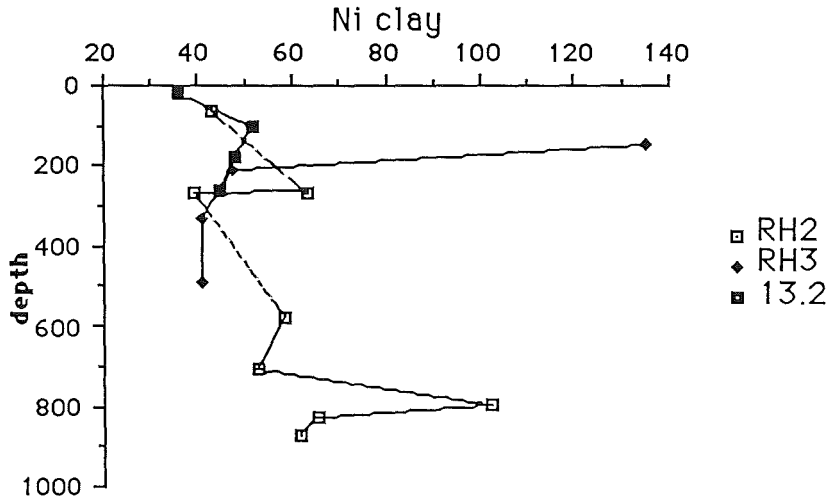
Ni clay
20
40
60
80
100
120
140
depth
0
200
400
600
800
1000
RH2
RH3
13.2

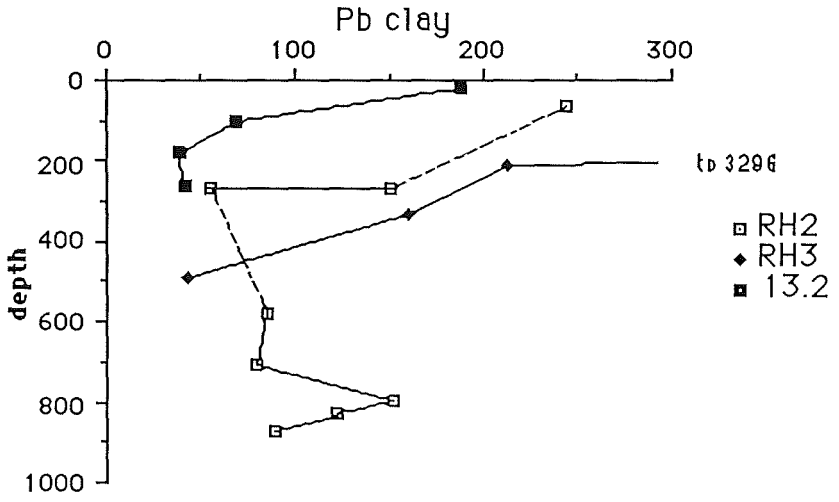
Pb clay
0
100
200
300
depth
0
200
400
600
800
1000
tp 3296
RH2
RH3
13.2

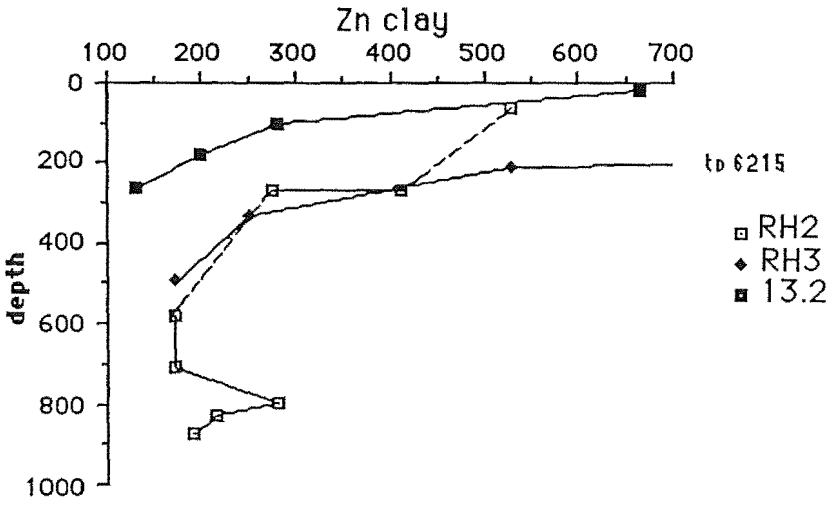
Zn clay
100
200
300
400
500
600
700
0
200
400
600
800
1000
depth
tp 6215
RH2
RH3
13.2

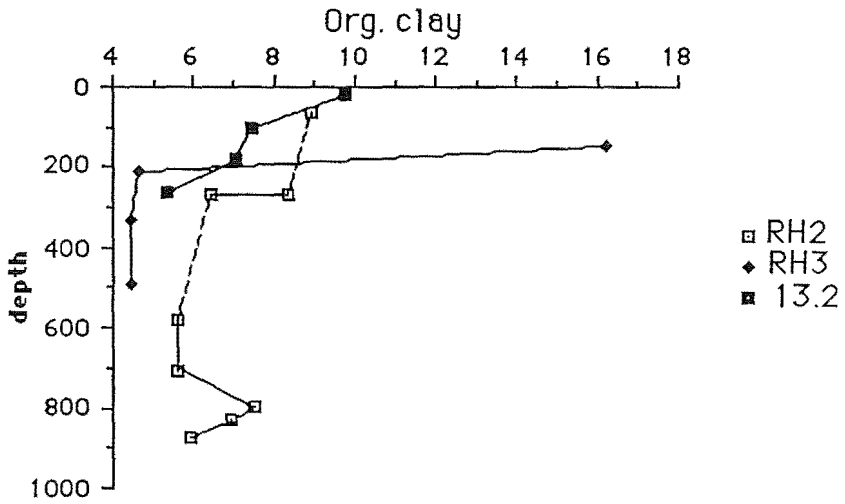
Org. clay
4
6
8
10
12
14
16
18
0
200
400
600
800
1000
depth
RH2
RH3
13.2

Figure 13 Dendogram for Combined Surface Samples

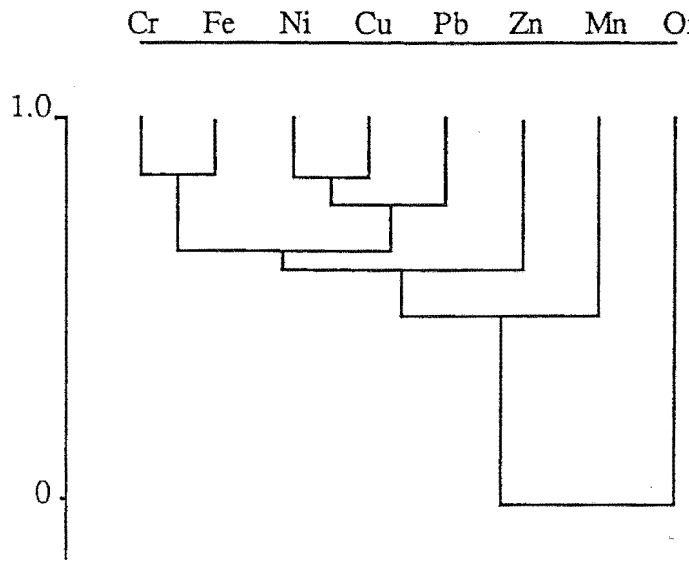

Figure 14 Dendogram for Combined Total Sample

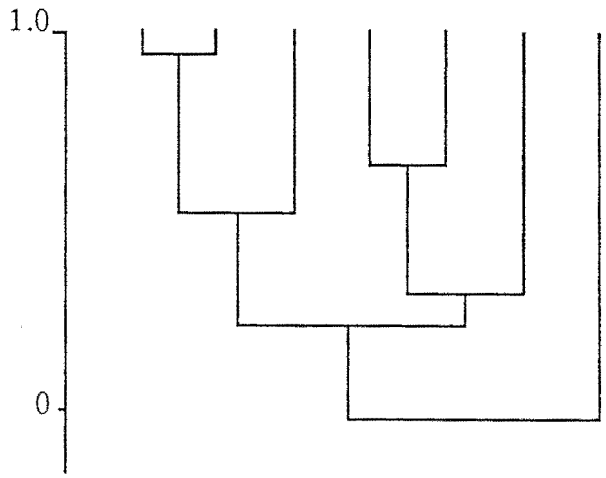

Figure 15 Dendogram for Combined Sand Samples

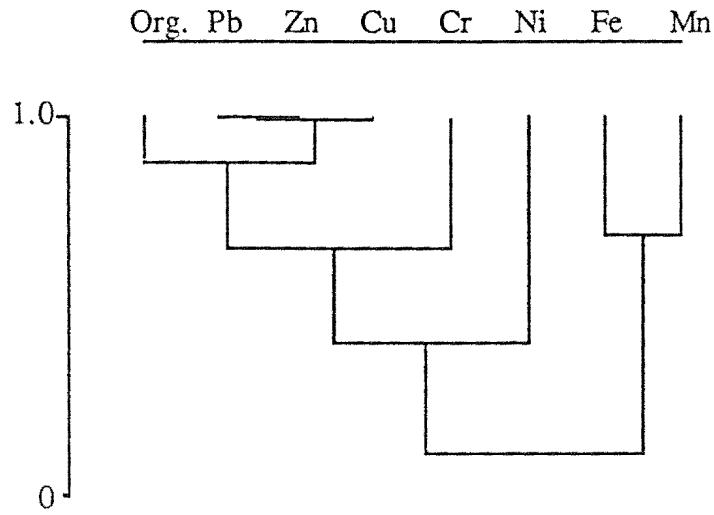

Figure 16 Dendogram for Combined Silt Samples

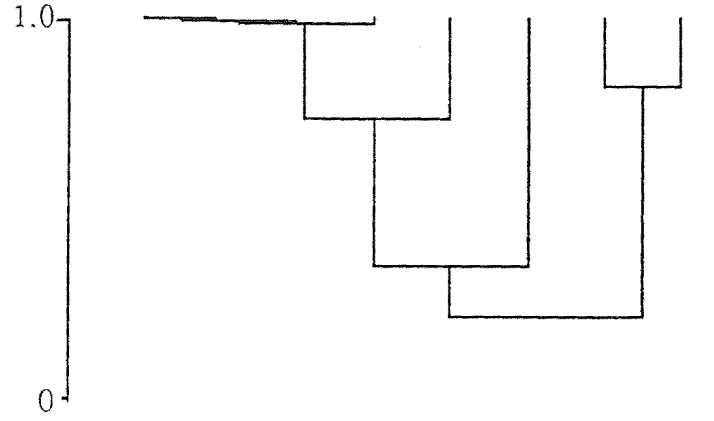

Figure 17 Dendogram for Combined Clay Samples

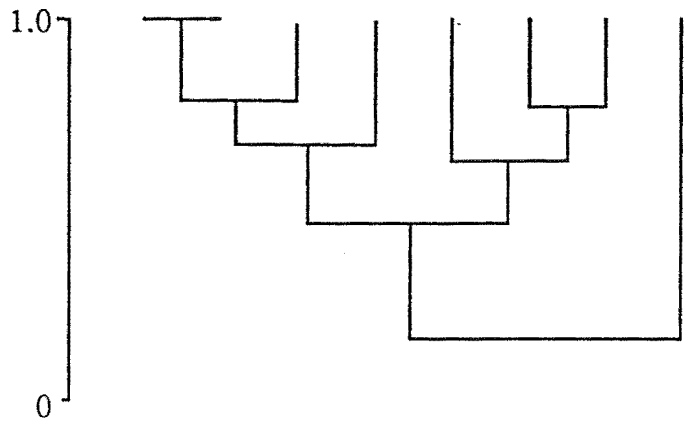

PLATE 1 The City Drain Outfall Viewed from Castle Rock

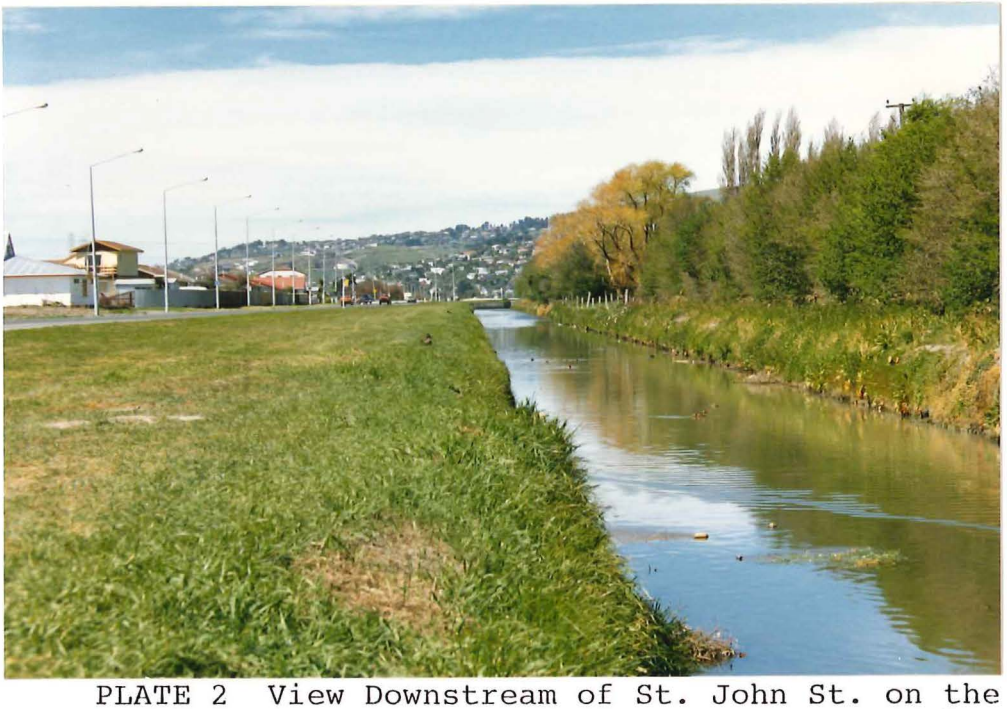

PLATE 2 View Downstream of St. John St. on the City Drain

PLATE 3 View Upstream of St. John St. on the City Drain

CHAPTER III

TRACE METALS IN SURFACE SAMPLES

3.1 INTRODUCTION

Surface samples were collected from the upper reaches of the storm water drain, at the sites shown in **Figure 2**, and from a transverse section across the outlet of the drain in the estuary using the method described in Section 6.2. Analyses was performed in the same manner as for core samples.

3.2 SAMPLING PLAN AND SITE DESCRIPTION

Surface, rather than core samples, were collected from St. John St., upstream to Bordesly St., as this section of the drain is composed of prefabricated concrete sections. Above Bordesly St. no samples could be collected as the drain is fully piped. Four batches of samples were collected at seven to eight weekly intervals, with a fifth batch collected a little over five weeks later. In retrospect a shorter time interval between collections would have been more useful, perhaps around four weeks.

The sites shown in **Figure 2** (S1, S2, S3, S4) were chosen for two reasons. Firstly access, and secondly, at these sites some sediment always accumulated. This was necessary as the intention was to collect samples from the same location over a period of time. In this way the metal ion concentrations could be studied with reference to both location and time.

Between St. John St. and Olliviers Rd. the drain is approximately 1.5 m wide at the base, and usually carries 5-15 cm of water. The concrete walls of the drain are pierced at regular intervals, both near the base and halfway up, by seepage holes. In addition, on a number of occasions, both water and sediment were observed entering the drain through joints between concrete slabs, and at junctions with tributary drains. Samples S10a and S10b, which were collected from the Hargood St. site, represent seepage hole, and intrusive material respectively.

The transverse surface samples were collected from adjacent to the site of core RH2 in order to investigate any change in metal concentration with respect to the outfall of the drain, and to demonstrate the localisation of high metal ion concentrations that often

occurs in sediments. **Figure 18** is a sketch of the locality, with the sites of sample collection labelled TS1-TS8.

3.3 RESULTS

The surface and transverse surface samples were analysed by both AAS and XRF in the manner described in Chapter 6. The results of these analyses are presented in **Table 3.0** (AAS), and **Table 3.1** (XRF). The high concentrations obtained for some metals were not expected as the sediment is predominantly medium to coarse sand. This may be explained by entrapment of fine, dense, metal rich particles by the coarser bed load sediment, and to a limited extent by association with iron (though not manganese) oxyhydrates.

3.3.1 Surface samples

To study the dependency of metal concentration in the samples on location in the drain the AAS results have been plotted in **Figure 19** as concentration versus distance from a reference point. The intersection of Olliviers Rd. and Tuam St. was chosen as the reference, as this was an easily identified location above the last sampling site. The lines of each plot have been labelled 1, 2,... 5, representing the first, then the second batch of samples collected and so on.

Monthly rainfall figures for Christchurch Airport from 1/4/87 to 1/10/87 are plotted in **Figure 20**. These are provided for comparison with the metal concentration versus time plots for the four sampling sites (**Figure 21**). Metal with metal, and metal with organic correlation coefficients are presented in **Tables 3.2-3.6**.

3.3.2 Transverse Surface Samples

A graphical representation of the results of the transverse sediment sample analyses may be seen in **Figure 22**. They are largely self explanatory and will be discussed below. Metal-metal and metal-organic correlation coefficients are presented in **Table 3.7**.

3.4 DISCUSSION

3.4.1 Variation of Surface Sample Metal Concentration with Location

All of the metals studied displayed a general decrease in concentration in a downstream direction although the trend was not always smooth. Manganese showed the least consitency in its pattern of variation, with two batches having marked increases at

the St. John St. site. All elements, and especially lead, zinc, and manganese, had on occaisions increased concentrations at the Aldwins Rd. site. The pattern of increase in concentration at Aldwins Rd. was mimiced by organic matter, with an important difference that whereas the % organic content increased sharply at the St. John St. site, metal concentrations increased only slightly or not at all. All of the metals, in particular copper, chromium, and nickel, appeared to reach steady concentrations between the Hargood St. and St. John St. sites, with the exception of manganese. Lead, zinc, and iron occaisionaly displayed marked increases (iron) or decreases (lead and zinc) between these two sampling stations. As the type of sediment supplied to the drain is probably mineralogically similar throughout the catchment, it is reasonable to assume that if the metals do not enter the drain evenly over the catchment area, then changes in metal concentrations in the Outfall Drain may reflect changes in inputs from tributary drains.

As may be seen from **Figure 2** there are two major tributary drains between Olliviers Rd. and St. John St. The first of these feeds in from the commercial area bounded roughly by Cashel St., England St., Worcester St., and Fitzgerald Ave., and joins the main drain on Bordesly St., just downstream of the sampling site. The second tributary drains an extensive area known as South Canal Reserve (SCR). The western part of the catchment is residential, the rest comprising vacant sites, a cemetary, and some minor lght industry. The SCR Drain meets the City Outfall Drain 30-40 m upstream of Hargood St. The Hargood St. sampling site is 1.5 m upstream of this junction.

Although the upper tributary has a smaller catchment, and therefore carries less water than the SCR Drain, it is expected that it will carry higher concentrations of metal ions and metal rich particulate due to the nature of the catchment use (extensive use of metal roofs and high traffic densities). The SCR Drain on the other hand, carries a higher water flow, due to its larger catchment, but is expected to have lower metal concentrations, partly because of its largely residential/"rural" character, and partly due to dilution of the metal burden by the higher water flow.

If the above is correct, the observed increase in metal concentrations at the Aldwins Rd. site may be explained by the combined "high" concentration inputs of the upper Outfall Drain and the Cashel St. tributary. Following from this the later sharp decrease in concentration can be attributed to "low" concentration inputs from groundwater seepage holes and the SCR Drain. The fact that some metals appear to be affected more than others and that the pattern of variation discussed above did not occur uniformly suggests that other factors also influence results. These are discussed below.

3.4.2 Variation of Metal Concentrations with Time and Rainfall

Plots of change in metal concentration versus time in days are presented site by site in **Figure 21**. Comparison of these plots against the monthly rainfall data plotted in

Figure 20 do not present an easily explained pattern. It is possible that if shorter collection intervals had been used, together with comparison against daily or weekly rainfall data a clearer picture of the processes taking place could have been obtained. However, neither the time, or the data to make this possible were available.

Plots of copper and chromium at the St. John St. site display only a slight similarity to rainfall, and match poorly at other sites. Nickel concentration varies little although a slight increase at the last collection (197 days) would be consistent with a heavy rainfall 2 days beforehand. Greatest variation in nickel concentration between sampling times is found at the two upstream sites which are less subject to dilution. As the element is present in low concentrations this is consistent with the view of nickel as being largely a background element with only slight anthropogenic inputs which are easily "swamped" by natural inputs and dilution. Lead, iron, and in particular zinc, match the rainfall pattern well (with the exception of iron and lead at the Bordesly St. site). At the Bordesly St. site iron continues to increase as rainfall decreases after 91 days, and lead has the reverse pattern to that of rainfall. Manganese does not match with the rainfall pattern, having the reverse of the rainfall pattern at all except the Aldwins Rd. site. The % organic content shows no consistent pattern when compared with rainfall. This is not unexpected as other factors such as temperature, light, and nutrient availability affect both allocthonous and autochthonous organic matter sources. Harrison and Wilson (1985a,b,c) carried out an extended study of urban runoff water and the suspended sediment load. They found that lead and iron associated largely with particulate (>0.45 μm) and manganese with dissolved (<0.45 μm) phases. Copper was intermediate in its behaviour and associated largely with colloidal, possibly humic, material. If these findings apply to this study, the lead, iron, and zinc results follow the rainfall pattern well because high rainfall levels remove large amounts of these metals from roofs, roads, and gutters, depositing some of the metal bearing particulate in the drain. It is known that after significant rainfall levels of lead in street dust fall significantly (Harrison and Wilson, 1985b; Simmonds and Fergusson, 1983). Manganese on the other hand, if it is in the dissolved phase, would be removed from the drain by high rainfall levels without the oppourtunity for adsorption or precipitation to the bed load sediment to occur. Thus during periods of low rainfall, when runoff water residence time is increased metals associated with the dissolved phase would be expected to increase in concentration, whereas particulate associated metals would decrease in concentration as "contaminated" sediments were slowly removed from the drain by residual water flow, being replaced by cleaner sediment entering the drain with deeper groundwater (see results for sample S10a).

3.4.3 Metal to Metal, and Metal to Organic Correlations

Correlation coefficients for metal pairs and metal with organic matter in all combined surface samples are presented in **Table 3.6.** Significant correlations are summarised in **Table 2.21.** Significant values of r for various values of n_{-2} may be found above **Table 2.3.** There are few significant correlations at individual sampling sites, probably due to the small number of samples, and the variability of results caused by the factors discussed above. When the results from all surface samples are combined the situation improves markedly. Pb-Cu, Pb-Cr, Pb-Ni, Cr-Fe, Cr-Ni, and Cu-Ni all correlate at the 0.001 level. Pb-Cu, Cr-Fe, and Cr-Ni correlations are all expected from either the literature or other parts of this study (see Chapters 2 and 4). However, the Pb-Cr correlation was not expected, and the strength of the Pb-Ni and Cu-Ni correlations was surprising. Although not proven, it could be that the Pb-Cr correlation arises from lead chromate, which is used as a pigment for yellow road paint, and that the stenght of the Pb-Ni and Cu-Ni correlation is due either coincidental to the Cr-Ni correlation or because the elements share a common source (such as metal corrosion). Zinc correlates with Pb, Cu, Cr, and Ni at the 0.01 level, as does Fe with Pb and Ni and Cr with Zn and Cu. Zinc correlates with Fe at the 0.02 level; Cu and Fe, and Mn with Fe and Pb at the 0.1 level. If the arguments above are accepted only the weakness of the Fe-Mn correlation is surprising, and this may be explained by the lack of time in which Fe/Mn oxyhydrates have to form and precipitate.

No significant metal to organic correlations were found. The reasons for this would logically be the short residence time of material in the drain preventing accumulation of metal ions in the organic matter, and that a great deal of the organic material present in the <563μm fraction was fragments of leaves, scraps of paper etc. Algae, which was abundant, constituted only a small portion of the organic matter dry weight, and although implicated as producing complexing agents for copper in natural waters, does not appear to have affected the concentrations of copper in the sediments studied.

3.4.4 Transverse Surface samples

The results for this work are plotted in **Figure 22**, which shows the concentration versus the distance from the first sample (TS1). Lead, chromium, manganese and organic matter all increase markedly in concentration across the drain outfall before falling off at the opposite bank. Iron, copper, and zinc follow the same pattern, though the increase in concentrations are smaller. The concentration of nickel does not vary to any significant degree.

Chromium, lead, zinc, and % organic show a slight dip in concentration on the northern bank at TS3; iron, zinc, and copper show a similar feature on the southern bank at TS7. There is no obvious reason why this should be so.

The results of this experiment demonstrates that concentrations can vary markedly over a short distance, and that metal ions become bound to the sediment close to the source of pollution. Obviously then, location, in terms of potential pollutant or diluent inputs into the environment, is an important factor to consider when setting up an environmental survey.

3.4.5 Comparison of AAS and XRF Results

The method of anlysis by XRF was identical to that used for the core samples, the results are tabulated in **Table 3.1.**

Comparison of chromium results from XRF and AAS shows a similar situation to that found for the core samples, with the XRF results being higher than those obtained by AAS, though in this case by only 20% compared with 46% for the core samples. Also, in the case of the surface samples the range of values obtained by AAS is greater than obtained by XRF (24.0-78.0 c.f. 17.0-82.0 ppm). There is no significant difference in the coefficient of variation (36.6% c.f. 35.0%). As with the core samples the AAS results for nickel again have a greater range, and higher mean concentration, than those obtained by XRF (19.2 c.f. 15.6 ppm). The mean zinc concentrations obtained by the two techniques were virtually identical (902 ppm,AAS; and 904 ppm,XRF), although the AAS results have a smaller cv (27.2% c.f. 34.5%). The reason for this is the greater range of results for XRF. The range is 58-1410 ppm, however the second lowest value is 587 ppm, hence if the 58 ppm value is regarded as an artifact, which it almost certainly is, and excluded, then the cv for the XRF results becomes 31%. The comparison for surface and core samples by AAS and XRF then becomes very similar.

The reasons for the differences between the AAS and XRF techniques has already been discussed in Section 2.4.5. The better agreement for surface than core samples arises from the greater similarity of the sediment from sample to sample, thereby reducing variation caused by matrix effects. Results for the major element concentrations of two samples may be found in Appendix A.

Table 3.0 Metal Concentrations by AAS for Surface samples

sample	element concentration (ppm unless stated)							
	Cr	Cu	Fe	Mn	Ni	Pb	Zn	Org.
S1	46.0	6.9	3.24	964	13.1	26.3	683	6.93
S2	39.7	36.0	2.67	1105	12.4	143	734	3.18
S3	39.7	71.8	3.34	1454	22.1	1103	816	3.35
S4	51.0	98.0	4.11	1311	36.1	696	920	1.98
S5	28.7	32.5	3.40	885	8.7	187	810	4.52
S6	28.7	20.0	3.37	982	11.5	132	872	-
S7	50.2	50.2	4.96	1062	15.3	463	803	2.19
S8	49.0	43.2	5.33	1592	25.1	535	757	3.40
S9	36.7	26.2	3.81	738	15.7	155	759	4.95
S10	32.4	33.5	3.25	1128	11.4	128	912	2.50
S10a	23.5	2.9	2.06	192	8.0	10.3	41.1	1.07
S10b	49.9	98.7	3.70	529	18.8	395	819	7.78
S11	65.9	80.3	4.78	1611	29.4	608	1397	4.66
S12	66.6	77.3	5.55	1340	29.7	538	1381	2.81
S13	24.0	15.0	2.92	1574	9.6	96.0	504	2.36
S14	22.8	19.0	2.72	1014	11.9	86.7	802	1.80
S15	39.1	99.0	3.94	1324	24.4	705	1172	3.67
S16	78.0	85.6	6.56	1551	30.0	900	1105	3.55
S17	22.6	18.4	3.66	810	12.8	98.3	484	4.10
S18	26.3	9.9	2.61	460	19.7	115	763	2.03
S19	54.5	136	4.76	755	35.2	715	1147	4.42
S20	66.2	298	4.52	874	45.0	1014	1245	2.95
TS1	36.5	11.2	2.30	-	11.3	45.8	96.4	1.95
TS2	39.5	10.6	2.44	203	8.5	47.2	109	2.65
TS3	37.3	11.5	2.58	161	8.1	44.7	90.4	2.64
TS4	41.5	14.0	2.81	284	8.9	57.7	116	3.43
TS5	43.2	20.0	2.76	317	11.2	56.7	131	3.54
TS6	48.3	19.3	2.54	724	10.4	62.4	132	4.17
TS7	41.7	13.0	2.41	346	10.4	57.1	91.0	3.07
TS8	37.9	12.0	2.77	105	9.5	52.5	104	2.42

Table 3.1 Metal Concentrations by XRF for Surface Samples

sample	element concentration (ppm)										
	Ba	Ce	Cr	La	Nb	Nd	Ni	V	Zn	Zr	Sr
S1	580	48	31	25	11	32	9	51	58	119	293
S2	536	49	41	28	10	27	11	45	803	152	291
S3	564	57	54	22	11	31	18	56	912	120	299
S4	529	53	62	23	14	24	22	56	903	120	299
S5	556	57	40	26	9	31	12	49	824	151	271
S6	529	42	33	29	9	30	11	44	959	142	290
S7	574	55	59	22	13	25	18	59	863	107	298
S8	567	53	59	27	15	26	17	64	665	126	289
S9	543	53	42	29	10	30	11	48	825	128	276
S10	555	48	35	21	10	35	11	46	1011	143	286
S10a	512	37	26	17	8	42	9	45	45	104	292
S10b	624	88	89	35	11	39	19	76	1076	154	277
S11	621	61	72	29	15	25	18	60	1410	120	281
S12	531	39	89	29	18	21	24	80	1243	129	299
S13	555	46	17	20	9	27	10	44	587	105	290
S14	535	39	32	20	10	30	11	44	1045	119	294
S15	555	53	65	22	14	33	21	68	1181	123	287
S16	505	79	82	13	18	30	25	83	1179	128	288
TS1	571	58	40	22	11	41	9	37	133	381	305
TS2	568	47	39	29	10	36	9	45	144	367	303
TS3	581	58	39	29	11	32	10	45	142	365	304
TS4	579	57	49	28	12	38	11	52	158	350	296
TS5	564	46	49	23	12	33	10	53	168	342	289
TS6	545	61	49	--	10	40	11	52	198	351	290
TS7	553	65	45	27	11	38	13	47	147	396	298
TS8	562	58	47	28	12	36	10	44	146	461	307

Table 3.2 Correlation Coefficients for St. John St. site n = 5

	Cu	Cr	Fe	Mn	Ni	Pb	Zn	Org.
Cu	1.000							
Cr	-0.364	1.000						
Fe	0.476	0.080	1.000					
Mn	-0.388	-0.319	-0.908	1.000				
Ni	-0.196	0.500	0.679	0.568	1.000			
Pb	0.991	-0.410	0.409	-0.282	-0.221	1.000		
Zn	0.956	-0.495	0.408	-0.208	-0.167	0.983	1.000	
Org.	-0.266	0.890	0.311	-0.616	0.487	-0.364	-0.484	1.000

Table 3.3 Correlation Coefficients for Hargood St. Site n = 5

	Cu	Cr	Fe	Mn	Ni	Pb	Zn	Org.
Cu	1.000							
Cr	0.827	1.000						
Fe	0.239	0.040	1.000					
Mn	0.838	0.458	0.444	1.000				
Ni	-0.662	-0.260	-0.594	-0.956	1.000			
Pb	0.577	0.869	0.340	0.243	-0.150	1.000		
Zn	0.162	-0.178	0.910	0.384	-0.511	0.044	1.000	
Org.	0.829	0.997	-0.027	0.463	-0.257	0.831	-0.239	1.000

Table 3.4 Correlation Coefficients for Aldwins Rd. Site n = 5

	Cu	Cr	Fe	Mn	Ni	Pb	Zn	Org.
Cu	1.000							
Cr	0.092	1.000						
Fe	0.058	0.767	1.000					
Mn	-0.502	0.037	-0.426	1.000				
Ni	0.889	0.449	0.160	-0.222	1.000			
Pb	0.129	-0.532	-0.895	0.272	0.119	1.000		
Zn	0.502	0.616	0.318	0.249	0.718	-0.278	1.000	
Org.	0.707	0.506	0.057	0.150	0.928	0.154	0.861	1.000

Table 3.5 Correlation Coefficients for Bordesly St. Site n = 5

	Cu	Cr	Fe	Mn	Ni	Pb	Zn	Org.
Cu	1.000							
Cr	0.253	1.000						
Fe	-0.437	0.668	1.000					
Mn	-0.941	-0.114	0.613	1.000				
Ni	0.938	0.150	-0.608	-0.948	1.000			
Pb	0.786	0.570	-0.022	-0.589	0.750	1.000		
Zn	0.436	0.700	0.168	-0.524	0.388	0.288	1.000	
Org.	-0.111	0.462	0.800	0.381	-0.416	0.140	-0.028	1.000

Table 3.6 Correlation Coefficients for all surface samples n = 20

	Cu	Cr	Fe	Mn	Ni	Pb	Zn	Org.
Cu	1.000							
Cr	0.619	1.000						
Fe	0.428	0.852	1.000					
Mn	0.032	0.401	0.426	1.000				
Ni	0.849	0.780	0.629	0.179	1.000			
Pb	0.754	0.709	0.620	0.417	0.820	1.000		
Zn	0.610	0.599	0.555	0.250	0.669	0.625	1.000	
Org.	-0.051	0.183	0.099	-0.090	-0.032	-0.054	-0.273	1.000

Table 3.7 Correlation Coefficients for TS samples n = 8

	Cu	Cr	Fe	Mn	Ni	Pb	Zn	Org.
Cu	1.000							
Cr	0.848	1.000						
Fe	0.649	0.397	1.000					
Mn	0.725	0.966	0.700	1.000				
Ni	0.511	0.298	0.841	0.539	1.000			
Pb	0.774	0.886	0.376	0.774	0.362	1.000		
Zn	0.854	0.779	0.452	0.609	0.295	0.670	1.000	
Org.	0.850	0.955	0.319	0.913	0.128	0.871	0.769	1.000

n = 7 for manganese

Figure 18 Location of Transept for Transverse surface samples and Cross Sectional View of the Transept

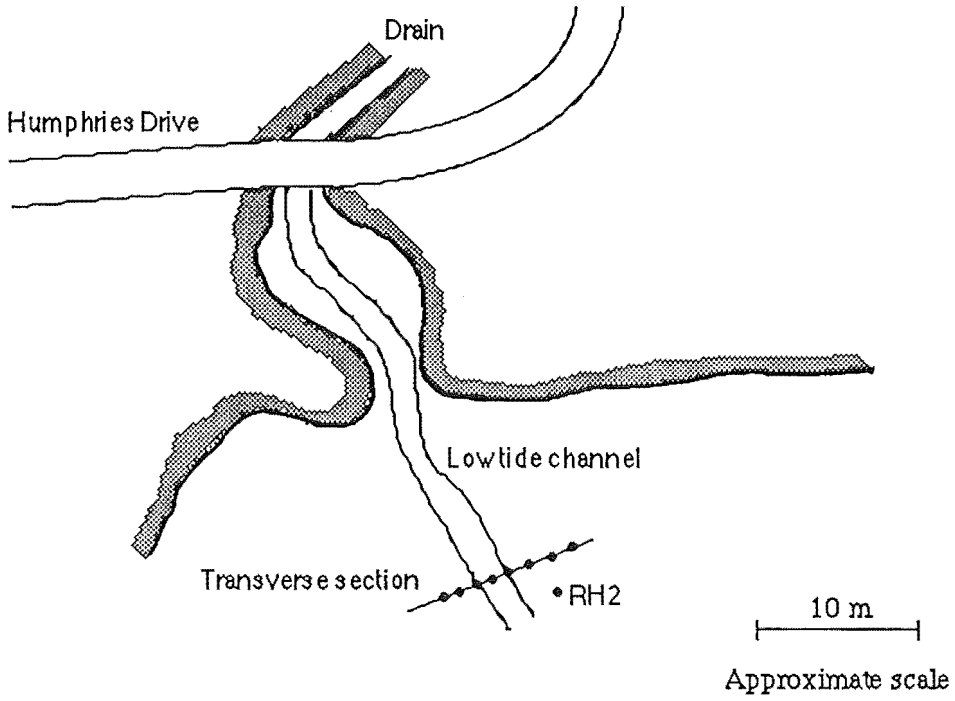

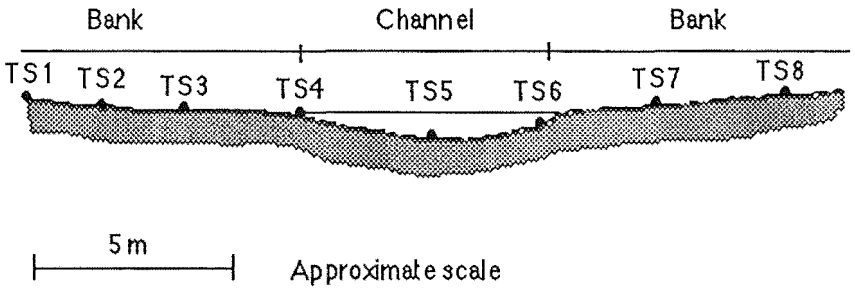

Figure 19 Metal Concentration Variation with Distance from the Central City

Reference point is the junction of Olliviers Rd. and Tuam St.

All concentrations are $\mu g\ g^{-1}$ unless stated.

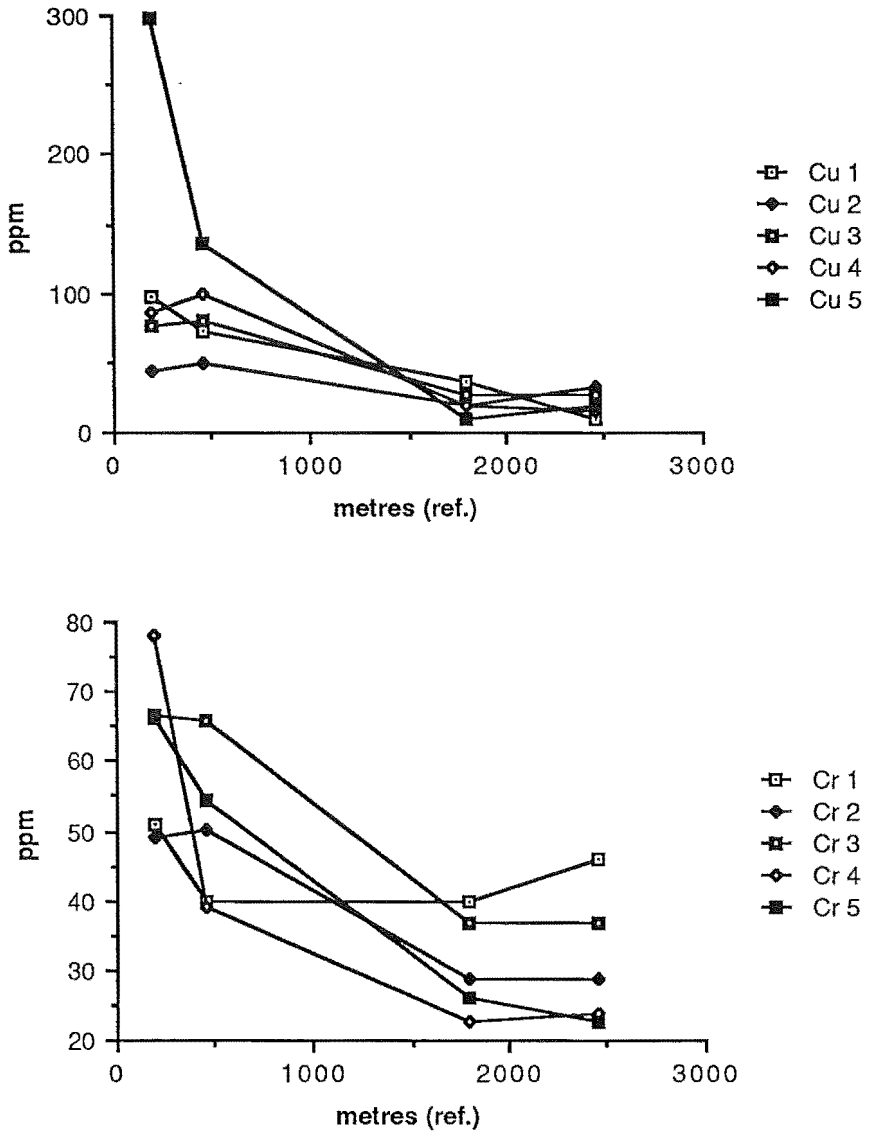

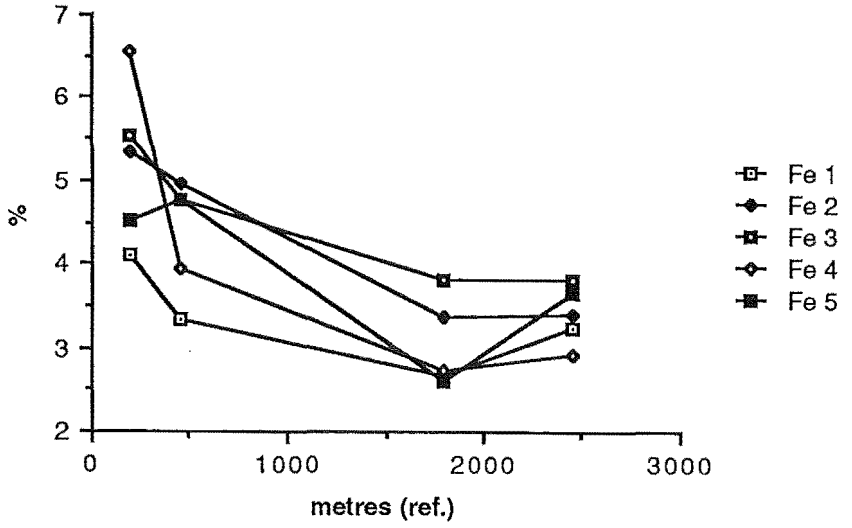
7
6
5
4
3
2
%
0
1000
2000
3000
metres (ref.)
Fe 1
Fe 2
Fe 3
Fe 4
Fe 5

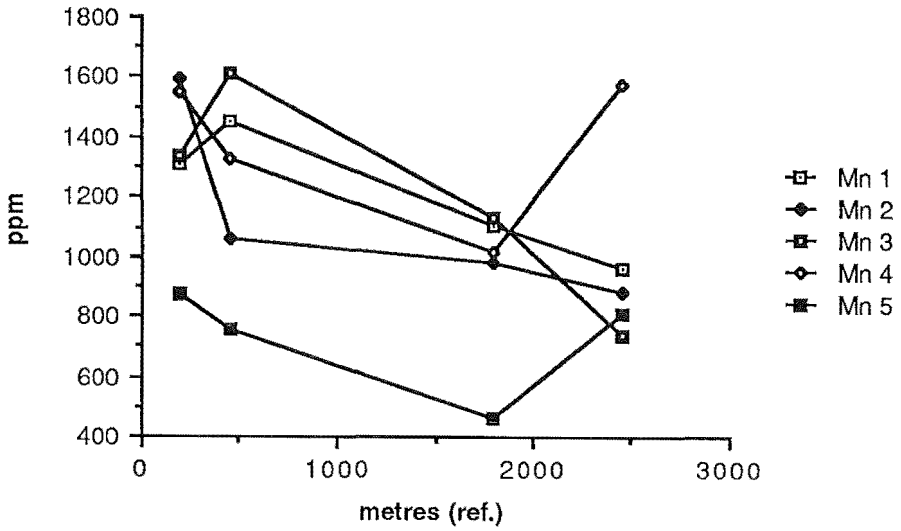
1800
1600
1400
1200
1000
800
600
400
ppm
0
1000
2000
3000
metres (ref.)
Mn 1
Mn 2
Mn 3
Mn 4
Mn 5

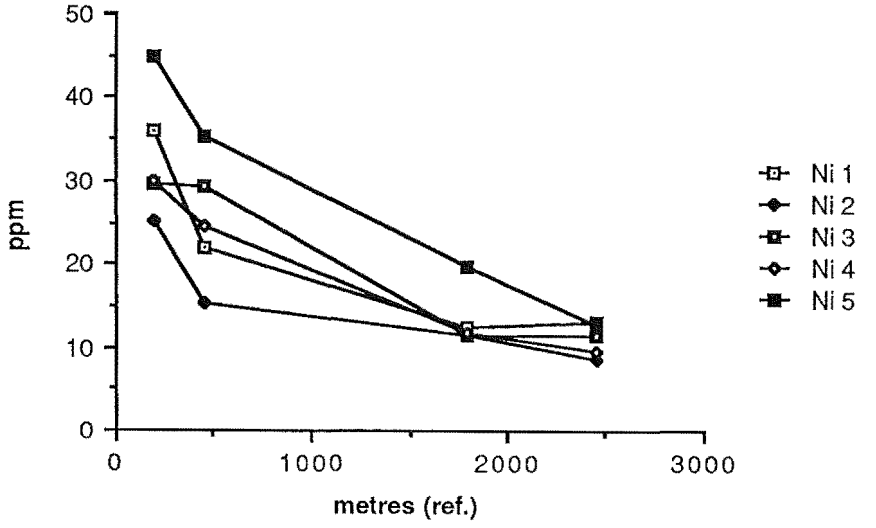
50
40
30
20
10
0
ppm
0
1000
2000
3000
metres (ref.)
Ni 1
Ni 2
Ni 3
Ni 4
Ni 5

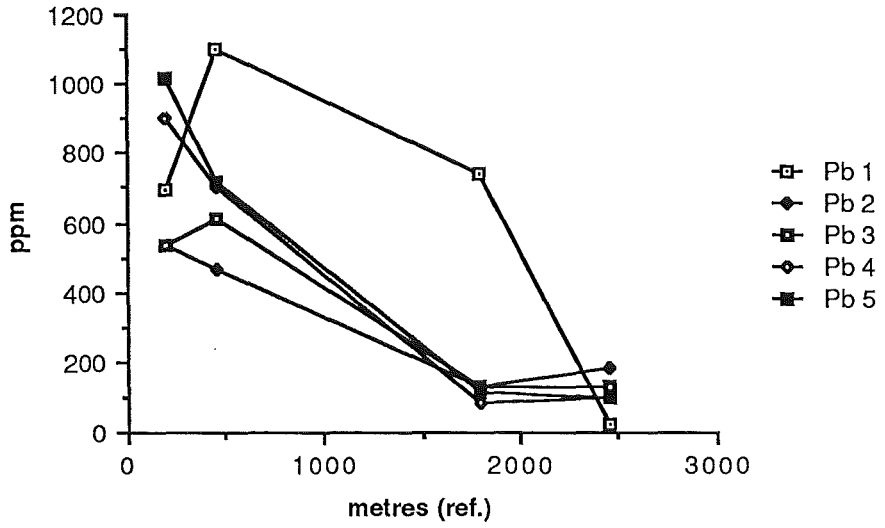
1200
1000
800
600
400
200
0
ppm
0
1000
2000
3000
metres (ref.)
Pb 1
Pb 2
Pb 3
Pb 4
Pb 5

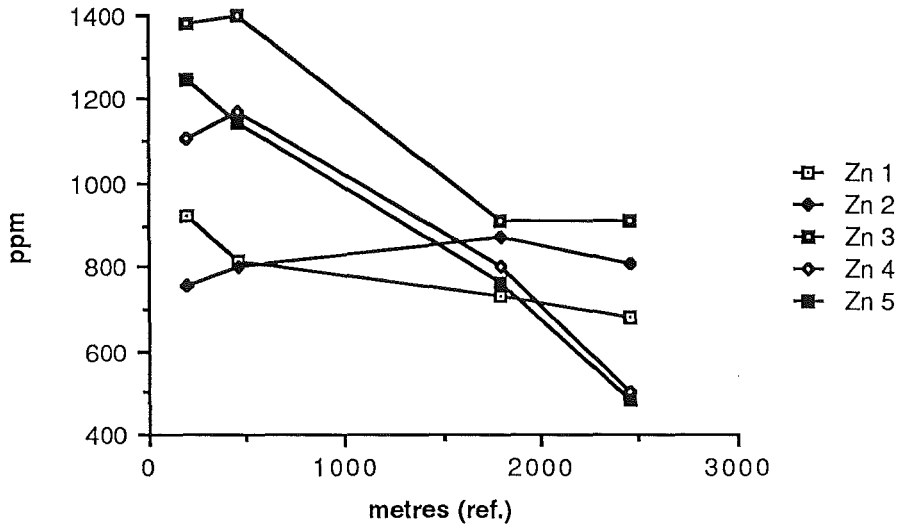
1400
1200
1000
800
600
400
ppm
0
1000
2000
3000
metres (ref.)
Zn 1
Zn 2
Zn 3
Zn 4
Zn 5

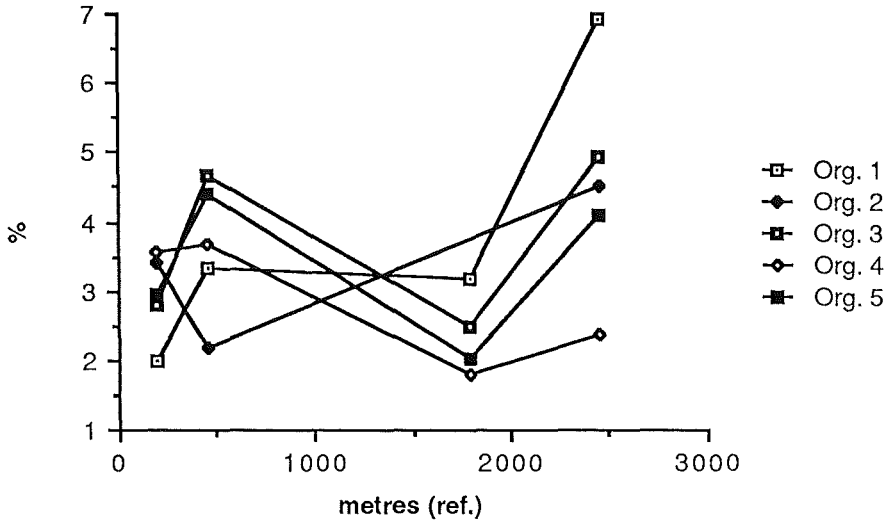
7
6
5
4
3
2
1
%
0
1000
2000
3000
metres (ref.)
Org. 1
Org. 2
Org. 3
Org. 4
Org. 5

Figure 20 Monthly Rainfall 1st April to 31st October

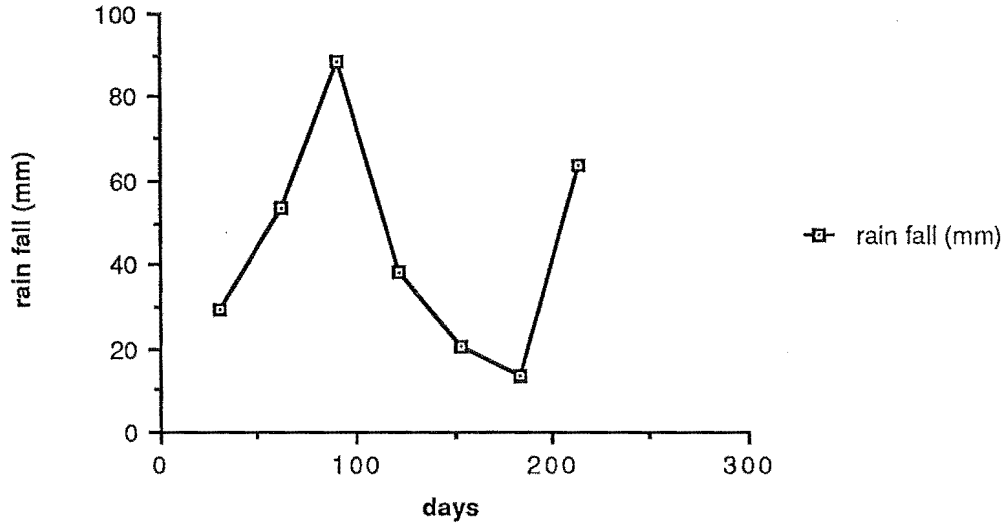

Figure 21 Change in Metal Concentration with Time

All concentrations are μg g^{-1} unless stated. Day 0 is 14/1/4

St. John St. Site.

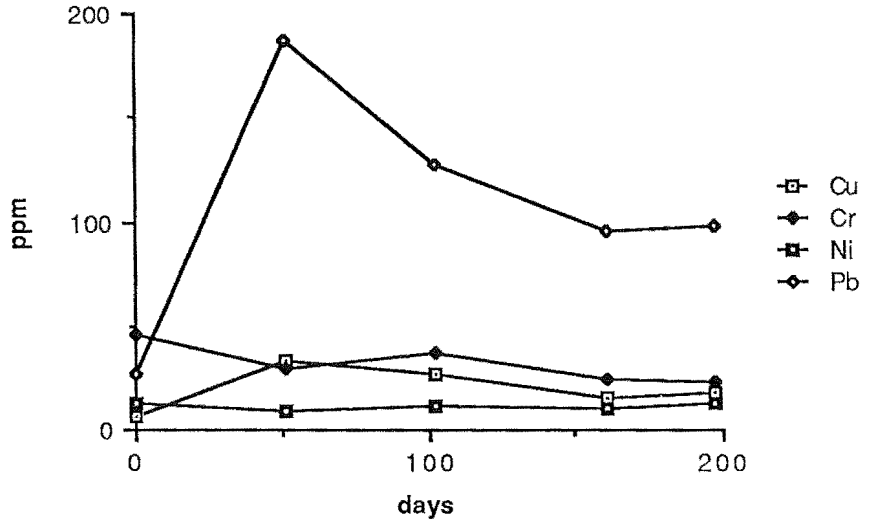

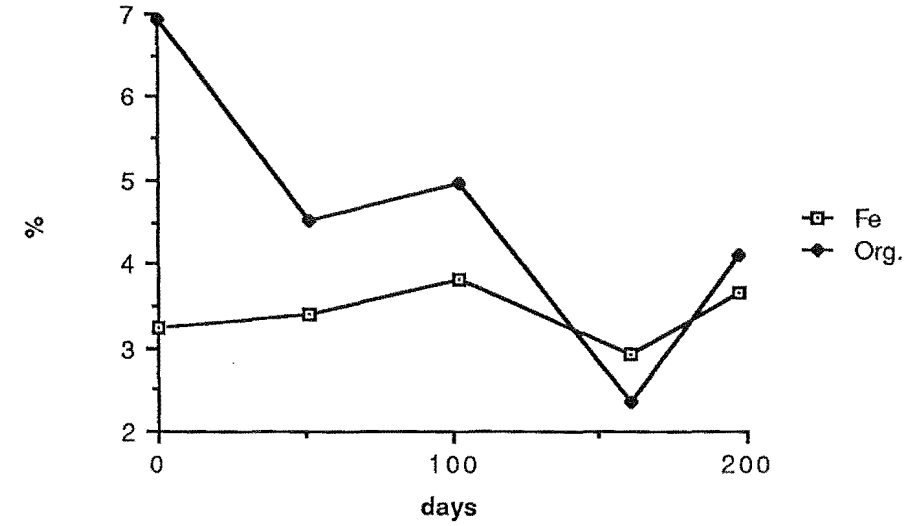

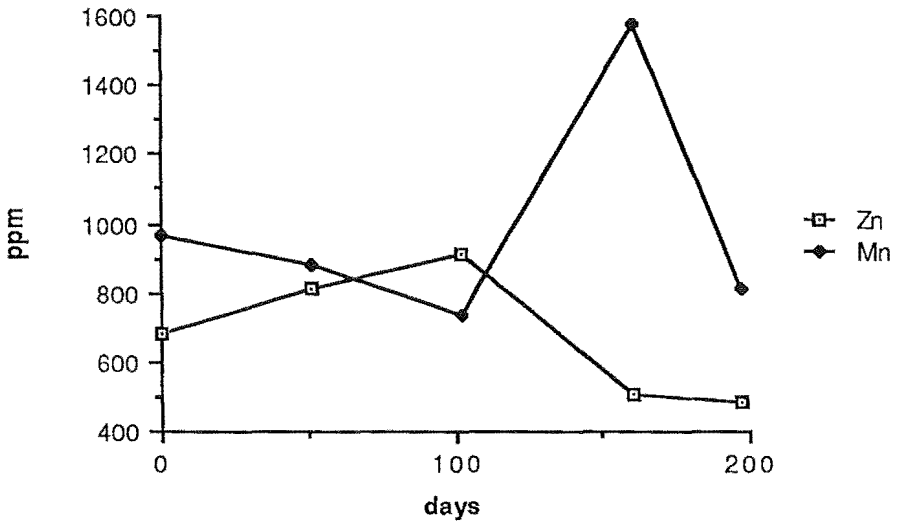

Hargood St. Site.

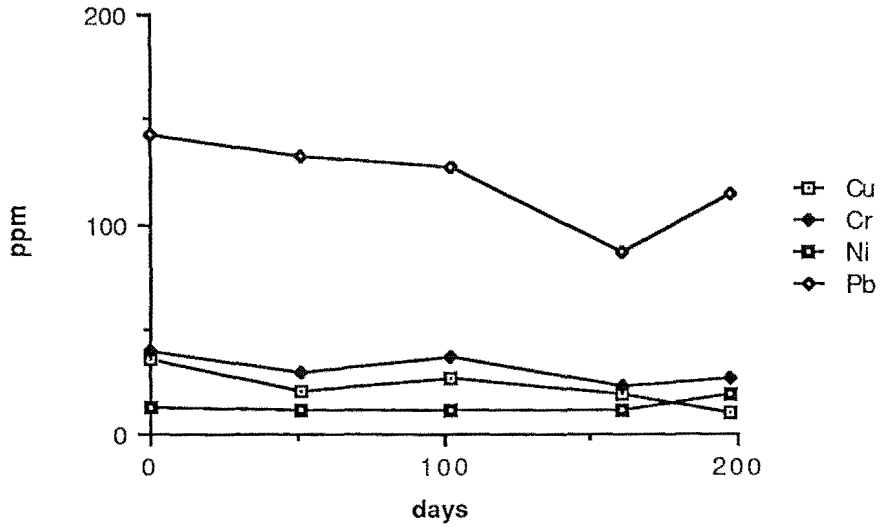

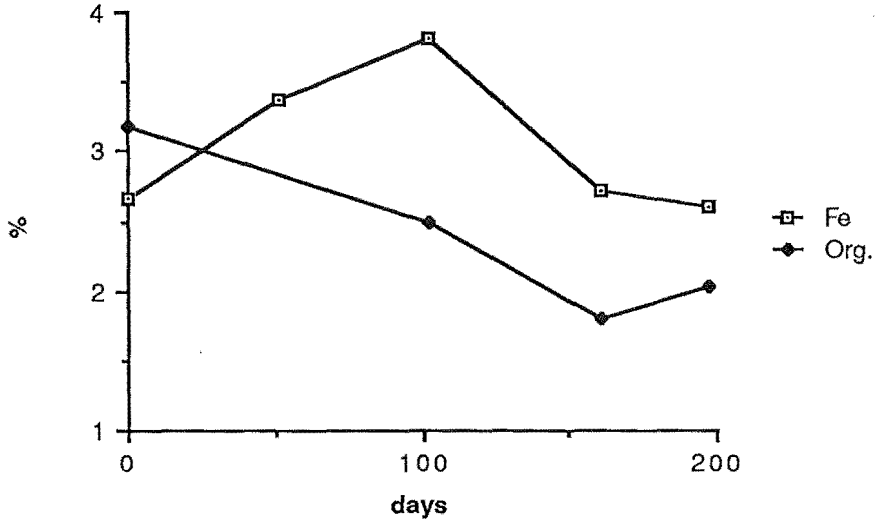

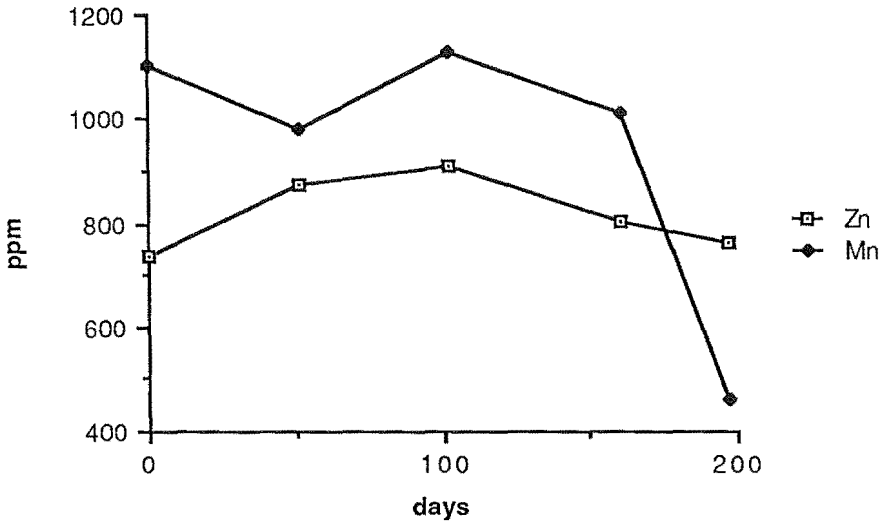

Aldwins Rd. Site.

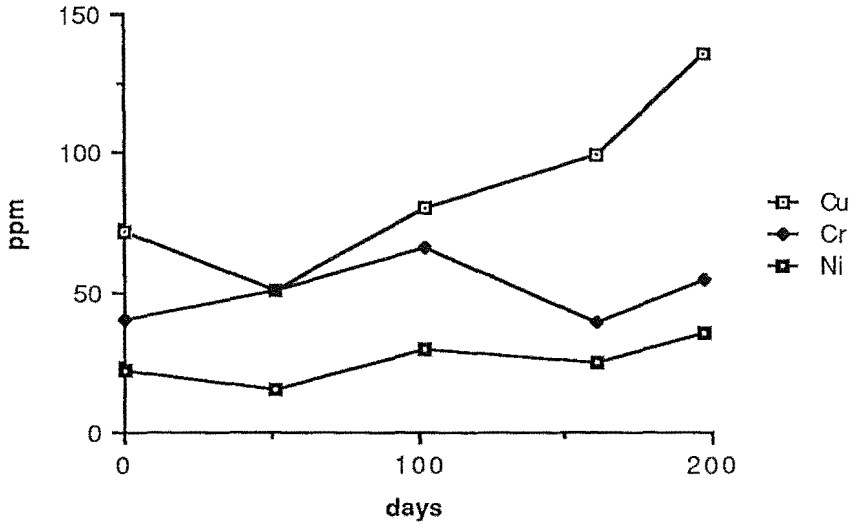

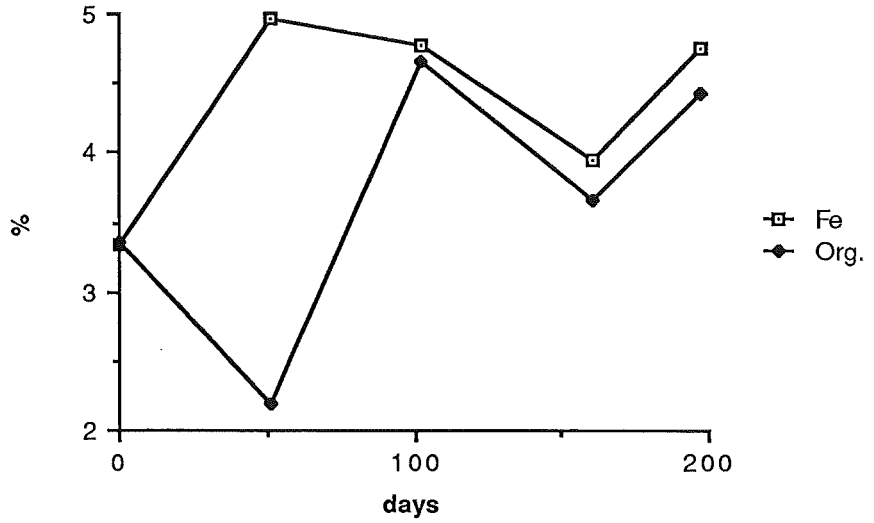

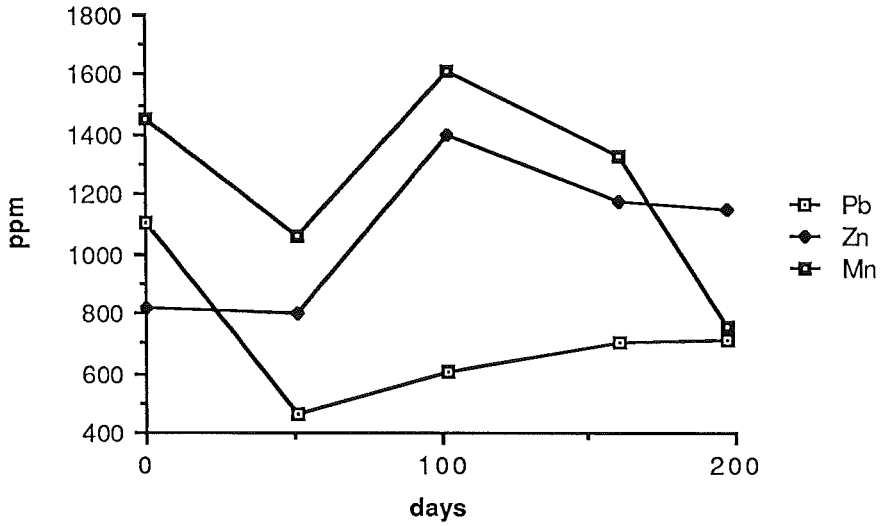

Bordesly St. Site.

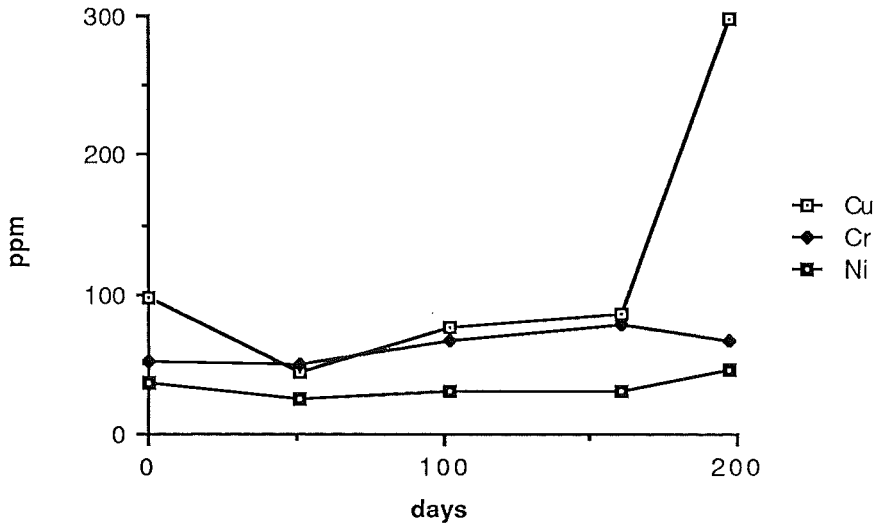

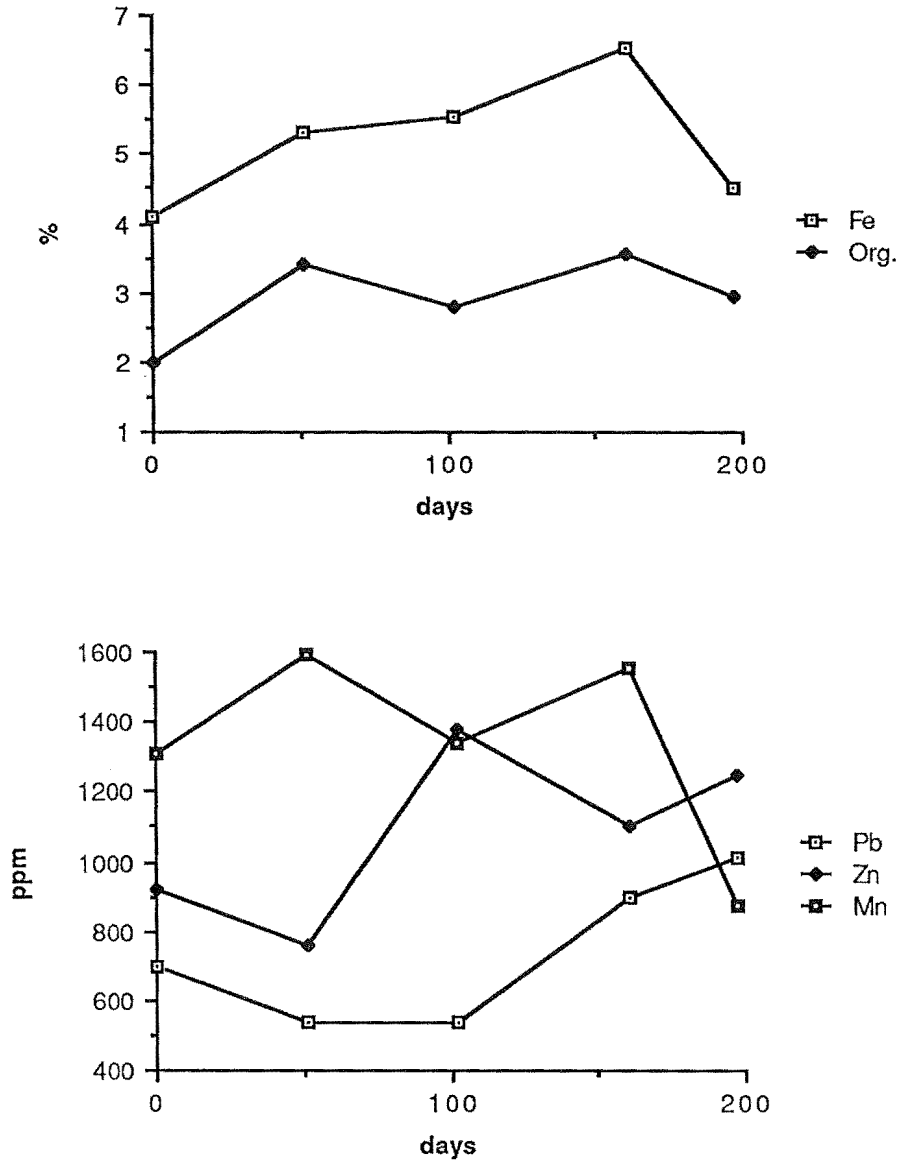

Figure 22 Change in Metal Concentration on a Transept Across the Drain Outfall

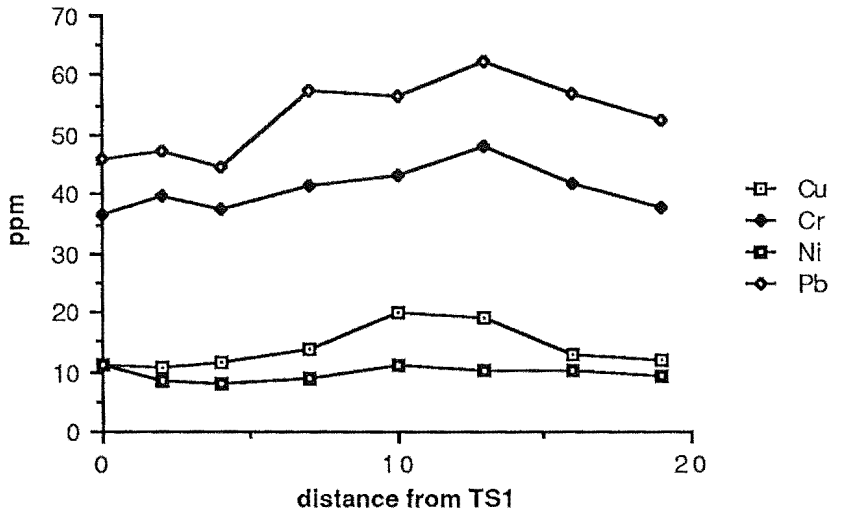

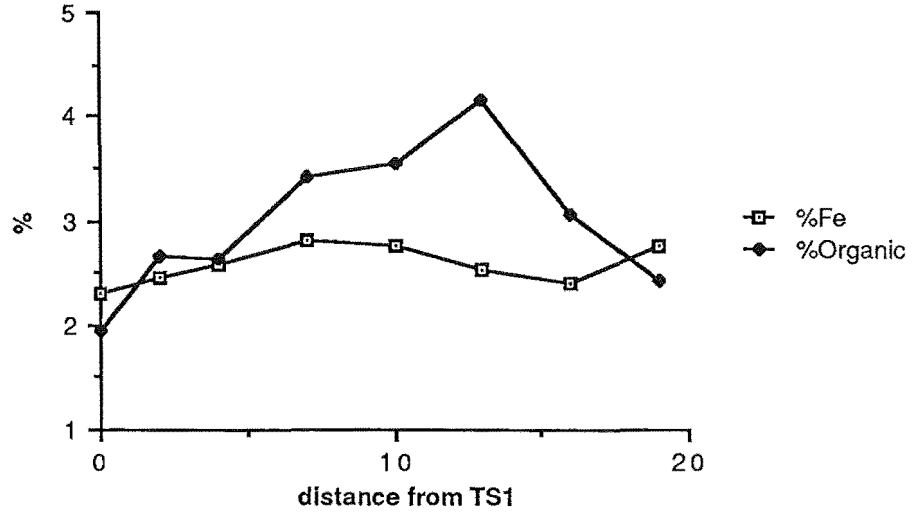
5
4
3
2
1
%
0
10
20
distance from TS1
%Fe
%Organic

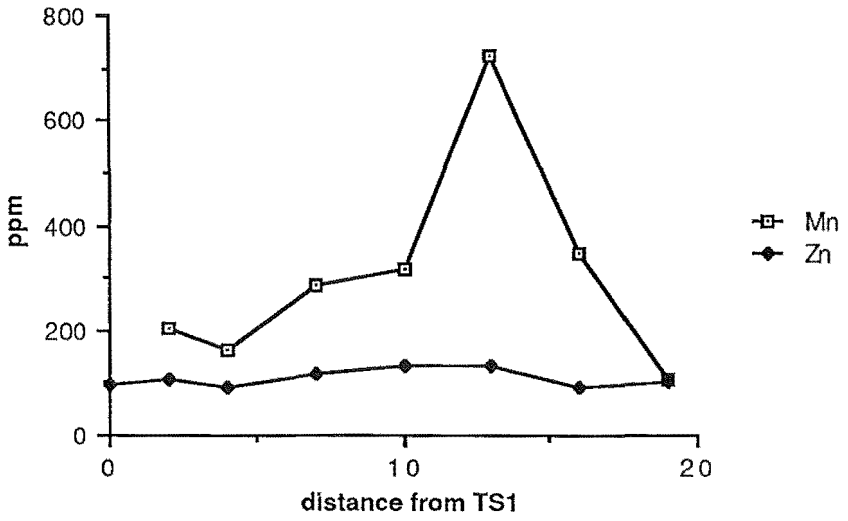
800
600
400
200
0
ppm
0
10
20
distance from TS1
Mn
Zn

CHAPTER IV

TRACE METAL DISTRIBUTION IN THE SILT-CLAY SIZE FRACTION

4.1 INTRODUCTION

A number of workers have reported a relationship between decreasing particle size and increasing heavy metal concentration in sediments, soil, and dust (Thorne and Nickless, 1981; Harrison and Wilson, 1985b; Hulse, 1983; Anderson, 1985; Burgess, 1985; Perhac, 1972; Fergusson and Ryan, 1984; Archer and Barratt, 1976). The increase in metal concentration with decreasing particle size does not appear to be linear, as demonstrated by Burgess (1985) who observed minima in the 83-44 μm and 213-165 μm particle size fractions and a maxima in the 165-111 μm range. Fergusson (1987) also observed a minima in the 165-111 μm range while Stewart (1984) reported the same effect being widespread in street dust samples. Salomons and Förstner (1984) explain minima in metal concentrations in geological samples by the domination of metal-poor quartz in the silt-fine sand fractions. The influence of the organic content of sediments on metal concentrations will vary from sediment to sediment and metal to metal. This will be discussed to a limited extent in this chapter.

The purpose of this section of work is to examine the particle size distribution from 63 μm to <1μm to see if behaviour similar to that described above occurs. The relationship of metal concentration to organic content and to hydrated iron manganese oxides will also be examined.

4.2 SAMPLE PREPERATION AND ANALYSIS

4.2.1 Sample Origin

The main sample used in this study was a composite made by batching three surface samples previously collected from the storm water drain at the intersections of Kidbrooke St., Dyers Rd., and Charlesworth St. with Linwood Avenue. The sample was wet sieved through a 63 μm nylon sieve to separate the clay and silt fraction from the sand fraction. After drying at 60 °C for approximately 70 hours the sample was crushed and prepared for subsampling. A separate sample was also taken from a site 40m downstream of St. John St. a few months later.

4.2.2 Subsampling and Analysis

Subsamples were obtained by using the pipette technique described by Lewis (1981). The method was modified by using sodium carbonate rather than sodium hexametaphosphate (calgon) as the dispersant, as doubts have been expressed about the reliability of calgon as a dispersant (Deely, pers. comm.1987; Hulse, pers. comm.1987). Each subsample contains a representative quantity of all particle sizes finer than a certain limit. Thus the 44 μm sample contains all particle sizes finer than 44 μm, the 32 μm size fraction contains all particle sizes finer than 32 μm and so on. The results of the pipette analysis can be seen in **Table 4.0**, where ss denotes the subsample; weight %, the % of each fraction in the total sample; and cum. weight %, the cumulative weight % of fractions in the total sample.

Each sample was separated into two portions by placing a section of an acid washed microscope slide into the bottom of each beaker, and then adding the slurry from the pipette. After the sample had been dried the slides were suitably mounted and used for XRD analysis. The material remaining in the beaker was digested in concentrated HNO_3 /40% HF and filtered into 25 ml (samples 1-5), 10 ml (6,7), or 5 ml (8,9) volumetric flasks. The solutions were then analysed by flame AAS in the manner described. No value for manganese in sample 9 was obtained as there was insufficient sample available for the standard additions method to be used, and reliable results could not be obtained using ETAAS.

Table 4.0 Pipette Analysis Results.

ss	phi(ϕ)	μm	mass (g)[1]	ϕ fraction	mass fraction[2]	mass fraction l^{-1}[1]	weight %	cum. weight %[3]
1	4.0+	63	0.4158	4.0-4.5	0.0658	3.29	16.62	16.62
2	4.5+	44	0.3500	4.5-5.0	0.0324	1.62	8.19	24.81
3	5.0+	32	0.3176	5.0-5.5	0.0539	2.69	13.62	38.43
4	5.5+	22	0.2637	5.5-6.0	0.0390	1.95	9.85	48.28
5	6.0+	16	0.2247	6.0-7.0	0.0859	4.29	21.70	69.98
6	7.0+	7.8	0.1388	7.0-8.0	0.0674	3.37	17.03	87.01
7	8.0+	3.9	0.0714	8.0-9.0	0.0332	1.66	8.39	95.40
8	9.0+	2.0	0.0382	9.0-10.0	0.0101	0.505	2.55	97.95
9	10.0+	<1	0.0281	10.0+	0.0081	0.405	2.05	100.00

1 uncorrected for Na_2CO_3 content, 20ml sample.

2 corrected for Na_2CO_3 content.

3 obtained by using (mass sample/l (mass sample x 50) -1) x 10

4.3 TRACE METAL CONCENTRATION- PARTICLE SIZE CORRELATION

4.3.1 Results: Particle Size, Organic Matter Distribution

The particle size distribution for the composite sample is shown in **Figure 23**. Shown also is the particle size distribution for the single sample. The purpose of the second sample was to find out whether or not it had a different particle size distribution to that of the composite sample i.e. to see whether the composite sample was representative of individual samples. As may be seen from **Figure 23**, the overall patterns are remarkably similar, notably a sharp drop in both curves at 22 μm (5.5 ϕ) which is at the centre of the medium silt size range. Since the single sample was collected in the spring, whereas the composite sample was collected before the winter, the higher percentage of coarse and medium silt in the single sample may, in the absence of obvious sediment inputs between sampling sites, be due to increased surface water runoff rates during the winter season carrying the larger particle sizes down the drain.

The organic matter distribution between fractions is presented for the two samples in **Figure 24**. The method of calculation used for these results is the same used for the individual metal ions described below. Again, while actual distributions differ, the patterns are similar. The main difference being that the single sample shows a rapid increase in organic matter content below 17 μm. This is not unexpected as decomposing plant and animal matter is common in this area of the drain. An interesting feature to note is the sharp drop in the organic matter content in the 22-17 μm fraction and the rise in the 45-32 μm fraction for both samples.

4.3.2 Results: Trace Metal Distribution

The trace metal concentrations were determined on the basis of corrected sample mass (i.e. mass of Na_2CO_3 added as a dispersant was subtracted). From this the metal ion concentration in each size fraction was determined using the following steps.

[M] μg g^{-1} x mass (corrected) of analysed subsample = μg M in subsample

μg M in $subsample_1$ - μg M in $subsample_2$ = μg M in $fraction_1$

μg M in $fraction_1$ ÷ fraction weight (corrected) = [M] μg g^{-1} in $fraction_1$

The results of these calculations are presented in **Table 4.3**. Negative concentration values were obtained occasionally and may arise in two ways. Firstly, if the subsample containing the larger particle sizes has a lower trace metal concentration than that of the one immediately following (due to dilution by quartz, feldspar, lithic or carbonate grains) then a negative value is to be expected. Secondly, because of the small

quanities of material analysed, and the number of operations performed on each sample accumulation of experimental errors could result in a small positive value becoming negative.

4.3.3 Discussion

The variation in the trace metal concentration with size fraction is expressed graphically in **Figure 25**. The results have been presented in order to group metals which show a similar pattern of variation. The groupings are Pb-Zn-Cu, Ni-Cr, and Fe-Mn. Whereas iron and manganese follow a similar pattern there are also differences. The minima and maxima for manganese are in general one fraction behind those for iron. Iron and manganese correlate negatively with each other (i.e. when the concentration of one increases the other decreases). The only major departure within the patterns for Pb, Zn and Cu is the maxima for lead in fraction 7 (4-2 μm) whereas both zinc and copper have minima. No obvious association for the lead-zinc-copper grouping with a transport mode has been found. Nickel and chromium follow each other closely from fraction 5 (16 μm) downwards, whereas at particle sizes larger than 16 μm the minima and maxima are again one size fraction out of phase. Another intersting feature to note is that there is also a similarity between iron and chromium on the one hand and manganese and nickel on the other. This suggests that hydrated iron oxides act as a scavanger for chromium, and hydrated manganese oxides for nickel. In their excellent review Metals in the hydrocycle Salomons and Förstner (1984) report that nickel,copper, and zinc associate with manganese in freshwater iron-manganese nodules, while Bowen (1979) found that hydrous iron oxides strongly absorbed chromium and that hydrous manganese oxides carried some nickel. Certainly in this work the correlation coefficient between iron and chromium is stronger than that between manganese and nickel (**Table 4.1**).

Correlations to note in **Table 4.1** are: Cu-Zn (0.805, 0.02, 7)*, Mn-Cu (0.745, 0.05, 6), Fe-Cr (0.781, 0.05 [just below 0.02], 7), Pb-Zn (0.681, 0.1, 7), Pb-Ni (0.695, 0.1, 7), Ni-Cr (0.688, 0.1, 7), and Mn-Fe (-0.674, 0.1, 6). Although most of the pairs above do not correlate strongly they do have a similar pattern of variation and it is possible that if the sample size was increased a better correlation would be obtained.

Surprisingly only two metal ions correlated with organic material. Chromium (0.636, 0.1, 6) and manganese (0.621, 0.1, 6). The correlation with chromium is most likely to be a false one as a plot of chromium concentration vs. organic material yields a cluster of seven points and one outlier, essentially yielding a line between two points. If the outlier is removed the correlation disappears. The graph of relative % organic material per fraction for the composite sample (**Fig. 24**) does however resemble the corresponding manganese graph.

* Using the format (r=correlation coefficient, p<n%, df=degrees of freedom)

Table 4.1 Metal-Metal and Metal-Organic Correlations*

	Cu	Cr	Fe	Mn	Ni	Pb	Zn	%Org.
Cu	1.000							
Cr	0.398	1.000						
Fe	0.121	0.781	1.000					
Mn	0.745	0.141	-0.674	1.000				
Ni	0.396	0.688	0.566	0.596	1.000			
Pb	0.394	0.533	0.327	0.276	0.695	1.000		
Zn	0.805	0.353	0.041	0.458	0.294	0.681	1.000	
%)rg.	0.352	0.636	-0.037	0.621	0.323	0.251	0.274	1.000

* Pearson's correlation coefficient is used throughout this work.

4.4 POWDER XRD ANALYSIS OF SAMPLES

4.4.1 Results

After mounting on a glass slide subsamples were analysed in the manner described in Section 6.4.3. Identification of minerals was carried out by comparison of the d-values for the sample pattern with either literature values (JCPDS, 1980; Brindly and Brown, 1980) or standard samples certified against American Petroleum Institute Clay Mineral Standards Project No. 49 (**Figs. 26-29**).

Peaks at d=4.24, 3.34, 2.45, 2.28, 2.12, 1.95, and 1.82 Å have been identified as arising from quartz. Illite peaks have been identified at d=9.85, 4.96, 4.49 Å and with less certainty at d=3.53, 2.57, and 1.95 Å. Chlorite peaks were identified at d=14.34, 7.06, and 4.74 Å and with less certainty at d=3.53, 2.64, 2.04 Å. Uncertain peak identification was caused by peaks close to, or overlapping each other (e.g. illite 3.33 and quartz 3.34 Å) or alternatively too small an intensity to be reliably identified.

The XRD patterns for the 4.0+ ϕ, 9.0+ ϕ, and 10.0+ ϕ subsamples are given in **Figures 30, 31, 32** respectively. The most significant change to occur in the progression from 4.0+ ϕ to 9.0+ ϕ is the marked reduction in the intensity of the quartz peaks. The pattern for 10.0+ ϕ (**Fig. 32**) is however quite different in character. The quartz peaks have virtually disappeared with the small peak to the left of the peak at d=3.25 Å possibly representing the I=100% quartz peak. No identification of the 10.0+ ϕ pattern could be made by comparison with either data files or standards. However, the general form of the pattern is similar to both the data file and the calculated patterns for

illite-clay interlayerings. It seems probable that the pattern is a result of the interlayering of illite and chlorite, possibly in a disordered manner and possibly with organic material playing some role (the sample was approximately 35% organic material). In sediments chlorite is often found as mixed layer structures with other clay minerals (Shelly, 1975). Montmorillinite can be ruled out as being a possible member of the mixed layer structures as exposure of the sample to ethylene glycol (which would have produced a shift to a higher d-value for the peak at d≈14.36 Å) and heat (which would have had the reverse effect) did not produce the expected d-value changes in the pattern.

4.4.2 Discussion

The reduction in quartz mentioned above does not occur uniformly, as may be seen from the data in **Table 4.2** which gives the intensity in c.p.s. of the I=100% peak for quartz, illite, and chlorite. Because of the good identification achieved for quartz it has been assigned as the internal standard against which other minerals may be compared. This comparison is a relative one only, as a number of factors can affect the intensity of the diffracted beam. In addition the amount of quartz present in each subsample varies making quantitative interpretation of results impossible.

Table 4.2 Intensity of I=100% Peaks for Quartz, Illite, and Chlorite.

subsample	Quartz		Illite			Chlorite		
	c.p.s.	%v	c.p.s.	%q	%v	c.p.s.	%q	%v
1	7819	100.0	2201	29.4	100.0	2058	26.3	100.0
2	7469	95.5	2315	31.0	100.6	1863	24.9	90.5
3	6868	87.8	2584	37.6	112.3	2177	31.7	105.8
4	6444	82.4	1859	28.8	80.8	1683	26.1	81.8
5	5911	75.6	2285	38.7	99.3	1958	33.1	95.1
6	7225	92.4	2094	29.0	91.0	1965	26.1	95.5
7	4520	57.8	2026	44.8	88.0	1422	31.5	69.1
8	2073	26.5	1891	91.2	82.2	1325	63.9	64.4
9			37837?			37837?		

%v: relative to mineral in subsample one.

%q: for illite and chlorite, relative to quartz in corresponding subsample; for quartz relative to I=100% peak in subsample one.

When the values of %v (for quartz) and %q (for illite and chlorite) are plotted (**Fig. 33**) a clear inverse relationship can be seen from 6.0+ ϕ onwards for quartz relative to the clay minerals. If the change in %v or %q for each mineral are calculated and plotted as Δ% illite, chlorite,and quartz (**Fig. 34**) then the inverse relationship

becomes slightly clearer and illite and chlorite show a close correlation (0.982, 0.001, 5) in their pattern of variation. Illite and chlorite show Δ% maxima in the 44-32 μm, 22-16 μm fractions with a steady rise for particle sizes finer than 4 μm (the beginning of the clay size fraction). Quartz follows the reverse pattern with slight minima at 44-32 μm and 22-16 μm, a sharp rise in the 8-4 μm range (very fine silt), and a sharp decline as the clay size fraction begins.

4.5 CONCLUSIONS

Although the concentrations of the metal ions increase with decreasing particle size this appears to be due to the decrease in the quantity of quartz present (which is frequently low in metal ion concentration), rather than increasing quanities of metal ions. The less quartz that is present the more the sample is composed of clays and iron-manganese hydrated oxides. The only metals to show marked increases at finer (<2 μm) size fractions were iron and manganese. This is likely to be colloidal material and coatings on clay particles (the negatively charged clay particles act as nucleation centres for the formation of the hydroxides). Three factors influence the variation of metal concentration with particle size. The first is the speciation which is an important factor in metal ion transport and distribution, i.e. whether the metal is bound to clay, or iron-manganese oxyhydrates, or organic matter. The second factor is the particle size, which influences the surface area available for metal ion transport. Smaller particles have a larger surface area available. The third factor is the quanity of quartz. It appears that quartz is the dominating factor until approximately the 8-4 μm size range. For particle sizes finer than this the effective surface area and metal speciation appear to become dominant.

The impact of organic matter on metal ion distribution is not clear. Although the proportion of organic matter does not correlate well with most metals it has features in common with the particle size distribution and with the % clay variation. In the first case a sharp drop at 5.5+ ϕ for both organic and mineral matter probably represents a transportation barrier, or fractionation of particle sizes during the repeated erosion-transportation-deposition cycle before final sedimentation. Whereas in the second case there is a sharp increase at < approx. 8 μm. This is not surprising as organic material is known to form coatings on clay particles and Fe-Mn hydrated oxides.

Table 4.3 Size Fraction Analysis Results.

subsample	[M] μg g^{-1}	μg in subsample	μg in fraction	[M] μg g^{-1} of size fraction
Mn				
1	1161	240	-33	-502
2	1755	277	120	3704
3	1079	157	-74	-1373
4	2007	231	-23	-590
5	2410	254	191	2224
6	1209	63	8	119
7	1897	55	-17	-512
8	7078	72	72	7129
9	-	-	-	-
Fe	%			%
1	4.67	9653	1148	1.74
2	5.39	8505	459	1.42
3	5.53	8046	3016	5.60
4	4.37	5030	-71	-0.18
5	4.84	5101	869	1.01
6	8.17	4232	1473	2.19
7	9.48	2759	1664	5.01
8	10.74	1095	-135	-1.34
9	24.12	1230	1230	15.19
Pb				
1	103	21.3	-1.6	-24.3
2	145	22.9	-2.1	-64.8
3	172	25.0	-1.2	-22.3
4	228	26.2	3.7	94.9
5	213	22.5	10.0	116
6	242	12.5	2.0	29.7
7	360	10.5	6.9	208
8	352	3.6	1.9	188
9	342	1.7	1.7	210

Table 4.3 continued

subsample	[M] μg g^{-1}	μg in subsample	μg in fraction	[M] μg g^{-1} of size fraction
Zn				
1	145	30.0	2.5	38.0
2	174	27.5	-13.0	-401
3	279	40.5	0.4	7.4
4	349	40.1	-7.5	192
5	451	47.6	23.6	275
6	464	24.0	13.5	200
7	360	10.5	-0.5	-15.1
8	1079	11.0	7.6	752
9	663	3.4	3.4	420
Cu				
1	38.9	8.0	2.0	30.4
2	38.2	6.0	0.1	3.1
3	40.6	5.9	1.5	27.8
4	37.9	4.4	0.4	10.3
5	38.4	4.0	1.6	18.6
6	46.7	2.4	1.0	14.8
7	47.7	1.4	-1.0	-30.1
8	236	2.4	1.6	158
9	148	0.8	0.8	98.8
Ni				
1	24.2	5.0	0.5	7.6
2	28.6	4.5	0.8	24.7
3	25.6	3.7	-0.4	-7.4
4	33.3	4.1	0.4	10.3
5	35.1	3.7	1.8	21.0
6	29.2	1.5	-0.4	-5.9
7	65.9	1.9	1.1	33.1
8	73.8	0.8	0.3	29.7
9	96.6	0.5	0.5	61.7

Table 4.3 concluded

subsample	[M] μg g^{-1}	μg in subsample	μg in fraction	[M] μg g^{-1} of size fraction
Cr				
1	48.3	10.0	2.0	30.4
2	50.9	8.0	0.5	15.4
3	51.2	7.5	1.3	24.1
4	54.1	6.2	0.0	0.0
5	59.3	6.2	2.7	31.4
6	67.7	3.5	1.5	22.3
7	68.7	2.0	1.2	36.1
8	73.8	0.8	0.3	29.7
9	96.6	0.5	0.5	61.7

Figure 23 Particle Size Distribution, Single and Composite Samples

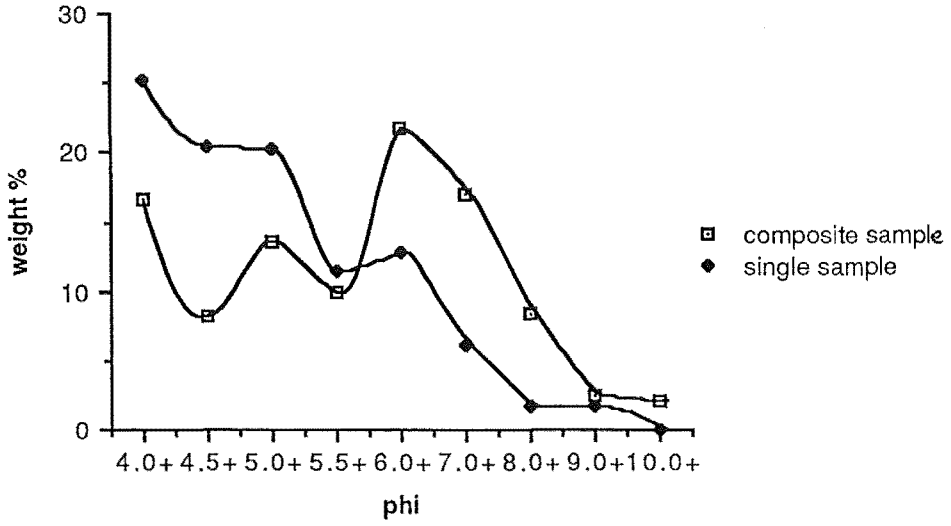

Figure 24 Organic Matter Distribution, Single and Composite Samples

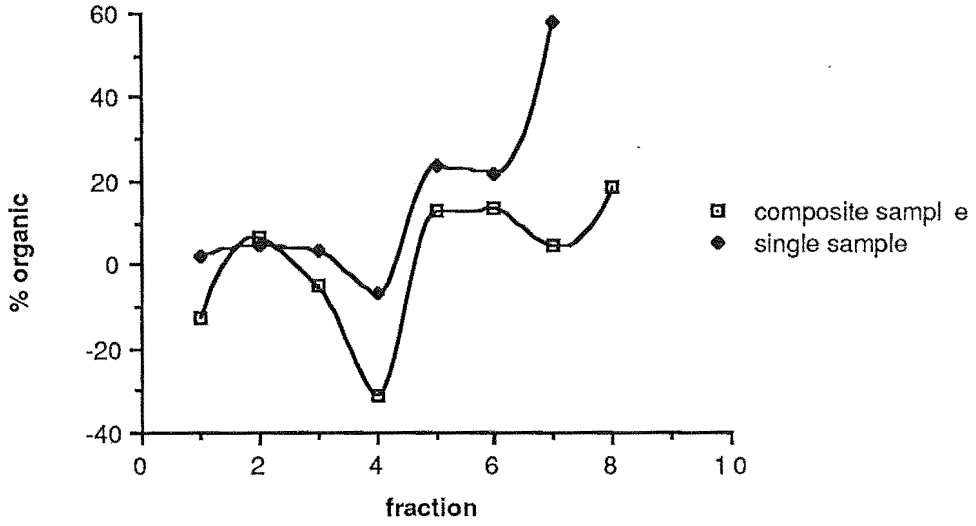

Figure 25 Change in Metal Concentration with Size Fraction

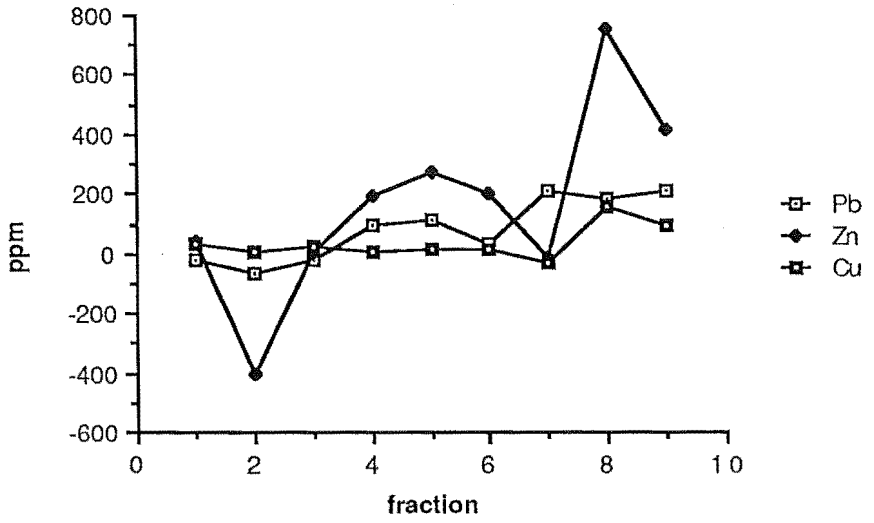

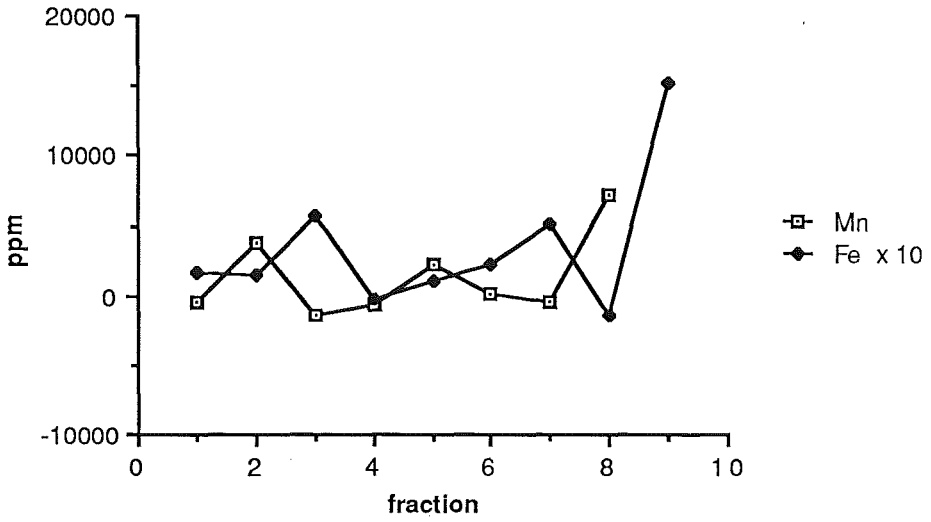
20000
10000
0
-10000
ppm
0
2
4
6
8
10
fraction
Mn
Fe x 10

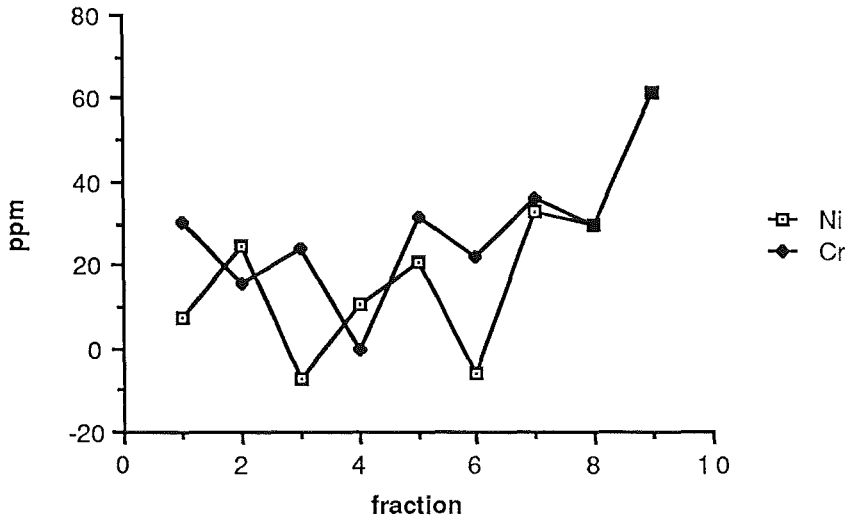
80
60
40
20
0
-20
ppm
0
2
4
6
8
10
fraction
Ni
Cr

Figure 26 Quartz standard

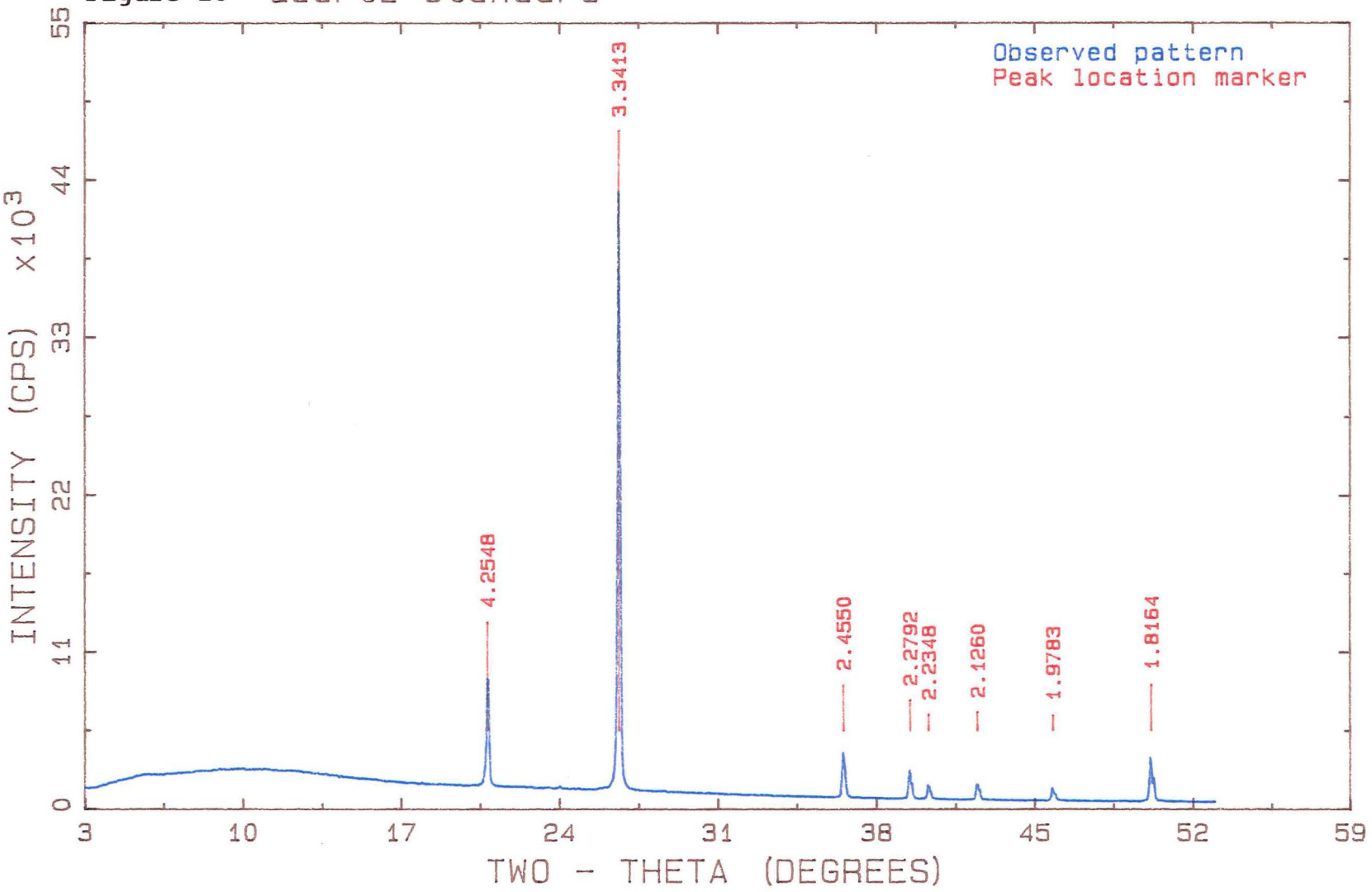

Figure 27 Illite standard

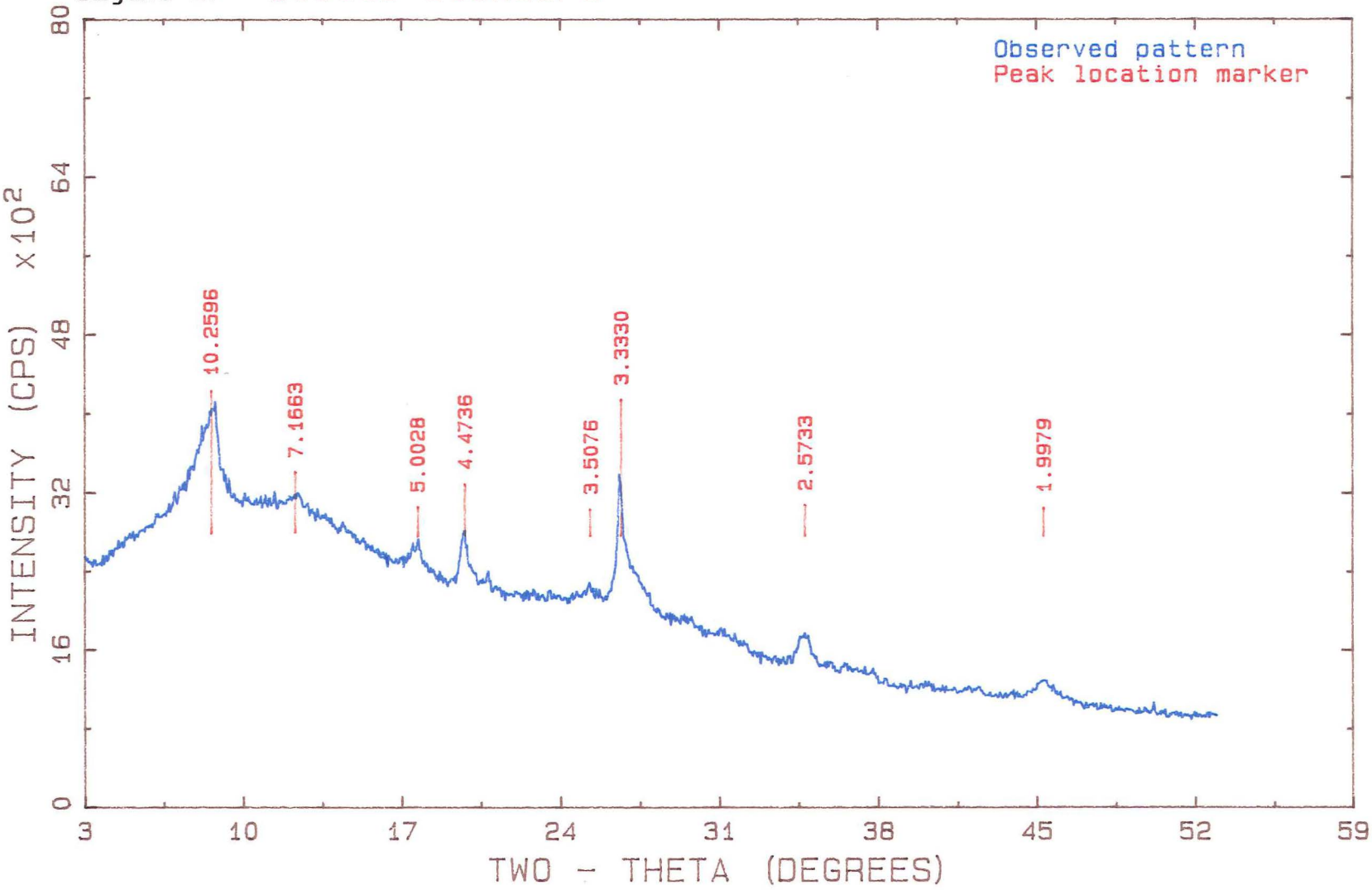

Figure 28 Montmorillinite standard

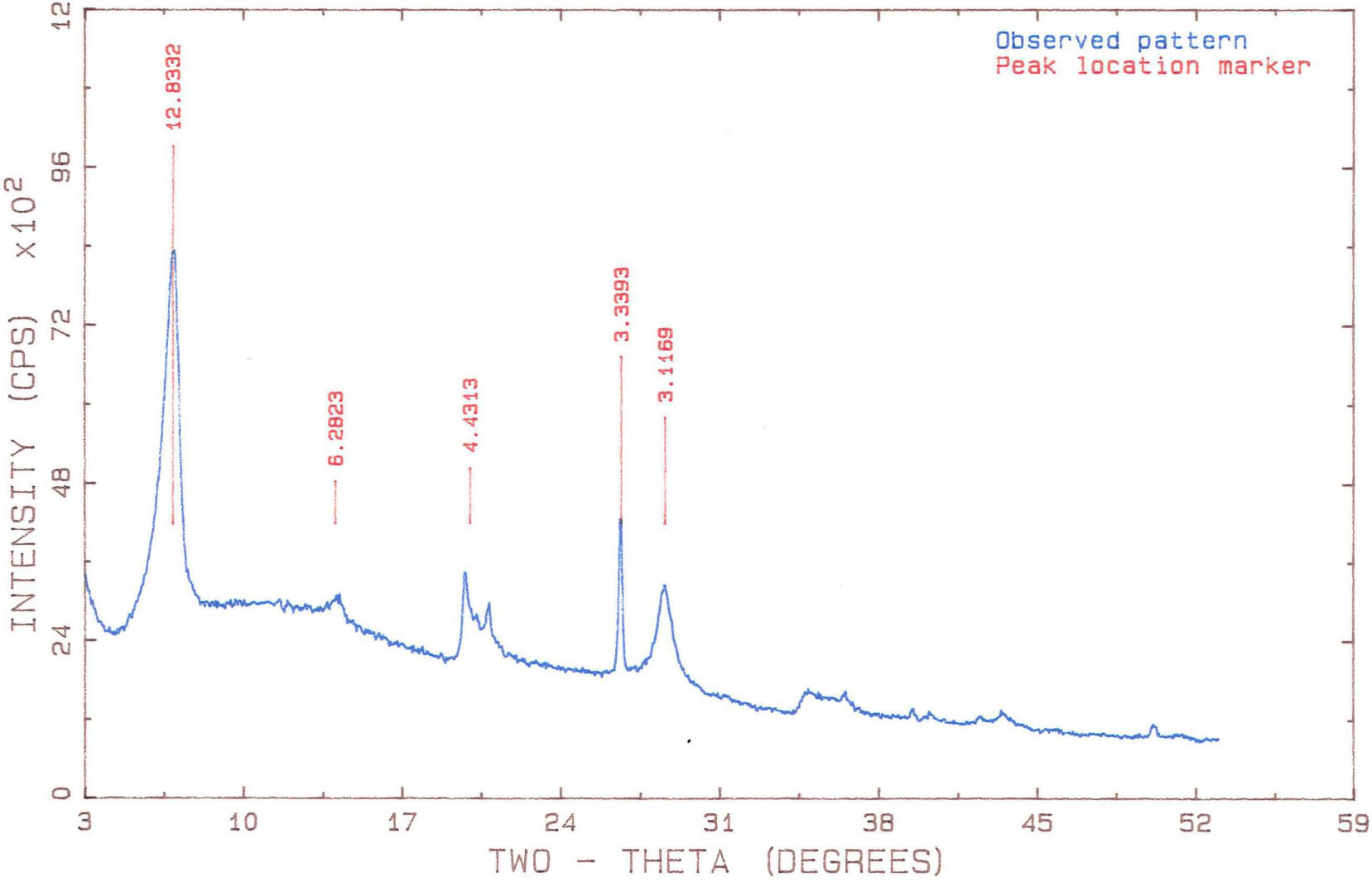

Figure 29 Kaolinite standard

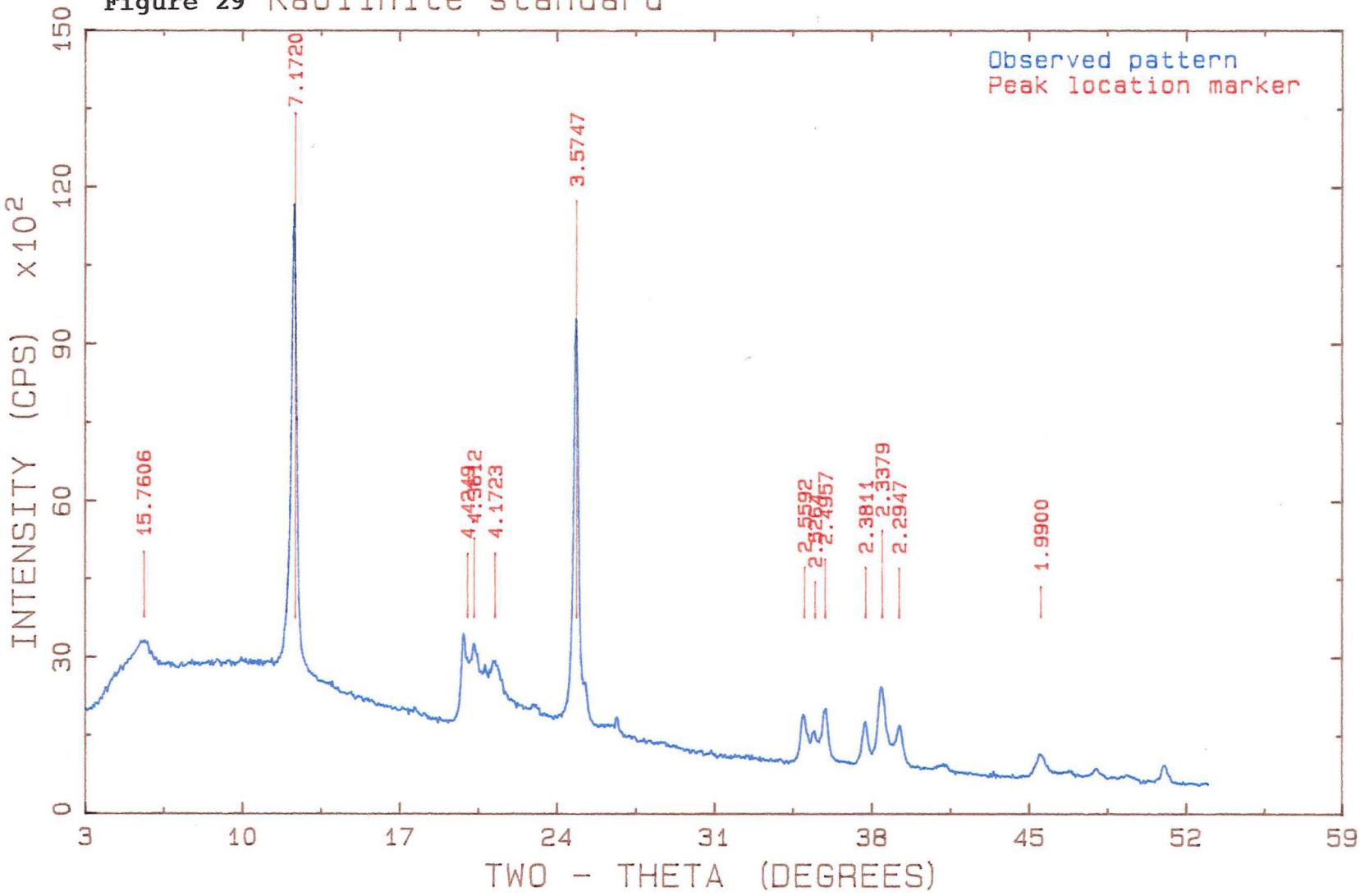

Figure 30 4+ Phi

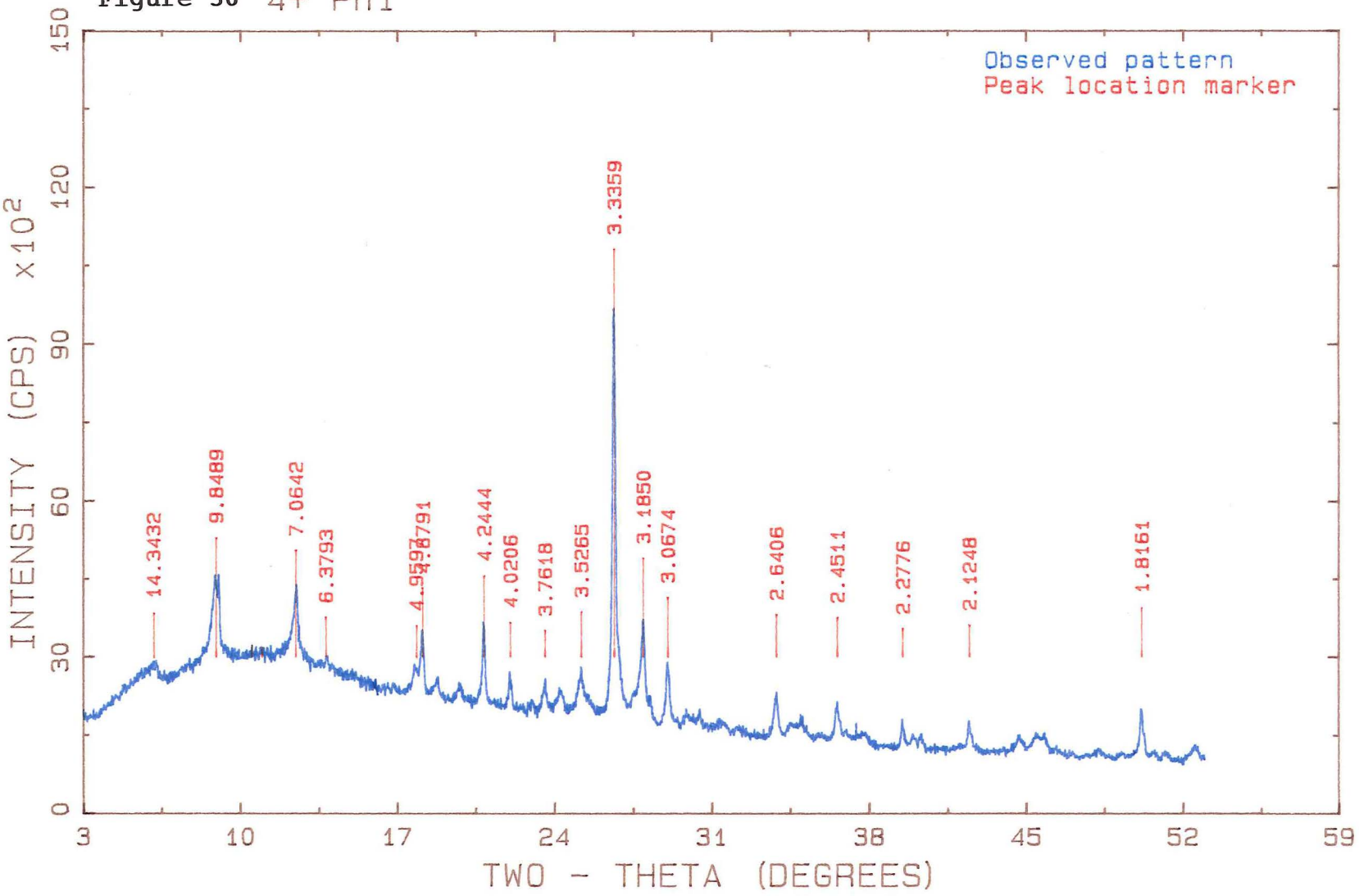

Figure 31 9+ Phi

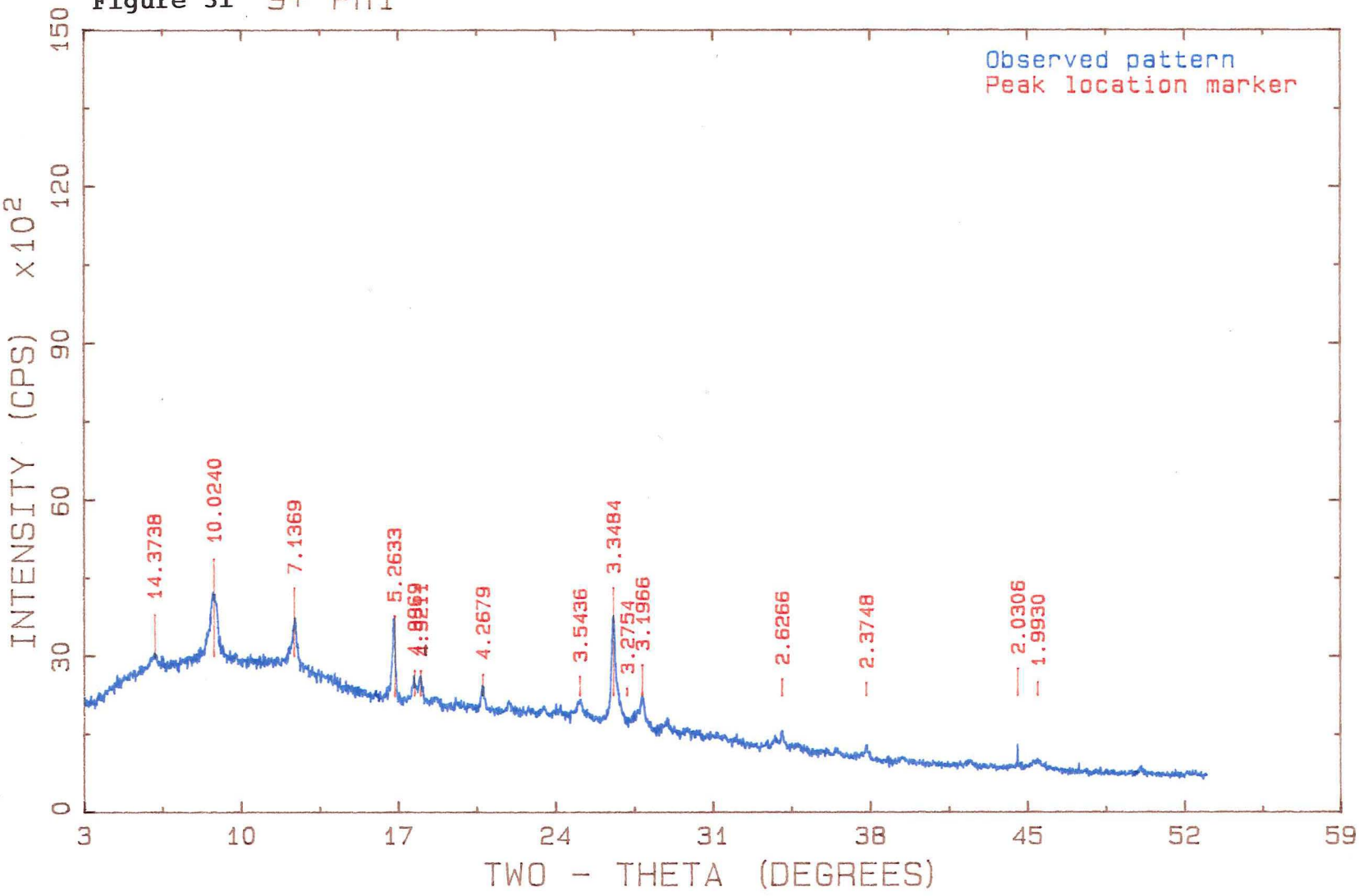

Figure 32 10+ Phi

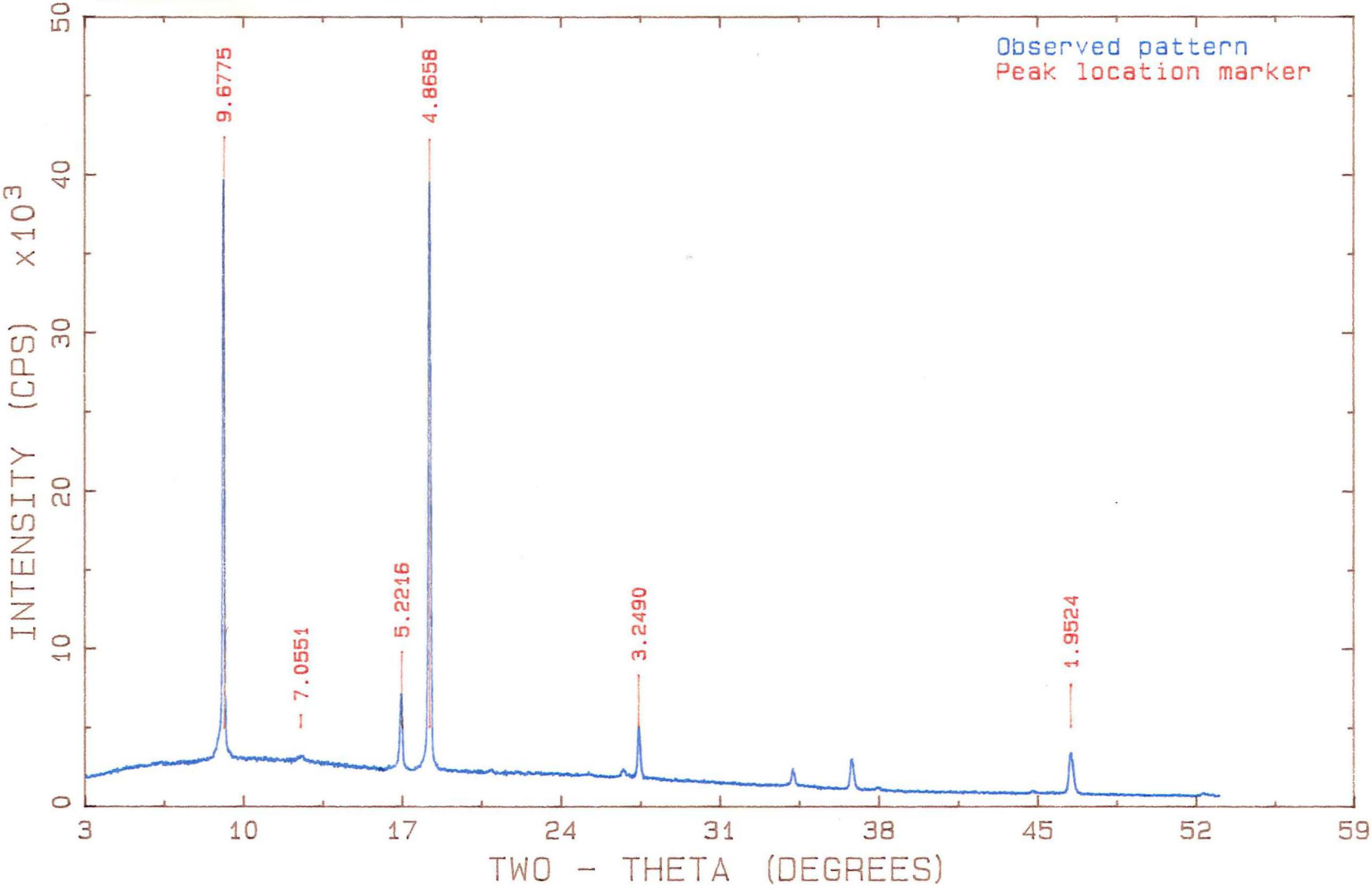

Figure 33 %v Quartz, and %q Illite and Chlorite

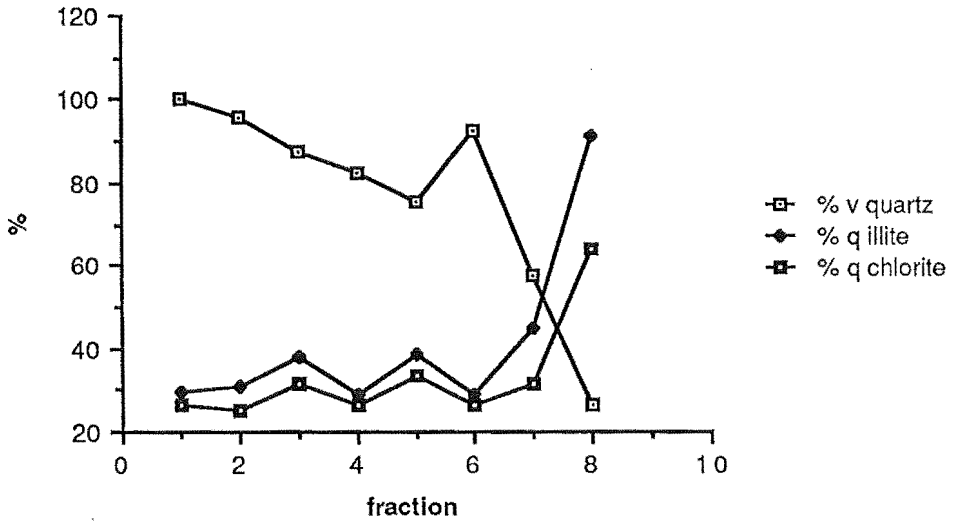

Figure 34 Δ % for Quartz, Illite, and Chlorite

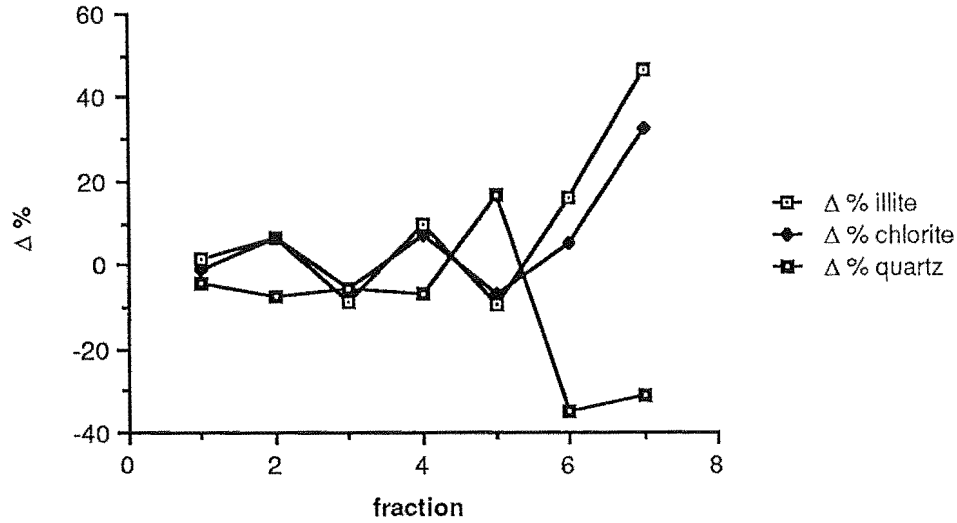

CHAPTER V

EVALUATION OF RESULTS AND CONCLUSIONS

5.1 INTRODUCTION

The purpose of this chapter is to evaluate the results descibed in earlier sections in terms of background levels, enrichment factors, and any trends observed with location, particle size, or other parameters. In addition, areas of further research are suggested and briefly discussed where appropriate.

5.2 BACKGROUND LEVELS AND ENRICHMENT FACTORS

5.2.1 Introduction and Results

Both local and internationally recognized background levels were considered for use in this study. A large number of background levels are available in the literature, often based on "average composition", as well as natural sediments (Bowen, 1979; and deGroot et al., 1976 give backgrounds derived from "average" and natural sediments respectively). For the reasons mentioned in Section 6.5.3, a local set of background values was preferred. Unfortunately, no such set existed, however a partial set, consisting of Fe, Mn, Cr, Ni, Zn, and Ba (and also Ce, La, Nd, V, and Zr), was obtained by averaging the results supplied by Lobb (pers. comm., 1987), for 3 sandstones, 1 mudstone, and 2 river sands from the Torlesse Group in the Canterbury region. A summary of these results for the elements Ba, Cr, Fe, Mn, Ni, and Zn is given in Appendix C.

Enrichment factors have been calculated in the manner described in Section 6.5.3, using Ba, Mn, and Fe as the conservative elements. Barium is considered to give the best results, unfortunately however, this element was analysed by XRF only, and, due to the sample size required, could not be determined in the sand, silt, and clay size fractions. Comparison of the enrichment factors obtained for the total samples led to the choice of iron as the next best conservative element for the calculation of enrichment factors in the sand silt, and clay size fractions, as iron was less enriched than manganese. The data in **Table 5.0** is a list of enrichment factors for all total samples with respect to barium, whereas **Table 5.1** contains the enrichment factors for total samples with respect to manganese, and **Table 5.2** contains enrichment factors for all samples with respect to iron.

Although lead was not one of the elements determined in local crustal material, enrichment factors have been calculated, with respect to iron, using the background value of 19 ppm given in Table 3.5 of Bowen (1979).

5.2.2 Discussion of Calculated Enrichment Factors

An enrichment factor of 3 has been chosen as representing a significant level of enrichment above the local crustal values. Caution should be excercised in the interpretation of these results, as the local crustal values are for the total sample. Thus enrichment factors for the size fractions are relative to the total crustal value, not to the corresponding background sand, silt, or clay. This is expected to make the greatest difference to the clay size fraction, which is mineralogically the most dissimilar to the total sample, and has a largely different mechanism of metal binding. A slight effect, due to particle size, is expected for the silt size faction, as this fraction has a significantly larger surface area for the development of Fe/Mn oxyhydrates than the sand size fraction, for which a slight lowering of the enrichment factor is expected.

Only manganese, lead, and zinc are enriched above the proposed threshold level. Nickel, although occasionally enriched to the 1.6-1.9 range never climbed above this, and even if the disparity between Chromium results by AAS and XRF are allowed for, by adding 46% to the enrichment factors (see Section 2.4.5), only three samples approached or passed the threshold level (RH2/8ac, 13.2/1c, and 13.2/3c).

Lead is the most often, and also the most highly enriched element (22 samples, see **Table 5.2**), with manganese the second most often enriched (16 samples), and zinc third (13 samples). Zinc however, is consistently more highly enriched than manganese. The reason for this is largely that lead is present at much lower levels in uncontaminated and unmineralised rocks than either zinc or manganese. Likewise, zinc is found at lower concentrations in crustal rocks than manganese, but is enriched only at, or near, the surface in the cores studied, suggesting that zinc pollution is of more recent origin than lead pollution. In contrast to both lead or zinc, manganese enrichment is low level (typically 3-3.5, and never higher than 4.94 for enriched samples) and spread almost uniformly throughout the cores with depth.

For all metals there is a trend towards decreasing enrichment in a downstream direction. This is best exhibited by lead, with enrichment factors of 15.0, 12.3, 7.9, 6.1, and 1.2, for the mean of all surface samples, RH3/1, RH1/1, RH2/2, and 13.2/1 respectively. In reality the enrichment factors of the surface samples at RH1 and RH2 will be higher, as RH1/1 is (as mentioned previously) the top 18 cm of the core, and RH2/2 was used rather than RH2/1 in all analyses, as it was suspected that RH2/1 may have become contaminated. The enrichment factors given for the averaged surface

samples will vary markedly depending upon rainfall and the sediment deposition rate (see Chapter 3).

In core RH2, manganese, lead, and zinc follow an almost identical pattern of enrichment, which is also similar to the variation of concentration with depth. All three metals drop markedly in enrichment at the "modern"-unit c boundary, although for lead this is a continuation of the drop from RH2/2 - RH2/8a. Again all three metals peak sharply at RH2/19 (a peak not matched by the concentration versus depth profiles), and again, rather weakly at RH2/21-22. Below this depth the enrichment factor for lead increases, manganese decreases, and zinc remains relatively constant. As the appearance of the sample and concentration of all metals, other than iron, do not change markedly at RH2/19, the high enrichment factors observed at this depth may be an artifact caused by the somewhat lower iron concentration than the samples above and below. However, as the concentration of iron in RH2/19 is within the normal range, and the enrichment factors calculated with respect to barium have the same pattern, it is likely that the calculated enrichment factor represents an actual pollution event.

Comparison of the calculated enrichment factors for Cr, Ni, Mn, Pb, and Zn with particle size fraction leads to the following conclusions. Chromium and nickel are most probably "background" elements. Not only are they seldom, or ever, enriched, but the pattern of enrichment versus size fraction changes from core to core, and even within cores. In the case of manganese cores RH1 and RH2 follow the pattern of enrichment silt > clay > sand, whereas core RH3 was found to have the pattern sand > silt > clay, and core 13.2 the pattern clay > silt > sand. For core 13.2 only the clay size fraction was found to approach the threshold level of 3 for enrichment. The pattern of enrichment factors versus size fraction for the remaining cores gives no firm indications as to a likely primary source of manganese, but rather suggests that manganese may be derived from both large, and small particles (minerals and lithic fragments, and coatings, discrete oxide particles [?], and metal rich particulate [?] respectively). For both lead and zinc the majority of samples were enriched in the order clay > sand > silt, with clay > silt > sand the second most common order of enrichment. Exceptions to these patterns were: lead in core 13.2 (except 13.2/1), RH2/2, and RH2/8b, with the pattern sand > clay > silt; and lead in RH3/3, with the pattern silt > clay > sand. While no clear reason is obvious for the former result, the latter is most probably due, with regard to the sampling location, to fine lead or lead rich particulate. The most common result (clay > sand > silt) is the same as that obtained for the concentration of lead versus size fraction in Section 2.4.2, and in the case of the lead enrichment factors probably reflects that result. The fact that zinc now displays the same behaviour as lead (the concentration of zinc, in contrast to lead declined clay > silt > sand) is reasonable, as lead and zinc correlate strongly, but can still not be explained.

5.3 SUMMARY AND CONCLUSIONS

In this Section three areas discussed earlier are evaluated. These are: (1) how much metal is present ? (2) change in metal concentration with regard to the location of the sample (i.e. depth and site), and (3) metal associations with regard to particle size and statistical correlations with other metals and organic matter.

The study of metals in sediments is complex due to the nature of the matrix, and the relatively low levels of the metals studied. As the bulk mineralogy of the sediments studied is fairly constant, variation in the metal concentrations due to changes in the mineralogy can largely be ignored. The greatest changes in the sediment are the organic matter content and particle size. The conditions in the sedimentary column favour manganese diagenisis, however, the results obtained in this study do not prove or disprove that manganese and other trace metals are being redistributed due to changes in sediment E_h and pH.

The question "how much metal is present?" relates basically to the issue of pollution. There are two differing definitions of pollution. One is to regard any enrichment of a substance above its naturally occurring level at a given site as a pollutant, whereas the other is adequatly summed up in the following quotation.

> *Introduction by man, directly or indirectly, of substances into the marine environment (including estuaries) resulting in such deleterious effects as harm to (sic) living resources, hazards to human health, hinderance to marine activities (including fisheries), impairing the quality for use of seawater and reduction of amenities.*
>
> UNESCO International Oceanographic Commission, as reported by Knox and Kilner (1973).

Clearly, with regard to the first definition, all of the sampling sites used in this study are polluted, although site 13.2 somewhat less so than the others. With regard to the second definition the site of core RH2 also becomes marginal, although should be regarded as polluted. Certainly the metal concentrations at site 13.2 compare favourably with those reported by Taylor (1976) for the Urr Water - a relatively unpolluted estuary in the United Kingdom. The concentrations of all metals, other than nickel, at site RH2 are, however, well above those reported for the Urr Water.

When examining the variation of metal concentrations and enrichment factors with location, a clear trend towards a decrease in a downstream direction may be seen, especially upon entering the estuary. This is considered to be due to dilution by both

water and less contaminated sediment. All cores except RH2 exhibited a decrease in metal concentration with depth. Core RH2 must be considered separately, as it is the only core collected to contain the top three of MacPherson's units (see **Table 1.1**). While the variation in metal concentration at this site, and other sites (Deely, 1987), lend support to, and the variation in enrichment factors for core RH2 do not contradict, MacPherson's hypothesis of sediment deposition in the AHE, neither do they confirm it as being correct. For a more positive stance to be taken, a dating of the upper and lower contacts of unit c is required.

The variation of metal concentration with particle size largely follows the expected trend of clay > silt > sand. The most notable exceptions are lead and zinc, which largely follow the pattern clay > sand > silt. The reason for this has not yet been determined and may be due to metal rich particulate, organic matter, or, given the complexity of most natural systems, a combination of these and other factors.

The metals chromium, copper, nickel, and iron are regarded as deriving largely from natural sources, with only slight, and occasional, enrichment above natural levels. Manganese has the characteristics of an element derived in significant quantities from both natural and anthropogenic activities. Zinc, and in particular lead, are derived largely from anthropogenic activities, most probably leaded petrol and galvanised roofing iron repectively.

5.4 RECOMMENDATIONS FOR FURTHER RESEARCH

The role of organic matter and iron/manganese hydrated oxides has not been determined in this, or other, studies on the Avon - Heathcote Estuary. The available evidence suggests that these components of the sediment play a major role in the heavy metal transport and binding, and therefore warrant more detailed study.

A method for the sequential extraction of trace metals from sediments has been reported by Tessier et al. (1979). No sequential extraction techniques were used in this study however, largely due to the doubts raised about the selectivity of the reagents used, and redistribution of trace metals during extraction (Kheboian and Bauer, 1987). It would be useful if a sequential extraction procedure could be developed that at least minimised the problems discussed by Kheboian and Bauer, and could then be calibrated against AHE sediments with a range of % clay, and % organic matter.

As mentioned in earlier sections the interpretation of the concentration versus depth profiles of this study, and MacPherson's interpretation of the AHE sediment units, is limited by the lack of dated horizons in the sediment column. An attempt to date Core RH2 using the ^{210}Bi "daughter" of ^{210}Pb in this study was discontinued due to time

constraints. A better technique, though having a longer ingrowth time, is the use of the ^{210}Po "grandaughter" of ^{210}Pb. Care must be taken however, that the site chosen for dating has not been subject to erosion, or that the amount eroded is accurately known.

A method for the removal of metal ions from natural waters by glauconitic greensand has been described by Spoljaric and Crawford (1978). Greensands are found near Christchurch in the Waipara Valley area (Wilson, 1963; Browne and Field, 1985). An interesting, though not entirely chemistry oriented, project would be to study the efficiency and viability of using local greensand to filter Christchurch storm water and treated sewage effluent.

Table 5.0 Enrichment Factors for Total Samples with Respect to Barium

sample	Cr	Fe	Mn	Ni	Zn
surface*	0.9	1.6	5.8	1.2	14.4
RH3/1	0.7	0.8	3.3	0.7	10.4
RH3/3	1.1	1.4	3.9	1.2	18.4
RH3/4	0.8	1.5	3.4	1.0	9.6
RH3/5	0.6	1.1	2.8	0.8	1.9
RH3/8	0.6	1.3	2.9	0.8	1.5
RH3/9	0.7	1.4	4.5	0.7	0.9
RH3/10	0.7	1.5	5.6	0.9	1.3
RH3/11	0.7	1.4	5.0	1.1	1.3
RH1/1	0.7	0.8	1.3	1.8	3.4
RH1/3	0.6	0.9	1.7	1.7	2.6
RH1/6	0.5	0.8	2.0	1.5	0.9
RH1/9	0.5	0.6	1.2	1.5	0.5
RH1/12	0.3	0.7	0.8	1.3	0.4
RH1/14	0.4	0.8	1.6	1.2	0.5
RH2/2	1.1	1.5	4.8	0.5	2.5
RH2/8a	-	-	-	-	-
RH2/8b	0.7	2.0	2.7	0.7	0.6
RH2/16	0.7	1.3	3.0	0.8	0.6
RH2/19	0.8	1.2	5.6	0.9	1.1
RH2/20	0.7	1.0	1.1	0.6	0.6
RH2/21	-	-	-	-	-
RH2/22	0.9	2.7	3.8	1.0	0.9
RH2/23	1.1	2.2	3.5	1.1	1.2
RH2/27	0.7	1.0	1.1	0.6	0.6
13.2/1	0.9	0.8	0.6	0.6	1.3
13.2/3	1.1	1.1	0.6	1.0	1.2
13.2/5	1.0	1.2	0.9	1.1	0.9
13.2/7	1.0	1.0	0.8	0.8	0.6

*taken from the mean of all surface samples.

Table 5.1 Enrichment Factors for Total Samples with Respect to Manganese

sample	Cr	Fe	Ni	Zn
RH3/1	0.2	0.2	0.2	3.2
RH3/3	0.3	0.4	0.3	1.8
RH3/4	0.3	0.5	0.3	2.8
RH3/5	0.2	0.4	0.3	0.7
RH3/8	0.2	0.4	0.3	0.7
RH3/9	0.2	0.3	0.2	0.2
RH3/10	0.1	0.3	0.2	0.2
RH3/11	0.1	0.3	0.2	0.3
RH1/1	0.5	0.7	1.3	2.5
RH1/3	0.4	0.6	1.0	1.6
RH1/6	0.2	0.7	0.7	0.5
RH1/9	0.4	0.5	1.0	0.4
RH1/12	0.7	0.9	1.6	0.5
RH1/14	0.3	0.6	0.8	0.3
RH2/2	0.2	0.3	0.1	0.5
RH2/8a	0.3	0.3	0.3	0.5
RH2/8b	0.3	0.5	0.3	0.2
RH2/16	0.2	0.4	0.3	0.2
RH2/19	0.1	0.2	0.2	0.2
RH2/20	0.1	0.4	0.1	0.2
RH2/21	0.2	0.4	0.2	0.2
RH2/22	0.3	0.4	0.3	0.2
RH2/23	0.3	0.6	0.3	0.3
RH2/27	0.6	0.9	0.6	0.5
13.2/1	1.5	1.3	0.9	2.2
13.2/3	1.8	1.7	1.6	2.0
13.2/5	1.1	1.3	1.2	0.9
13.2/7	1.2	1.3	1.0	0.8

Table 5.2 Enrichment Factors for All Samples with Respect to Iron

sample	Cr	Mn	Ni	Zn	Pb
surface*	0.6	3.7	0.8	9.1	15.0
RH3/1	0.9	4.4	0.9	13.7	12.3
RH3/3	0.8	2.9	0.9	13.6	26.3
RH3/3s	0.7	4.2	0.6	17.1	21.8
RH3/3z	0.8	3.4	0.9	16.0	93.7
RH3/3c	0.8	3.1	1.8	22.3	41.7
RH3/4	0.6	2.2	0.7	6.2	10.7
RH3/5	0.6	2.6	0.7	1.8	2.2
RH3/5s	0.5	4.1	0.4	1.7	2.1
RH3/5z	0.5	3.1	0.4	1.3	3.0
RH3/5c	0.6	3.4	1.1	3.2	4.6
RH3/8	0.5	2.3	0.6	1.1	1.9
RH3/8s	0.5	4.1	0.4	1.4	1.0
RH3/8z	0.5	2.9	1.0	0.6	1.3
RH3/8c	0.6	2.9	1.0	1.6	3.6
RH3/9	0.5	3.4	0.5	0.7	0.6
RH3/10	0.5	3.7	0.6	0.9	0.8
RH3/11	0.5	3.6	0.8	0.9	0.6
RH3/11s	0.4	1.4	0.3	0.6	2.1
RH3/11z	0.4	2.4	0.7	0.4	2.7
RH3/11c	0.7	2.1	1.1	1.2	4.8
RH1/1	0.7	1.4	1.9	3.5	7.9
RH1/1s	0.8	1.2	0.7	2.3	2.9
RH1/1z	0.8	3.6	0.5	3.7	5.1
RH1/1c	0.7	2.3	0.7	4.4	6.1
RH1/3	0.6	1.8	1.9	6.4	2.9
RH1/3s	0.9	1.4	0.8	1.8	2.1
RH1/3z	0.6	2.4	0.4	2.3	2.7
RH1/3c	0.6	2.1	0.5	3.4	4.8
RH1/6	0.5	2.5	1.8	1.2	3.1
RH1/9	0.9	2.2	2.2	0.9	5.4
RH1/9s	0.8	2.2	0.9	0.5	0.9
RH1/12	0.7	1.1	1.8	0.6	3.4
RH1/14	0.5	2.0	1.5	0.6	2.5
RH1/14s	0.7	1.0	0.9	0.4	0.9

* taken from the mean of all surface samples

Table 5.2 Continued

sample	Cr	Mn	Ni	Zn	Pb
RH2/2	0.9	3.2	0.3	1.7	6.1
RH2/2s	1.0	1.5	0.8	1.5	6.4
RH2/2z	0.6	3.6	0.3	1.0	0.9
RH2/2c	1.4	1.9	0.9	2.8	4.6
RH2/8a	1.0	3.1	0.4	1.4	2.9
RH2/8as	1.1	1.6	0.8	0.8	1.2
RH2/8az	1.3	2.8	0.4	0.8	0.5
RH2/8ac	1.9	2.7	1.2	2.2	2.8
RH2/8b	0.5	1.9	0.5	0.9	1.0
RH2/8bs	0.8	0.9	0.8	0.5	1.0
RH2/8bz	0.4	2.6	0.5	0.5	0.3
RH2/8bc	0.5	1.6	0.5	1.0	0.7
RH2/16	0.6	2.4	0.7	0.5	1.2
RH2/16s	0.9	1.0	0.9	0.6	1.0
RH2/16z	0.5	2.7	0.5	0.5	0.5
RH2/16c	0.5	2.3	1.0	0.8	1.4
RH2/19	0.7	4.9	0.8	0.9	2.4
RH2/19s	1.0	1.0	0.9	0.6	1.1
RH2/19z	0.5	2.5	0.5	0.5	0.5
RH2/19c	0.6	2.2	1.1	1.0	1.6
RH2/20	0.4	2.5	0.3	0.4	1.1
RH2/21	0.6	2.9	0.5	0.6	1.3
RH2/21s	0.7	0.7	0.9	0.5	0.9
RH2/21z	0.5	3.1	0.5	0.3	0.5
RH2/21c	0.6	4.3	1.6	1.2	2.3
RH2/22	0.6	2.4	0.6	0.5	1.4
RH2/22s	0.8	0.5	1.0	0.5	0.8
RH2/22z	0.5	2.3	0.6	0.5	0.4
RH2/22c	0.5	1.6	1.1	1.0	1.9
RH2/23	0.5	1.6	0.5	0.5	1.3
RH2/23s	0.7	0.9	0.8	0.3	0.8
RH2/23z	0.5	3.8	0.6	0.6	0.5
RH2/23c	0.6	2.0	1.1	0.9	1.6
RH2/27	0.7	1.1	0.6	0.6	2.8

Table 5.2 Concluded

sample	Cr	Mn	Ni	Zn	Pb
13.2/1	1.2	0.8	0.7	1.7	1.2
13.2/1s	1.5	0.9	1.0	1.7	3.7
13.2/1z	1.7	1.2	1.2	1.6	2.1
13.2/1c	2.6	2.4	1.2	6.2	6.1
13.2/3	1.0	0.6	0.9	1.1	0.9
13.2/3s	1.3	0.8	1.4	1.3	3.1
13.2/3z	1.4	0.7	1.2	0.8	0.5
13.2/3c	2.0	2.7	1.9	2.8	2.4
13.2/5	0.8	0.8	0.9	0.7	0.8
13.2/5s	1.1	0.9	1.4	0.9	2.2
13.2/5z	1.2	1.2	2.0	0.7	0.3
13.2/5c	1.5	2.7	1.7	1.9	1.3
13.2/7	0.9	0.8	0.7	0.6	0.6
13.2/7s	1.1	0.8	1.2	0.2	2.6
13.2/7z	1.2	1.3	1.5	0.8	0.5
13.2/7c	1.4	2.5	1.5	1.2	1.3

CHAPTER VI

EXPERIMENTAL AND STATISTICAL PROCEDURES

6.1 INTRODUCTION

The purpose of this chapter is to detail the collection and handling of samples, and the subsequent analysis and statistical evaluation of the results obtained. A brief account of the instumental tecniques used is given, and also a list of reagents, and the level of impurities in these when known.

6.2 SAMPLE COLLECTION, HANDLING, AND STORAGE

6.2.1 Surface and Transverse Surface Samples

All surface samples were collected from the top two centimetres of sediment using an acid washed plastic scoop. The samples were then transferred into new, labelled, plastic bags, which were then securely sealed with rubber bands. Upon arrival in the laboratory the bags were opened and placed in a clean oven at 55 °C until the sample was dry. After this stage the transverse sediment samples were crushed between several layers of plastic using a stainless steel rolling pin. It was not necessary to crush the surface samples in this manner as they were low in clay and silt, and could be easily dissaggregated by hand when necessary. Both sets of samples were then stored in acid washed polypropylene jars until required for analysis. The acid used for washing all equipment throughout this study was AR 2 mol l^{-1} HNO_3. Surface samples were then labelled S1, S2 ... in order of collection (samples were collected from the same sites in the same order each time), while the transverse surface samples were labelled TS1-TS8.

6.2.2 Core Samples

A total of four cores were collected, one of these by Dr. J Robb (Burgess, 1985). For the cores collected during this study the following procedure was used.

One and a half metre lengths of "D" class acid washed PVC piping, of internal diameter 55 mm, were driven as deeply as possible into the sediment. The depth of penetration was dependent upon the sediment and water conditions. For example, the water depth of 80 cm at RH1 allowed only a short core to be collected, whereas, at RH3 although the water was only 10-20 cm deep considerable difficulty was experienced in collecting any core at all. Seven attempts were made at this location before a sucsessful

core was collected. Two problems existed at this site arising from the variability of the sediment. In places the full length of the core could be pressed into the sediment by hand, releasing vast quantities of gas, a sample of which was collected and analysed by GCMS, and shown to be methane, with no hydrogen sulphide being detected. When the core was capped and retrieved, the sediment within lacked any cohesion and ran out of the core as a slurry. As little as two metres away, however, no gas would be present. The sediment was soft for the first 30 cm or so, and then became very stiff. Retrieval of the cores was difficult, as even when digging to a depth of 1 m the sediment would not come to the surface when the capped core was removed. Eventually a PVC constriction was fitted to the mouth of the coring device to prevent the sediment from slipping out, and a post hole digger was used to dig alongside, and down to the bottom of the core, allowing the sediment column to be broken off at the base.

After removal the ends of the core were sealed by plastic covered corks and then covered by plastic bags sealed with rubber bands. Until the cores could be opened (1-3 days) they were stored at 4 °C. The cores were opened by cutting two groves down the full length of the piping on opposite sides, leaving a small amount of plastic remaining. This could then be easily cut through with a Stanley knife, the contaminated sediment being carefully scrapped away with a piece of acid washed glass. After being logged, the cores were covered with a sheet of glad wrap and partially dried by either air drying or using a 2.5 kW heat lamp suspended 15 cm above the sediment.

The cores were then divided along any natural boundaries and sections were then split into approximately 4 cm samples. Each sample was placed in a labelled polyethylene bag and dried in an oven at 55 °C until dry, then crushed in the manner described in section 6.2.1 where necessary. The crushed samples were then sieved through a stainless steel 563 μm sieve, before being stored in an airtight acid washed polypropylene jar. Samples were labelled according to the core of origin, and location from the top of the core. For example, the ninth segment down in the second core collected bears the lable RH2/9. Two samples bear the same number, RH2/8a, and RH2/8b. This is because they come from the same level in the core, but above and below a unit boundary respectively.

Seperation of the sediment into its component sand, silt, and clay fractions was carried out as per Burgess (1985). As large volumes of doubly distilled water come into contact with the clay and silt during the seperation it was thought that metal ions may be desorbed from the clay to the surronding solution, particularily in the presence of high concentrations of sodium chloride. The higher the ionic potential (z/r) of an element the more strongly sorbed to the clay it will be. All elements in this study have substantially higher z/r than Na^{1+}, it is therefore assumed that no significant desorption took place (using data from Fergusson, 1982).

6.3 DIGESTION AND ANALYSIS OF SAMPLES

Initially the method used was that of Anderson (1985) and Burgess (1985), who both slightly modified the method found to be most suitable by Hulse (1983). However, in an attempt to improve the reliability of results, and the overall ease of analysis, the quantities of sediment digested, and HF used were adjusted. This was nescessary as, in general, the metal ion concentrations were higher than those in the studies of Anderson, Burgess, and Hulse, and the quantities of sediment digested could normally be reduced. The quantities of sediments and reagents used are summarised in **Table 6.0**. Another major change made was the use of the standard additions technique for Fe and Mn, as this was found to greatly improve the results obtained.

Table 6.0 Sediment Digestion Summary

sample	weight (g)	digestion mixture
sand	0.5	3 ml conc. AR HNO_3 and 12 ml AR 40% HF
silt	0.25	3 ml conc. AR HNO_3 and 10 ml AR 40% HF
totals*	0.5	
DRS-1[a]	0.25	
LS-1[a]	0.5	
SD-N-1[a]	0.25	
clay	<0.2	3 ml conc. AR HNO_3 and 8 ml AR 40% HF
surface	0.2	

* because the concentration varied greatly some samples were analysed in larger or smaller quntities.

[a] Standards or special samples, see section 6.5.2.

The samples were weighed into previously tared acid washed plastic beakers using an acid washed glass spatula. The acid was then added and the sample was evaporated to dryness on a steam bath. This step was repeated before the sample was taken up in 6-7 ml of AR 2 mol l^{-1} HNO_3. The digested samples were filtered through acid rinsed Whatman 540 grade hardened ashless filter paper into 25 ml volumetric flasks. The residue was repeatedly washed with 1-2 ml portions of doubly distilled water, before the volume was made up to 25ml. Initially 40 grade paper was used, but this was found to slightly contaminate the sample with zinc. The efficiency of the digestion procedure in removing silica can be estimated by the amount of residue remaing after digestion of the sample. After one digestion cycle sample 13.2/1 was reduced in mass from 1.0422g to 0.2375g, a 77% reduction. When the digestion procedure was repeated the mass of the residue decreased a further 51%, a total mass loss of 89%.

Samples were analysed principally by two methods, AAS (digested samples) and XRF (undigested samples). These methods, and the instrumental parameters used in this study, are described below as well as the preparation of samples for XRF analysis.

6.4 INSTRUMENTAL METHODS

6.4.1 Atomic Absorption Spectrscopy (AAS)

1) Theory: The principle of AAS is to measure the absorption of radiation from a line source by a gaseous atomic species. An AA spectrophotometer consists basically of the following items: a radiation source, atomiser (e.g. burner), monochromator, and photomultiplier. The radiation source most commonly used is a hollow cathode lamp. the cathode of which is made of the analyte element. The lamp produces a series of line emissions, the intensity of which is governed by the lamp current. One of these lines (the analytical line) is isolated by a monochromator of suitable slit width. The beam from the lamp is positioned so as to pass through the flame from the burner. Absorption of the beam is measured as a decrease in the intensity of the analytical line, and is converted into an amplified electrical signal before the result is output as an absorbance. Absorbance is related to concentration by the Beer-Lambert law...

$$\log \frac{I_i}{I} = k_\upsilon.b.c = A$$

Where I_i = incident radiation intensity, I = transmitted radiation intensity, k_υ = the molar absorption coefficient, b = the path legth through the flame, c = the concentration, and A = the absorbance (Christian, 1978).

2) Interferences: Absorption is proportional to the number of atoms of analyte present in the flame, and hence to concentration - a linear relationship. However, non linear calibration curves are often obtained. There are two major classes of interferences that produce this non linear response. (1) Spectral, and (2) chemical.

Spectral interferences result from the overlap of emission lines, and can be reduced by careful choice of the analytical wavelength, and slit width. Chemical interferences such as ionisation, oxidation, and molecular species, may be overcome by including more easily ionised substances, decreasing the concentration of oxygen in the flame, and/or including releasing agents, and background correction using a deuterium lamp. In the latter case the absorbance of the radiation from the deuterium lamp by the atomised sample is measured and electronically subtracted from the signal. The processes taking place in the flame may be seen in **Figure 35**, those in bold type are to be optimised.

Figure 35 Flame Processes

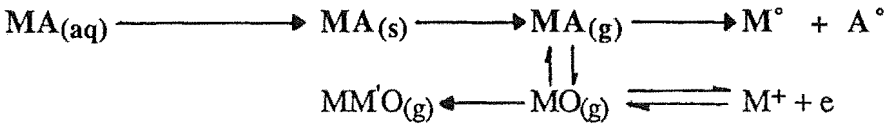

3) Analytical Procedure: Instrumental parameters used for the Varian AA-1475 series AAS used in this study are presented in **Table 6.1.** Absorbances were obtained using the "run mean" and single beam modes. Calibration curves were obtained by measuring the absorbances of a series of dilute standards. The concentration of the sample solutions was then determined graphically for elements other than iron and manganese, which were determined by linear regression.

The concentration chosen for the dilute standards varied from element to element, but were chosen to cover, as much as possible, the linear range of the absorbance curve. The concentrations are listed in **Table 6.2.** Dilute standards were prepared from the stock 1000 $\mu g\ ml^{-1}$ solutions listed in section 6.6.

Table 6.1 Instrumental Parameters

element	λ (nm)	slit (nm)	lamp (mA)	bkgrd corrector	atten.	flame[a]
Cr	357.9	0.2	7	off	out	N/A[c]
Cu	324.8	0.5	3	on	out	A/A
Fe[b]	248.3	0.2	6	off	out	A/A
Mn[b]	279.5	0.2	5	on	out	A/A
Ni	232.0	0.2	4	on	in	A/A
Pb[b]	217.0	1.0	4	on	in	A/A
Zn	213.9	1.0	5	on	in	A/A

[a] N/A = N_2O/C_2H_2; A/A = air/C_2H_2. [b] Fe,Pb are phototron lamps, Mn is activion, all others are varian. [c] best results with a reducing flame, air 27: N_2O 50.

Table 6.2 Concentration Ranges for Dilute Standards

	Cu	Cr	Fe*	Mn*	Ni	Pb	Zn
0	0.00	0.00	0.00	0.00	0.00	0.00	0.00
1	0.25	1.00	0.75	0.75	0.50	1.50	0.20
2	0.50	2.00	1.50	1.50	1.00	3.00	0.40
3	0.75	3.00	2.25	2.25	1.50	4.50	0.60
4	1.00	4.00	3.00	3.00	2.00	6.00	0.80

*succesive spikes for standard additions

6.4.2 X-Ray Fluorescence (XRF)

A number of samples were analysed in the Geology Department using a method based on that of Norrish and Hutton (1969), with modifications after Harvey et al. (1973), and Schroeder et al. (1980).

1) Theory: In XRF the atoms within the sample are excited by a primary X-ray beam. In returning to the ground state a secondary X-ray of longer wavelength than the primary beam is emitted by the sample atom. The primary beam is generated by striking a target (Au or Cr depending on the analyte element) with a stream of high energy electrons. This causes the ejection of an inner shell electron from the target atoms. The vacancy thus created is filled by an electron from a still higher energy shell and so on. Each transition produces an X-ray at an angle and wavelength characteristic of that transition and element. Secondary X-rays are generated from the sample atoms in similar fashion.

The calculation of the analyte concentration is made by correcting the count ratio for the analyte element for the absorbing and enhancing effects of all other elements present. The derivation of the formulas used is described in Harvey et al., and Schroeder et al.

2) Interferences: There are two main interferences to be considered in XRF. The first is similar in principle to the absorption and enhancement effect found in AAS and is due to the fluorescent activity of other elements in the sample. The second is that the technique assumes that the sample is homogeneous, whereas in fact rocks and minerals are heterogeneous.

For the analysis of major elements (Fe, Mn, Ca, Na, K, P, Ti, Si, Al, and Mg), in particular Si, Al, Fe, and Mg particle size becomes critical. It is easier, and involves less contamination, to dissolve the sample in a suitable flux rather than grind to a fine enough powder. The dissolution of the sample also minimises the matrix effects as the interfering elements have been diluted. The addition of a heavy absorber such as La_2O_3 greatly increases the absorption and so further reduces matrix effects. In the case of trace element analysis dissolution of the sample is not practical, and so the sample is finely ground and mass correction factors, which are dependant on the concentration of, for example Fe and Mg, are applied.

3) Sample Preparation and Analytical Procedure: Samples were analysed either as pressed pellets (trace analysis), or fusion beads (major elements) in 32 mm format. Pressed pellets were prepared in the following manner. The sample was ground for 150 sec. in a tungsten carbide tima, which was carefully washed between samples. Five grams of sample were then thoroughly mixed with 4-5 drops of spec. pure mowiol

solution (polyvinyl alcohol). The mowiol acts as a binder to prevent the sample from powdering. The sample was then transferred to a mould and formed into a pellet at high pressure. After numbering, and drying for 24 hours the sample is ready for analysis.

Preparation of fusion beads is rather more time consuming, and only an outline is given below. The sample and flux (0.30 and 1.61 grams respectively) are dried in an oven overnight and then transfered to a tared Pt crucible. A small quantity of $NaNO_3$ is added to ensure oxidising conditions in the melt, and the crucible is ignited in the furnace at 1000 °C for 10 minutes. The crucible is then allowed to cool, is weighed, and heated for a further 10 minutes. A glass bead is formed by pouring the melt onto a polished aluminium platten and pressing with a highly polished plunger. After annealing the bead can be trimmed, labelled, and stored over a desiccant until analysed.

The loss of mass on ignition (LOI) is equal to the mass of H_2O, CO_2, and organic matter lost, minus the mass gained, largely by the oxidation of Fe(II) to Fe(III). The crucibles used are a 5% Au/Pt alloy. The gold prevents the melt from wetting the crucible, making handling easier. The flux used was a mixture of lithium tetraborate (47%), lithium carbonate (36.7%), and lanthanum oxide (16.3%).

Samples were analysed on an automated Phillips PW 1400 spectrophotometer, with a PW 1732/10 X-ray generator, using the experimental parameters summarised in **Table 6.3**. An estimate of the detection limits and % error for the elements is provided in **Table 6.4**.

Table 6.3 Summary of Instrumental Parameters

element	filter	collimator	detector	crystal	kV	mA	angle (2θ)	line
Sr	no	fine	s	LiF_{200}	60	45	25.140	K_α
Zr	no	fine	s	LiF_{200}	60	45	22.530	K_α
Nb	no	fine	s	LiF_{200}	60	45	21.380	K_α
Ba	no	fine	f	LiF_{200}	60	45	87.280	L_α
La	no	coarse	f	LiF_{200}	60	45	138.985	L_α
V	no	fine	f	LiF_{220}	60	45	123.270	K_α
Cr	no	fine	f	LiF_{220}	60	45	107.115	K_α
Ni	no	coarse	f	LiF_{200}	60	45	48.710	K_α
Zn	no	coarse	s	LiF_{200}	60	45	41.780	K_α
Nd	no	coarse	f	LiF_{220}	60	45	99.220	L_β
Ce	no	coarse	f	LiF_{200}	60	45	71.730	L_β

f = flow proportional, s = scintillation counter

Table 6.4 Detection Limits and Estimated % Error for XRF

element	Sr	Zr	Nb	Ba	V	Cr	Nd	Ce	Zn	Ni	La
detection limit[a]	1	2	2	10	5	3	3	3	2	3	3
% error	1	2	5	10	5	5	10	5	3	3	3

[a] in ppm

6.4.3 X-Ray Powder Diffraction (XRD)

X-ray powder diffraction was used to identify mineral species present in the silt and clay size fractions.

1) Theory: The wavelength of X-ray radiation is on a par with the d-spacings of crystaline materials. Hence an incident X-ray beam will be diffracted by a crystaline substance. The angle of diffraction, θ, is defined by the Bragg eqution which states ...

$$n\lambda = 2.d.\sin\theta$$

where n = an integer value 1, 2, 3 ...

λ = the x-ray wavelength (e.g. Cu K_α = 1.5418 nm)

d = the spacing between the lattice planes

θ = the angle of diffraction, which is experimentally determined

The basic components of a diffractometer may be seen in **Figure 36**.

Figure 36 Diagrammatic Representation of a Diffractometer

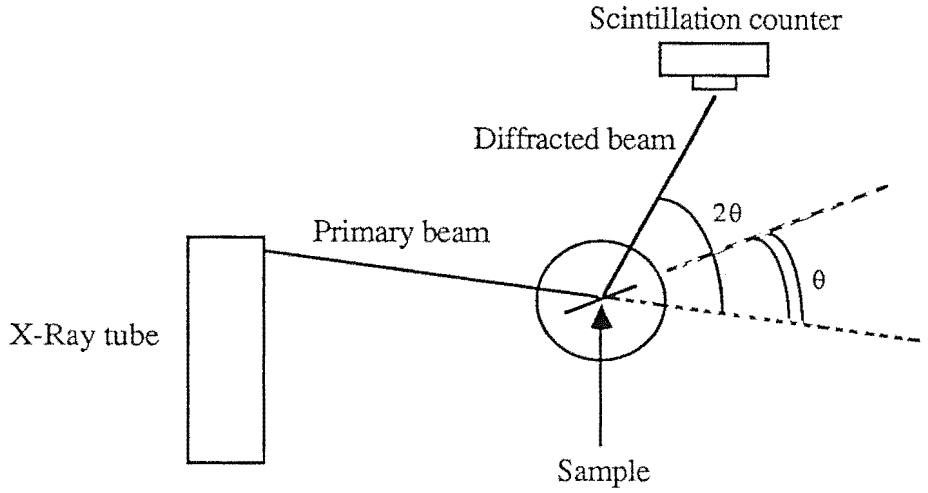

Each mineral analysed will produce a pattern of peaks of characteristic intensity and 2θ values. Identification is made by comparison of this pattern against either standards or data files.

2) Procedure: The sample was prepared by either: (a) grinding under ethanol in an agate mortar, spreading the slurry over a glass slide and allowing the ethanol to evaporate; or (b) taking an aliquot of an aqueous sample suspension and placing this in a beaker containg a glass slide. The water was evaporated off leaving an even coating of the sample on the slide. Both methods produce the sample with an ordered arrangement. Reference is made in the text as to which technique was used.

Analysis was performed with a Phillips PW 1729 x-ray generator, controlled by a Phillips PW1710 diffractometer controller, using a MAC-XT personnel computer as a terminal and for data analysis. The diffraction patterns used in the text were prepared on an HP 7475A plotter. The generator settings were 50 kV and 35 mA, while the scintillation counter scanned from 3-53° 2θ at 0.02° intervals, and a residence time of 1 sec. per step (50 sec. per degree). For the reference samples run at a later stage the step increment was increased to 0.05°, and the count time to 3 sec. (60 sec. per degree). The raw data was transformed from column to formatted form by the program PROCESS, then mathematically modelled and peaks selected with the aid of SHADOW. The programs HXRDPLT and HXRSCRN were used in the preparation of hardcopy.

6.5 STATISTICAL ANALYSIS

6.5.1 Data Evaluation

Results for any sample analysed more than three times were screened by an applicable statistical test to eliminate outliers. Where it was suspected that either the highest or lowest value was an outlier Dixon's Q-test (Grubbs, 1969) was used. For both the highest and lowest values as suspect the range/σ test of David et al. (1954) as reported by Grubbs was used, and for either the highest or lowest two values the Grubbs test was used. Of the three sediments tested (SD-N-1, DRS-1, and LS-1) SD-N-1 and LS-1 (a local soil) had vaues rejected by Dixon's Q-test. As only three samples of LS-1 were analysed, the rejection of those values may be due to the lack of data, however, the sample was not of enough importance to warrent further analysis. The Q-test, and a table of critical values are contained in Appendix B. A summary of the statistical values for LS-1 may be found in section 5. .

6.5.2 Error Evaluation

Error evaluation in any analytical work is critical. To obtain an estimate of the error involved in the experimental method used in this study two sediments were analysed, both initially in batches and then one or the other with every batch of samples digested.SD-N-1 is an international standard of the IAEA (IAEA,1985), DRS-1 was

prepared during this study by sieving (563 μm), and grinding the top 20 cm of a reject core collected near the site of RH3. The results obtained were treated in the following manner:

(1) Potential outliers were tested in the manner described above.
(2) The mean and standard deviation of the accepted data points were calculated.
(3) The coefficient of variation or cv (i), and the 95% confidence interval (ii) were caculated.

(i) $cv = \frac{\sigma}{mean} x\ 100$ (ii) $95\%\ CI = x \pm \frac{1.96.s}{n}$

The results may be seen in **Table 6.5**,and the raw data in Appendix D. A summary of the results obtained for DRS-1 and SD-N-1 is given in **Table 6.6**.

Table 6.5 Coefficient of Variation and % Error Based on 95% CI, for SD-N-1 and DRS-1

	Cr		Cu		Fe		Mn		Ni		Pb		Zn	
	cv	±%	cv	±%	cv	±%	cv	±%	cv	±%	cv	±%	cv	±%
SD-N-1[1]	37	12	14	5	21	3	15	5	32	11	21	8	11	3
SD-N-1[2]	8.5	4	11.5	5	23.5	13	6.5	5	16	8	12	6	6.5	4
DRS-1	16	6	22	9	25	10	26	10	31	13	13	5	11	5

[1] IAEA recommended. [2] this study.

Table 6.6 Summary of Results for SD-N-1 and DRS-1

	SD-N-1[1]			SD-N-1[2]			DRS-1		
	x	s	n*	x	s	n	x	s	n
Cr	148.3	55.1	136	139	11.5	15	27.0	4.27	24
Cu	72.2	10.2	117	68.6	7.2	16	25.5	5.55	24
Fe	3.64	0.39	154	2.94	0.69	13	3.27	0.83	23
Mn	777	120	147	755	97	8	816	214	24
Ni	31.0	10.0	116	30.9	4.98	15	14.7	4.6	24
Pb	120	25	87	105	12.5	15	147	19.4	23
Zn	439	48.6	167	412	30.0	16	598	66.9	23

[1] IAEA recommended [2] this study *n = the total number of accepted determinations, x and s are based on accepted laboratory means.

6.5.3 Analysis of Results

Accepted results can be examined for anthropogenic pollution in a number of ways. Two methods are commonly used. The first is to subtract local or international sediment values from the experimentally determined concentration. This approach has a number of drawbacks, in particular when subtracting an international set of values, as the sediment composition seldom matches perfectly, and this affects the concentration of metal ions present. Even when local sediments are used for comparison, subtle differences in composition or history may cast some doubt on the interpretation. The second method commonly in use is the comparison of a conservative element in both the background and sample sediment with the analyte element in both sediments. This is done using the equation below (after Fergusson et al., 1986).

$$E = \frac{[M]_s}{[M]_c} \times \frac{[X]_c}{[X]_s}$$

Where $M_{s,c}$ is the concentration of the analyte in the sample and crust respectively, $X_{s,c}$ is the concentration of the conservative element in the sample and crust respectively, and E is the enrichment factor.

A good conservative element should not be affected by anthropogenic activities, and should correlate well with other metal ions and the sediment type. In this study both barium and manganese are possibilities. Barium was determined by XRF for all total samples (but not sand, silt, or clay) and fulfills the criteria of a conservative element extremely well. Manganese was determined in all samples by AAS, and in a limited number of samples by XRF. Manganese is somewhat less suitable as it does exhibit some variation probably due to anthropogenic effects. Evaluation of enrichment factors and background levels is carried out in Chapter V.

6.6 REAGENTS AND CHEMICALS

The following is a brief list and description of the reagents and chemicals used in this study. Where stated by the manufacturer the concentration of relevant impurities are also given.

Standards: all 1000 $\mu g\ ml^{-1}$

Cu	AR $CuSO_4.5H_2O$	Fe, 0.01%; Ni, 0.01%
Cr	AR $K_2Cr_2O_7$	

Fe	AR $NH_4Fe(SO_4)_2.12H_2O$	Cu, 0.002%; Pb, 0.002%; Mn, 0.001%; Zn, 0.003%
Mn	AR $MnSO_4.4H_2O$	Fe, 0.002%; Pb, 0.001%; Zn, 0.05%; Ni, 0.002%
Ni	AR $(NH_4)_2SO_4,NiSO_4.6H_2O$	Cu, 0.002%; Fe, 0.001%; Pb, 0.002%; Zn, 0.002%
Pb	AR $Pb(NO_3)_2$	
Zn	AR $ZnSO_4.7H_2O$	

Acids: impurities are listed only for the concentrated acids

AR HF 40%	Cr, 2×10^{-6}%; Cu, 2×10^{-6}%; Ni, 2×10^{-6}%; Pb, 5×10^{-6}%; Mn, 5×10^{-6}%; Zn, 5×10^{-6}%; Fe, 2×10^{-5}%
AR HNO_3 16 mol l^{-1}	Cu, 1×10^{-5}%; Fe, 2×10^{-5}%; Pb, 1×10^{-5}%; Mn, 4×10^{-5}%
AR HNO_3 2 mol l^{-1}	

Miscellaneous:

AR NaCl	Fe (total), 0.0003%; Cu, 0.0002%; Pb, 0.0002%
AR Na_2CO_3	
Doubly distilled water	

ACKNOWLEDGEMENTS

I wish to extend my sincere thanks to my supervisor Dr, J. E. Fergusson for his assistance and advice. Dr. S. Weaver and Mr. S. Brown (Dept. of Geology) deserve thanks for allowing me to freely use their X-Ray facilities and laboratory. Numerous members of the technical and clerical staff of the Chemistry Department have made my task considerably easier by willingly attending to requests for their services, promptly and proffessionaly, and to them I am grateful.

Also deserving thanks are Carol Jean, for proof reading the finished manuscript, and especially Annette, for helping draft the map (several times), doing more than her share of chores, and being there.

Lastly I would like to thank my friends and colleagues, both in and out of the university, who provided encouragement, advice, and light relief. Although not the most "useful resource" that I have gained from my time at this establishment, they are certainly the most treasured.

REFERENCES

Ackermann, F. A. (1980). Procedure for Correcting the Grain Size Effect in Heavy Metal Analysis of Estuarine and Coastal Sediments. *Environmental Technology Letters*, 1: **518-527**.

Anderson, T. (1985). Geochemistry of Christchurch River Sediments: The Avon River: Unpublished BSc. Hons. Part III Report.Dept. of Chemistry, University of Canterbury.

Archer, A. and Barratt, R. S. (1976). Lead Levels in Birmingham Dust. *The Science of the Total Environment*, 6: **275-286**.

Aston, S. R. and Chester, R. Estuarine Sedimentary Processes. In: Burton, J. D. and Liss, P. S. Estuarine Chemistry. London: Academic Press; (1976): 37-53.

Bowen, H. J. M. Environmental Chemistry of the Elements. London: Academic Press; (1979).

Brindley, G. W. and Brown, G. Crystal Structures of Clay Minerals and their Identification. London: Mineralogical Society; (1980).

Brkovic-Popovic, I. and Popovic, M. (1977). Effects of Heavy Metals on Survival and Respiration Rate of Tubificid Worms: Part 1. Effects on Survival. *Environmental Pollution*, 13: **65-72**.

Browne, G. H. and Field, B. D. The Lithostratigraphy of Late Cretaceous to Early Pliestocene Rocks of Northern Canterbury, New Zealand. N.Z.G.S. Record 6. Lower Hutt: New Zealand Geological Survey; (1985).

Burgess, V. (1985). Analysis of Christchurch Estuary Sediments: Unpublished BSc. Hons. Part III Report. Dept. of Chemistry, University of Canterbury.

Burton, J. D. Basic Properties and Processes in Estuarine Chemistry. In: Burton, J. D. and Liss, P. S. Estuarine Chemistry. London: Academic Press; (1976): 1-36.

Campbell, J. A. and Whitekar, R. A. (1969). Eh/pH Diagrams. *Journal of Chemical Education*, 46: **90-92.**

CDB. (1972). Report on Flood Relief Works, Outfall Drain and South Canal Reserve Drain: Christchurch Drainage Board, Unpublished Report, 13/7/72.

Chao, T. T. and Theobald Jr, P. K. (1976). The Significance of Secondary Iron and Manganese Oxides in Geochemical Exploration. *Economic Geology*, 71: **1560-1569.**

Christian, G. D. Flame Spectroscopy. In: Bauer, H. H. et al. Instrumental Analysis. Boston: Allyn and Bacon; (1978): 256-294.

The Concise Oxford Dictonary of Current English. 7th ed. Oxford: Oxford University Press; (1982).

Crosby, S. A. et al. (1983). Surface Areas and Porosities of Fe (III)- and Fe (II)-Derived Oxyhydroxides. *Environmental Science and Technology*, 17: **709-713.**

Dawson, B. S. W. Trace Elements in Three Soil Monosequences and Iron-Manganese Concretions from Westland and Canterbury New Zealand: Unpublished Ph.D. Thesis, Chemistry Dept. University of Canterbury; (1982).

Day, J. P. (1977). Lead Pollution in Christchurch. *New Zealand Journal of Science*, 20: **395-406.**

de Groot et al. Processes Affecting Heavy Metals in Estuarine Sediments. In: Burton, J. D. and Liss, P. S. Estuarine Chemistry. London: Academic Press; (1976): 131-157.

Deely, J.Unpublished First Year Ph.D. Report. Geology Dept. University of Canterbury; (1987).

Deely, J. (1987). Pers. comm.

Duchart, P. et al. (1973). Distribution of Trace Metals in the Pore Waters of Shallow Water Marine Sediments. *Limnology and Oceanography*, 18: **605-610.**

Fergusson, J. E. et al. (1986). The Elemental Composition and Sources of House Dust and Street Dust. *The Science of the Total Environment*, 50: **217-221.**

Fergusson, J. E. Inorganic Chemistry and the Earth. Sydney: Pergamon Press; (1982).

Fergusson, J. E. (1987). The Significance of the Variability of Analytical Results for Lead, Copper, Nickel, and Zinc in Street Dust. *Canadian Journal of Chemistry*, 65: **1002-1006.**

Fergusson, J. E. and Ryan. D. E. (1984). The Elemental Composition of Street Dust from Large and Small Urban Areas Related to City Type, Source and Particle Size. *The Science of the Total Environment*, 34: **101-116.**

Forstner, U. Inorganic Pollutants, Particularily Heavy Metals in Estuarines. In: Olausson, E. and Cato, I. Chemistry and Biogeochemistry of Estuaries. Chichester:Wiley; (1980): 307-348.

Forstner, U. and Wittmann, G. T. W. Metal Pollution in the Aquatic Environment. Berlin: Springer-Verlag; (1981).

Grubbs, F. E. (1969). Detecting Outlying Observations in Samples. *Technometrics*, 11: **1-21.**

Harrison, R. M. and Wilson, S. J. (1985a). The Chemical Composition of Highway Drainage Waters I. Major Ions and Selected Trace Metals. *The Science of the Total Environment*, 43: **63-77.**

Harrison, R. M. and Wilson, S. J. (1985b). The Chemical Composition of Highway Drainage Waters II. Chemical Associations of Trace Metals in the Suspended Sediment. *The Science of the Total Environment*, 43: **79-87.**

Harrison, R. M. and Wilson, S. J. (1985c). The Chemical Composition of Highway Drainage Waters III. Run Off Water Speciation Characteristics. *The Science of the Total Environment*, 43: **89-102.**

Harvey, P. K. et al. (1980). An Accurate Fusion Method for the Analysis of Rocks and Chemically Related Materials by X-Ray Fluorescence Spectrometry. *X-Ray Spectrometry*, 2: **33-44.**

Hulse, C. A. Geochemistry of Christchurch River Sediments. Christchurch: Unpublished BSc. Hons. Part III Report. Dept. of Chemistry, University of Canterbury; (1983).

Hulse, C. (1987). Pers. comm.

IAEA. Intercomparison of Trace Element Measurements in Marine Sample SD-N-1/2. Monaco: IAEA Laboratory of Marine Radioactivity; (1985); (Report Number 24).

Jaffe, D. and Walters, J. K. (1977). Intertidal Trace Metal Concentrations in Some Sediments from the Humber Estuary. *The Science of the Total Environment*, 7: **1-15**.

JCPDS (Joint Committee on Powder Diffraction Standards). Mineralogical Powder Diffraction File Data Book. Swathmore, pensylvania; (1980).

Jenne, E. A. Controls on Mn, Fe, Co, Ni, Cu, and Zn Concentrations in Soils and Water: the Significant Role of Hydrous Mn and Fe Oxides. In: Trace Inorganics in Water. Advances in Chemistry Series. Washington D. C.: American Chemical Society; (1968); 73.

Kheboian, C. and Bauer, C. F. (1987). Accuracy of Selective Extraction Procedures for Metal Speciation in Model Aquatic Sediments. *Analytical Chemistry*, 59: **1417-1423**.

Knox, G. A. and Kilner, A. R. The Ecology of the Avon-Heathcote Estuary. Unpublished report to the CDB by The Estuarine Research Unit. Dept. of Zoology, University of Canterbury; (1973).

Lewis, D. W. Practical Sedimentology: Apteryx; (1981).

Lobb, A. (1987). Personal communication, 16/12/87.

MacPherson, J. M. Environmental Geology of the Avon-Heathcote Estuary: Unpublished Ph.D. Thesis, Geology Dept. University of Canterbury; (1978).

Moore, J. W. and Ramamoorthy, S. Heavy Metals in Natural Waters. Applied Monitering and Impact Assesment. New York: Springer-Verlag; (1984).

Norrish, K. and Hutton, J. T. (1969). An Accurate X-Ray Spectrographic Method for the Analysis of a Wide Range of Geological Samples. *Geochimica et Cosmochimica Acta,* 33: **431-453.**

Nriagu, J. O. (1979). Global Inventory of Natural and Anthropogenic Emmissions of Trace Metals to the Atmosphere. *Nature*, 279: **409-411.**

Nriagu, J. O. Lead and Lead Poisoning in Antiquity. New York: Wiley Interscience; (1983).

Pederson, E. et al. (1978). Second study of the Incidence and Mortality of Respiratory Organs Amongst Workers at a Nickel Refinery. *Annals of Clinical and Laboratory Science (Abstract)*, 8: **503.**

Perhac, R. M. (1972). Distribution of Cd, Co, Cu, Fe, Mn, Ni, Pb, And Zn in Dissolved and Particulate Solids from Two Streams in Tennesse. *Journal of Hydrology*, 15: **177-186.**

Postma, H. Sediment Transport and Sedimentation. In: Olausson, E. and Cato, I. Chemisrty and Biogeochemistry of Estuaries. Chichester: Wiley; (1980): 153-186.

Presby, B. J. and Trefry, J. H. Sediment-Water Interactions and the Geochemistry of Interstitial Waters. In: Olausson, E. and Cato, I. Chemistry and Biogeochemistry of Estuaries. Chichester: Wiley; (1980): 187-232.

Purchase, N. G. and Fergusson, J. E. (1986). The Distribution and Geochemistry of Lead in River Sediments, Christchurh, New Zealand. *Environmental Pollution*, 12: **203-216.**

Purves, D. Trace Element Contamination of the Environment. (Revised Edition). Amsterdam: Elsevier; (1985).

Ramamoorthy, S. and Rust, B. R. (1978). Heavy Metal Exchange Processes in Sediment-Water Systems. *Environmental Geology*, 2: **165-172.**

Robb, J. (1987). Pers. comm.

Robbins, J. A. and Callender, E. (1975). Diagenesis of Manganese in Lake Michigan Sediments. *American Journal of Science*, 275: **512-533.**

Salomons, W. and Forstner, U. Metals in the Hydrocycle. Berlin: Springer-Verlag; (1984).

Sanders, N. K, (trans.). Poems of Heaven and Hell from Ancient Mesopotamia. Harmondsworth: Penguin Books; (1971).

Schroeder, et al. (1980). Analysis of Geological Materials Using an Automated X-Ray Fluorescence System. *X.R.S.*, 9: **198-205.**

Shelly, D. Manual of Optical Mineralogy. Amsterdam: Elsivier; (1975).

Simmonds, P. R. Heavy Metals in the Christchurch Environment: Unpublished MSc. Thesis, Chemistry Dept. University of Canterbury; (1982).

Simmonds, P. R. and Fergusson, J. E. (1983). Heavy Metal Pollution at an Intersection Involving a Busy Urban Road in Christchurh, New Zealand. Part 1. The Level of Cr, Mn, Fe, Ni, Cu, Zn, Cd, and Pb in Street Dust. *New Zealand Journal of Science*, 26: **219-228.**

Spoljaric, N. and Crawford, W. A. (1978). Glauconitic Greensand: A Possible Filter of Heavy Metal Cations From Polluted Waters. *Environmental Geology*, 2: **215-221.**

Stewart, C. Studies on Christchurch Street Dust: Unpublished BSc. Hons. Part III Report. Dept. of Chemistry, University of Canterbury; (1984).

Stokes, P. M. Adaption of Green Algae to High Levels of Copper and Nickel in Aquatic Environments. In: Hutchinson, T. C. Proceedings of the First International Conference on Heavy Metals in the Environment. Toronto, Canada: University of Toronto Institute for Environmental Studies; (1975); vol. II: 137-154.

Swallow, K. et al. (1980). Sorption of Copper and Lead by Hydrous Ferric Oxides, 15.

Taylor, D. (1976). Distribution of Heavy Metals in the Sediment Of an Unpolluted Estuarine Environment. *TheScience of the Total Environment*, 6: **259-264.**

Tessier, A. et al. (1979). Sequential Extraction Procedure for the Speciation of Particulate Trace Metals. *Analytical Chemistry*, 51: **844-850.**

Thorne, L. T. and Nickless, G. (1981). The Relationship Between Heavy Metals and Particle Size Fractions Within the Severn Estuary (U. K.). *The Science of the Total Environment*, 19: **207-213.**

Timperly, M. H. and Allan, R. J. (1974). The Formation and Detection of Metal Dispersion Halos in Organic Lake Sediments. *Journal of Geochemical Exploration*, 3: **167-190.**

Weaver, C. E. and Pollard, L. D. Developments in Sedimentology 15. The Chemistry of Clay Minerals. Amsterdam: Elsevier Scientific Publishing Company; (1973).

WHO. Environmental Health Criteria 3. Lead. Geneva: WHO and UNEP; (1977).

Wilson, D. D. Geology of the Waipara Subdivision (Amberly and Motanau Sheets S68 and S69). New Zealand Geological Survey Bulletin n. s. 64. Wellington: R. E. Owen Govt. Printer; (1963).

Wilson, G. S. (1987). Personal communication, 29/12/87.

APPENDIX A

XRF RESULTS FOR MAJOR ELEMENTS

N.B. The results for all elements except Fe and Mn are presented as the % oxide in the sample.

sample	SiO_2	TiO_2	Al_2O_3	Fe	Mn	MgO	CaO	K_2O	P_2O_5
RH3/1	74.67	0.38	11.01	1.90	0.0310	0.82	1.03	2.13	0.16
RH3/3	64.53	0.54	11.84	3.24	0.0387	1.09	1.31	2.25	0.49
RH3/11	67.08	0.59	14.39	3.08	0.0465	1.61	1.33	2.88	0.14
RH1/1	70.48	0.44	12.73	2.35	0.0387	1.17	1.03	2.55	0.11
RH1/6	73.87	0.40	12.46	1.92	0.0465	0.98	0.92	2.58	0.09
RH1/14	73.38	0.40	12.06	1.80	0.0387	0.99	0.92	2.45	0.08
RH2/2	70.63	0.50	12.77	2.34	0.0465	1.11	1.15	2.43	0.14
RH2/16	70.72	0.55	13.77	2.49	0.0465	1.3	1.17	2.77	0.13
RH2/22	67.97	0.59	14.26	2.94	0.0542	1.46	1.15	2.91	0.12
RH2/27	71.66	0.44	12.49	1.94	0.0387	1.11	0.95	2.61	0.08
13.2/1	73.10	0.39	11.45	1.70	0.0232	0.87	2.22	2.25	0.10
13.2/5*	56.90	0.39	10.56	1.88	0.0310	1.03	0.85	2.10	0.09
S2	73.82	0.39	10.64	1.85	0.0387	0.83	1.09	2.07	0.19
S13	75.47	0.34	10.65	2.77	0.0387	0.76	1.02	2.08	0.17

* SiO_2 and Al_2O_3 are low, probably due to a faulty fusion bead.

APPENDIX B

Dixon's Q-test

n	Criterion	P=0.05
3	$r_{10}=\frac{x_2-x_1}{x_n-x_1}$ if smallest value is suspect	0.941
4		0.765
5		0.642
6	$=\frac{x_n-x_{n-1}}{x_{n-1}-x_1}$ if largest value is suspect	0.560
7		0.507
8	$r_{11}=\frac{x_2-x_1}{x_{n-1}-x_1}$ if smallest value is suspect	0.554
9		0.512
10		0.477
	$=\frac{x_n-x_{n-1}}{x_n-x_2}$ if largest value is suspect	
11	$r_{21}=\frac{x_3-x_1}{x_{n-1}-x_1}$ if smallest value is suspect	0.576
12		0.546
13		0.521
	$=\frac{x_n-x_{n-2}}{x_n-x_2}$ if largest value is suspect	
14	$r_{22}=\frac{x_3-x_1}{x_{n-2}-x_1}$ if smallest value is suspect	0.546
15		0.525
16		0.507
17	$=\frac{x_n-x_{n-2}}{x_n-x_3}$ if largest value is suspect	0.490
18		0.475
19		0.462
20		0.450
21		0.440
22		0.430
23		0.421
24		0.413
25		0.406

APPENDIX C

LOCAL CRUSTAL BACKGROUND LEVELS

sample	Fe_2O_3	MnO	Ba	Cr	Ni	Zn
sandstone	3.59	0.04	469	39	14	60
sandstone	2.58	0.02	405	35	11	41
mudstone	5.45	0.02	648	78	26	105
mudstone	4.00	0.04	680	49	17	68
river sand	2.74	0.01	617	34	13	44
river sand	4.70	0.03	712	65	24	86
mean*	2.69	207 ppm	589	50	18	67
std. dev (s)	0.78	94	123	18	6.2	25
c.v. %	29	45	21	36	35	37
$\pm$ %	23	36	18	29	28	30

* Calculated as the metal, not the oxide.

For a full list of data see Lobb (pers. comm., 1987).

APPENDIX D

RAW DATA FOR SD-N-1, DRS-1, AND LS-1

	Metal						
	Cr	Cu	Fe %	Mn	Ni	Pb	Zn
SD-N-1	158	76.0	3.17	754	29.0	121	458
	148	72.0	3.04	768	29.0	120	426
	145	73.0	3.04	781	26.5	119	435
	147	65.0	3.14	785	27.0	123	465
	130	66.2	3.05	783	24.0	110	386
	213*	60.3	2.68	654	40.2	98.1	431
	142	51.2	2.36	502*	26.9	107	437
	146	73.6	2.43	715	29.4	97.3	423
	147	76.0	2.24	802	30.7	85.9	370
	117	65.3	2.40		32.7	86.5	392
	137	68.7	2.66		28.6	113	404
	150	59.0	1.83		30.0	101	376
	123	69.0	3.95		41.6	96.4	435
	124	74.0	4.39		32.6	91.0	383
	139	77.0			36.0	107	388
	134				55.0*	179*	387
DRS-1	27.0	27.0	3.99	611	17.0	139	655
	29.0	27.0	2.93	832	18.0	155	641
	25.0	29.0	4.31*	1075	19.0	147	636
	27.0	27.0	3.69	956	21.0	114	680
	20.0	31.0	3.85	472	18.0	156	653
	25.0	28.0	3.64	966	19.0	167	508
	26.0	32.0	3.76	1164	21.0	166	575
	27.0	32.0	4.91	1423	20.0	164	627
	33.1	22.1	1.48	683	14.3	192	619
	33.9	28.6	4.36	898	11.3	175	768
	30.8	27.1	3.60	516	8.6	154	639
	34.6	29.3	3.06	609	12.0	153	651
	24.6	23.6	2.80	566	11.8	147	601

Appendix D concluded

	30.8	22.9	2.90	663	8.8	139	616
	28.6	26.2	2.90	899	9.2	136	647
	28.4	24.3	2.46	720	8.3	119	558
	30.8	23.8	2.21	835	11.6	110	423
	21.6	27.0	3.73	888	22.1	144	575
	23.1	24.9	3.13	699	15.1	137	592
	25.0	25.4	3.12	721	20.0	145	518
	22.1	25.4	3.93	911	11.3	155	642
	20.1	24.5	2.5	813		126	523
	31.6	25.8	1.91	857		140	489
	22.6	26.9		810			
LS-1	50.0	16.0	3.89	453	12.1	35.7	81.6
	40.0	14.7	3.49	451	14.1	35.7	66.0*
	46.7	15.9	3.61	321*	15.2	22.9*	81.3

* Rejected using the methods described in Section 6.5.1.